Electronic Supporting Information for:

Rational Design of Novel Organometallic *N*-Acylhydrazones with Potent Antiparasitic Activity on *Trypanosoma Cruzi* and *Brucei*

Patricia M. Toro-Sánchez [a,*], Andrea Lucero [b], David Villaman [c], Mauricio Moncada-Basualto [d], Rodrigo Arancibia [c], Shane R. Wilkinson [e], Pedro Levín [f], Jonathan Cisterna [g], Iván Brito [h], Concepción López [i,*]

[a] Instituto de Ciencias Aplicadas (ICA), Facultad de Ingeniería, Universidad Autónoma de Chile, 5 Poniente 1670, Talca, Chile.

[b] Facultad de Ingeniería y Ciencias, Universidad Adolfo Ibáñez, Av. Padre Hurtado 750, Viña del Mar, Chile.

[c] Facultad de Ciencias Químicas, Universidad de Concepción, Concepción, Chile.

[d] Instituto Universitario de Investigación y Desarrollo Tecnológico, Universidad Tecnológica Metropolitana, Santiago, Chile.

[e] School of Biological and Chemical Sciences, Queen Mary University of London, Mile End Road, London E1 4NS, UK.

[f] Departamento de Química de los Materiales, Facultad de Química y Biología, Universidad de Santiago de Chile, Av. Libertador Bernardo O'Higgins 3363, Santiago, Chile.

[g] Departamento de Química, Universidad Católica del Norte, Antofagasta 1249004, Chile.

[h] Departamento de Química, Universidad de Antofagasta, Av. Universidad de Antofagasta 02800, Campus Coloso, Antofagasta, Chile.

[i] Departament de Química Inorgànica i Orgànica, Secció de Química Inorgànica, Facultat de Química, Universitat de Barcelona, Martí i Franquès 1-11, E-08028 Barcelona, Spain.

*Corresponding author

E-mail addresses: patricia.toro@uautonoma.cl (P. M. Toro-Sánchez), conchi.lopez@qi.ub.edu (C. López).

(64 pages)

Contents

Figure S15. Crystal packing and the hydrogen bond N1–H1···O1 (-x, -y, 1-z) in **4b**. Donor-Acceptor distance (Å): N1–H1···O1, 2.884(5); C11–H11···O5, 3.360(8).

Figure S16. Crystal packing and the hydrogen bond N1–H1···O1 (1-x, 2-y, 2-z) in **5b**. Donor-Acceptor distance (Å): N1–H1···O1, 2.912(9); C11–H11···O5, 3.330(12).

Figure S17. UV-Vis spectra of a freshly prepared solution of **4a** in a DMSO:Buffer solution (20:80) were recorded every 3 h up to 24 h and are shown in **A**. To facilitate visualization, a selection of those obtained at t = 0, 12, and 24 h is presented in **B**.

Figure S18. UV-Vis spectra of a freshly prepared solution of **5a** in a DMSO:Buffer solution (20:80) were recorded every 3 h up to 24 h and are shown in **A**. To facilitate visualization, a selection of those obtained at t = 0, 12, and 24 h is presented in **B**.

Figure S19. UV-Vis spectra of a freshly prepared solution of **6a** in a DMSO:Buffer solution (20:80) were recorded every 3 h up to 24 h and are shown in **A**. To facilitate visualization, a selection of those obtained at t = 0, 12, and 24 h is presented in **B**.

Figure S20. UV-Vis spectra of a freshly prepared solution of **7a** in a DMSO:Buffer solution (20:80) were recorded every 3 h up to 24 h and are shown in **A**. To facilitate visualization, a selection of those obtained at t = 0, 12, and 24 h is presented in **B**.

Figure S21. UV-Vis spectra of a freshly prepared solution of **4b** in a DMSO:Buffer solution (20:80) were recorded every 3 h up to 24 h and are shown in **A**. To facilitate visualization, a selection of those obtained at t = 0, 12, and 24 h is presented in **B**.

Figure S22. UV-Vis spectra of a freshly prepared solution of **5b** in a DMSO:Buffer solution (20:80) were recorded every 3 h up to 24 h and are shown in **A**. To facilitate visualization, a selection of those obtained at t = 0, 12, and 24 h is presented in **B**.

Figure S23. UV-Vis spectra of a freshly prepared solution of **6b** in a DMSO:Buffer solution (20:80) were recorded every 3 h up to 24 h and are shown in **A**. To facilitate visualization, a selection of those obtained at t = 0, 12, and 24 h is presented in **B**.

Figure S24. UV-Vis spectra of a freshly prepared solution of **7b** in a DMSO:Buffer solution (20:80) were recorded every 3 h up to 24 h and are shown in **A**. To facilitate visualization, a selection of those obtained at t = 0, 12, and 24 h is presented in **B**.

Figure S25. ^{1}H-NMR spectrum (300 MHz) of compound **4a** in DMSO-d_6.

Figure S26. ^{1}H-NMR spectrum (300 MHz) of compound **5a** in DMSO-d_6.

Figure S27. ^{1}H-NMR spectrum (300 MHz) of compound **6a** in DMSO-d_6.

Figure S28. ^{1}H-NMR spectrum (300 MHz) of compound **7a** in DMSO-d_6.

Figure S29. ^{1}H-NMR spectrum (300 MHz) of compound **4b** in DMSO-d_6.

Figure S30. ^{1}H-NMR spectrum (300 MHz) of compound **5b** in DMSO-d_6.

Figure S31. ^{1}H-NMR spectrum (300 MHz) of compound **6b** in DMSO-d_6.

Figure S32. ^{1}H-NMR spectrum (300 MHz) of compound **7b** in DMSO-d_6.

Figure S33. ^{1}H NMR spectrum (400 MHz) of compound **4c** in DMSO-d_6.

Figure S34. ^{1}H NMR spectrum (400 MHz) of compound **5c** in DMSO-d_6.

Figure S35. ^{1}H NMR spectrum (400 MHz) of compound **6c** in DMSO-d_6. The inserted plot shows an expansion of the region 8.0 – 7.5 ppm.

Figure S36. ^{1}H NMR spectrum (400 MHz) of compound **7c** in DMSO-d_6. The inserted plot shows an expansion of the region 8.0 – 7.4 ppm.

Figure S37. [^{1}H–^{1}H] NOESY spectrum (400 MHz) of compound **4a** in DMSO-d_6.

Figure S38. ^{1}H-NMR spectra (400 MHz) of complex **4b** in DMSO-d_6 registered at variable temperatures (300 to 340 K).

Figure S39. Zoom-in of the NH and aromatic region of the ^{1}H-NMR spectra (400 MHz) of **4b** recorded at different temperatures (300 to 340 K).

Figure S40. Cyclic voltammograms of **4a** at different scan rates of 0.1 – 2.00 V s^{-1} in DMSO (TBAP 0.1 M, HMDE, Pt, non-aqueous Ag/AgCl).

Figure S41. Cyclic voltammograms of **4b** at different scan rates of 0.1 – 2.00 V s^{-1} in DMSO (TBAP 0.1 M, HMDE, Pt, non-aqueous Ag/AgCl).

Figure S42. Cyclic voltammograms of **5a** at different scan rates of 0.1 – 2.00 V s^{-1} in DMSO (TBAP 0.1 M, HMDE, Pt, non-aqueous Ag/AgCl).

Figure S43. Cyclic voltammograms of **6a** at different scan rates of 0.1 – 2.00 V s^{-1} in DMSO (TBAP 0.1 M, HMDE, Pt, non-aqueous Ag/AgCl).

Figure S44. Cyclic voltammograms of **7a** at different scan rates of 0.1 – 2.00 V s^{-1} in DMSO (TBAP 0.1 M, HMDE, Pt, non-aqueous Ag/AgCl).

Figure S45. Cyclic voltammograms of **7b** at different scan rates of 0.1 – 2.00 V s^{-1} in DMSO (TBAP 0.1 M, HMDE, Pt, non-aqueous Ag/AgCl).

Figure S46. Differential pulse voltammograms of **5b** (**A**) and **6b** (**B**) derivatives. All experiments were performed in DMSO (TBAP 0.1 M, HMDE, Pt, non-aqueous Ag/AgCl).

Figure S47. Comparative plot of the SI values obtained for NAH compounds (**4a**, **5a**, **6a**, **6b**, **7a**, and Nfx) in *T. cruzi* (**A**) and *T. brucei* (**B**).

Figure S48. Comparative plot of all the NAH compounds (types **E**, **F**, and **G**, and **I** with R^2 = H) of their anti-*T. cruzi* activity (EC_{50}) and selectivity (SI).

3. Supplementary Table

Table S1. Crystal data, experimental details, and refinement parameters for complexes [Re{(η^5-C_5H_4)-C(O)-NH-N=CH-(2-C_4H_2S-4-NO_2)}$(CO)_3$] (**4b**), [Fe(η^5-C_5H_5){(η^5-C_5H_4)-C(O)-NH-N=C(Me)-(2-C_4H_2S-4-NO_2)}] (**5a**), [Re{(η^5-C_5H_4)-C(O)-NH-N=C(Me)-(2-C_4H_2S-4-NO_2)}$(CO)_3$] (**5b**) and [Re{(η^5-C_5H_4)-C(O)-NH-N=CH-(2-C_4H_2S-5-NO_2)}$(CO)_3$] (**6b**).

Table S2. Bond lengths [Å] and angles [°] for **4b**.

Table S3. Bond lengths [Å] and angles [°] for **5a**.

Table S4. Bond lengths [Å] and angles [°] for **5b**.

Table S5. Bond lengths [Å] and angles [°] for **6b**.

Table S6. Hydrogen bonds for **4b**.

Table S7. Hydrogen bonds for **5a**.

Table S8. Hydrogen bonds for **5b**.

Table S9. Hydrogen bonds for **6b**.

Table S10. Summary of experimental ultraviolet-visible spectroscopic data: position of the bands detected [wavelengths λ_i (nm)] and logarithms of their molar extinction coefficients [log ε_i (ε_i in M^{-1} cm^{-1})] for the new organometallic NAHs (**4a,b – 7a,b**) [Types **H** and **I** in Figure 3).

4. Supplementary References

Contents

1. Supplementary Experimental Part:

1.1. General Comments.

The following chemical reagents were purchased from commercial suppliers and used as received: benzhydrazide (98%) (**1c**), 5-nitro-2-thiophenecarboxaldehyde (98%) (**3I**), trifluoroacetic acid (CF_3COOH, 99%) and ethanol (≥ 99.5%). 4-nitro-2-thiophenecarboxaldehyde (**2I**), 2-acetyl-4-nitrothiophene (**2II**) and 2-acetyl-5-nitrothiophene (**3II**) were synthesized as described in the literature [S1,S2]. The IR and high-resolution mass spectra (HRMS) were performed using the equipment indicated in the experimental section, *section 2.1* (*chemical and methods*) of the manuscript. ^{1}H-NMR spectra were recorded at room temperature on a Bruker Advance 400 spectrometer using DMSO-d_6 (99.9%) as the solvent.

*1.2. Description of the method used for the preparation of organic acylhydrazones (**4c–7c**).*

The organic acylhydrazones were readily prepared following the procedure described in the literature [S3,S4]. A few drops of CF_3COOH were added to a mixture formed by 1.0 mmol amount of benzyhydrazyde (**1c**) (136 mg) and the equimolar amount of the appropriate (4- or 5-)nitro-2-thiophenecarboxaldehyde (**2I** or **3I**) (157 mg, 1.0 mmol) or 2-acetyl-(4- or 5-)nitrothiophene (**2II** or **3II**) (171 mg, 1.0 mmol), and 15 mL of anhydrous ethanol (Scheme S1). The reaction mixture was then stirred under N_2 atmosphere at 80 °C for 5 h. After this period, the solid formed was separated by filtration, washed with ethanol, and dried in a vacuum.

*1.3. Yields and characterization data for compounds **4c – 7c**.*

Compound 4c. Light brown. Yield: 85% (234 mg, 0.85 mmol). Anal. (%) Calc. for $C_{12}H_9N_3O_3S$: C, 52.36; H, 3.30 and N, 15.26. Found: C, 51.89; H, 3.43 and N, 14.70. HRMS (*m/z*): 276.0433 and calc. for $[M + H]^+$ $C_{12}H_9N_3O_3S$: 276.0437. FT-IR selected data (ν in cm^{-1}): 3447 [ν(NH)] and 1650 [ν(-C(O)-)]. ^{1}H-NMR data: δ 7.51 – 7.63 (m, 3H, C_6H_5), 7.90 (d, 2H, J = 7.4, C_6H_5), 8.11 (s, 1H, C_4H_2S), 8.67 (s, 1H, CH=N), 8.84 (s, 1H, C_4H_2S), 12.11 (s, 1H, NH).

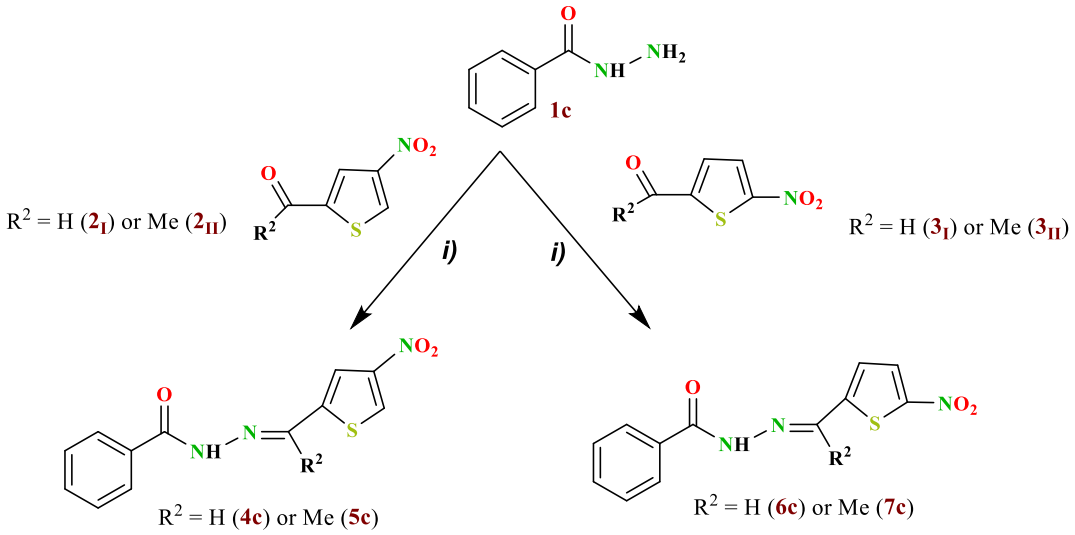

Scheme S1. Synthesis of the organic acylhydrazones **(4c – 7c)**. Reagents and conditions: *i)* equimolar amounts of the reagents, in absolute ethanol at 80 °C for 5 h, and in the presence of catalytic amounts of CF_3COOH.

Compound 5c. Light brown solid. Yield: 90% (260 mg, 0.90 mmol). Anal. (%) Calc. for $C_{13}H_{11}N_3O_3S$: C, 53.97; H, 3.83 and N, 14.52. Found: C, 53.49, H, 4.10 and N, 14.05. HRMS (*m/z*): 290.0597 and calc. for $[M + H]^+$ $C_{13}H_{11}N_3O_3S$: 290.0594. FT-IR selected data (ν in cm^{-1}): 3298 [ν(NH)] and 1646 [ν(-C(O)-)]. ^{1}H-NMR data: δ 2.42 (s, 3H, Me), 7.50 – 7.61 (m, 3H, C_6H_5), 7.86 (s, 2H, C_6H_5), 8.05 (s, 1H, C_4H_2S), 8.80 (s, 1H, C_4H_2S), 11.00 (s, 1H, NH).

Compound 6c. Deep yellow. Yield: 89% (245 mg, 0.89 mmol). Anal. (%) Calc. for $C_{12}H_9N_3O_3S$: C, 52.36; H, 3.30 and N, 15.26. Found: 53.25; H, 3.40 and N, 15.17. HRMS (*m/z*): 276.0445 and calc. for $[M + H]^+$ $C_{12}H_9N_3O_3S$: 276.0437. FT-IR selected data (ν in cm^{-1}): 3249 [ν(NH)] and 1641 [ν(-C(O)-)]. ^{1}H-NMR data: δ 7.52 – 7.64 (m, 4H, C_6H_5), 7.90 (d, 2H, C_4H_2S and C_6H_5), 8.13 (d, 1H, J = 4.3, C_4H_2S), 8.66 (s, 1H, CH=N), 12.23 (s, 1H, NH).

Compound 7c. Crystal yellow. Yield: 83% (240 mg, 0.83 mmol). Anal. (%) Calc. for $C_{13}H_{11}N_3O_3S$: C, 53.97; H, 3.83 and N, 14.52. Found: C, 55.09; H, 3.98 and N, 14.41. HRMS (*m/z*): 290.0601 and calc. for $[M + H]^+$ $C_{13}H_{11}N_3O_3S$: 290.0594. FT-IR selected data (ν in cm^{-1}): 3302 [ν(NH)] and 1646 [ν(-C(O)-)]. ^{1}H-NMR data: δ 2.41 (s, 3H, Me), 7.50 – 7.62 (m, 4H, C_6H_5), 7.85 (ps-d, 2H, C_4H_2S and C_6H_5), 8.10 (d, 1H, J = 4.4, C_4H_2S), 11.10 (s, 1H, NH).

2. Supplementary Figures

Figure S1. High-resolution mass spectra of compounds **4a**, **4b** and **4c** (see also *section 2.2.1* of the manuscript).

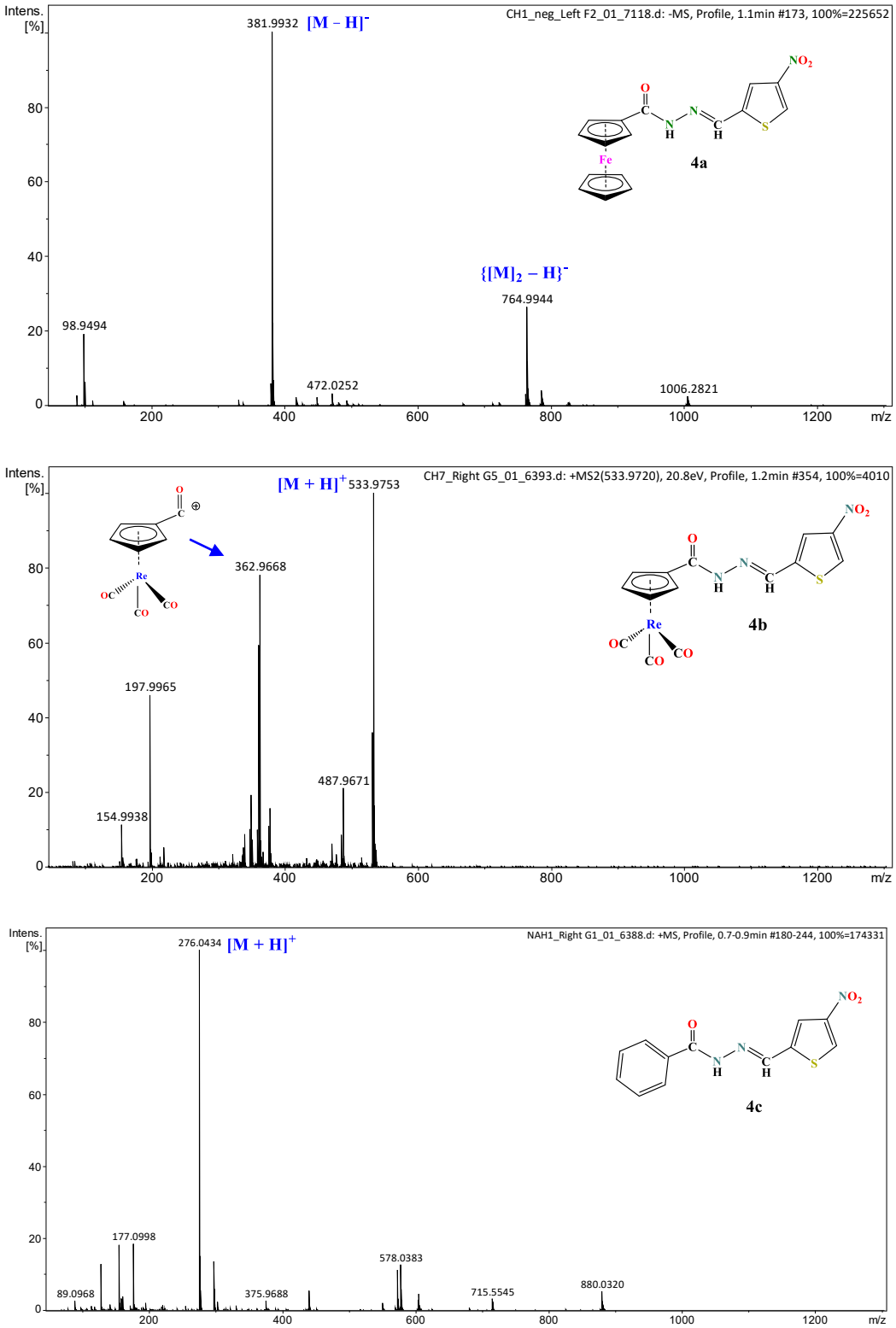

Figure S2. High-resolution mass spectra of compounds **5a**, **5b**, and **5c** (see also *section 2.2.1* of the manuscript).

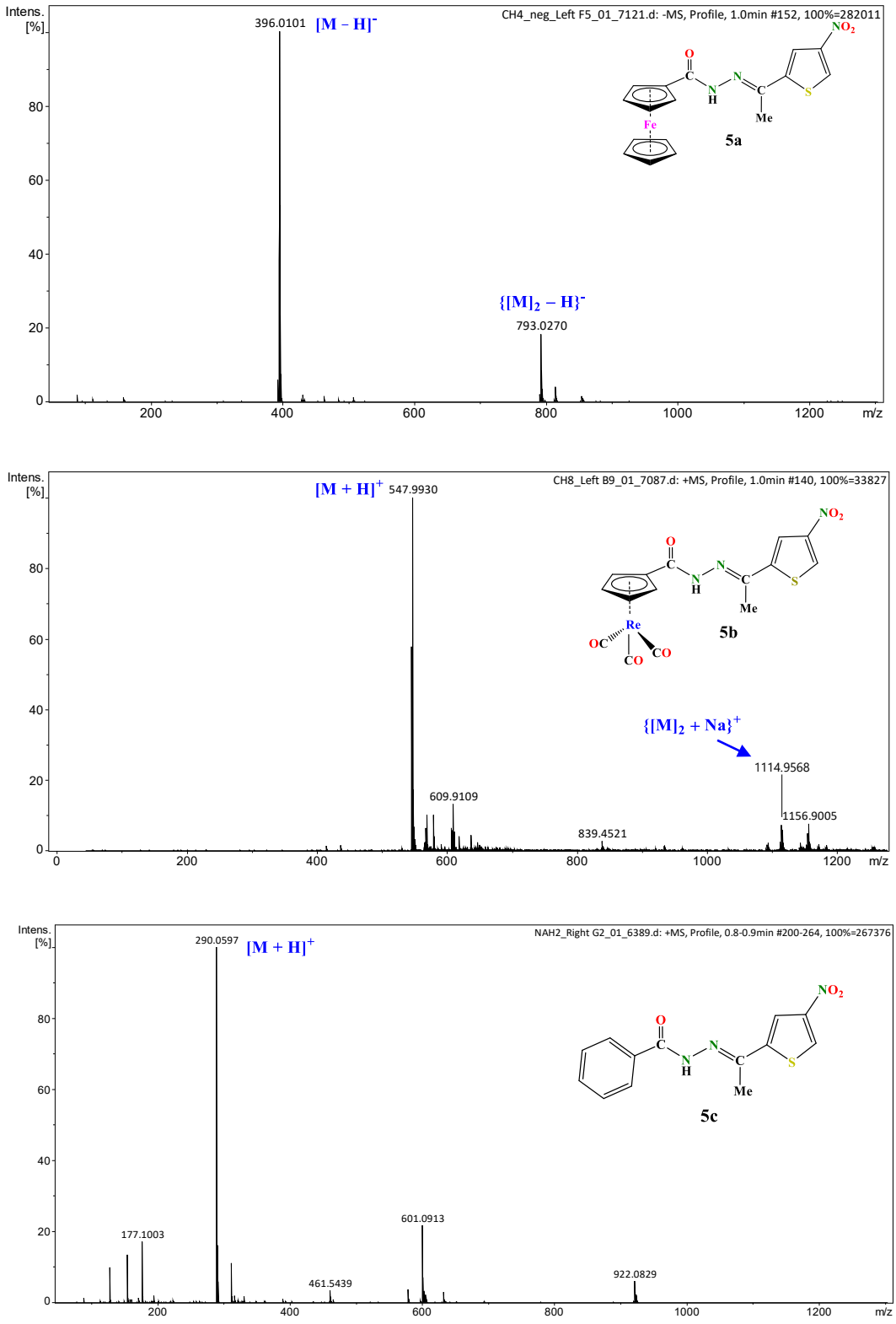

Figure S3. High-resolution mass spectra of compounds **6a**, **6b**, and **6c**. (see also *section 2.2.1* of the manuscript).

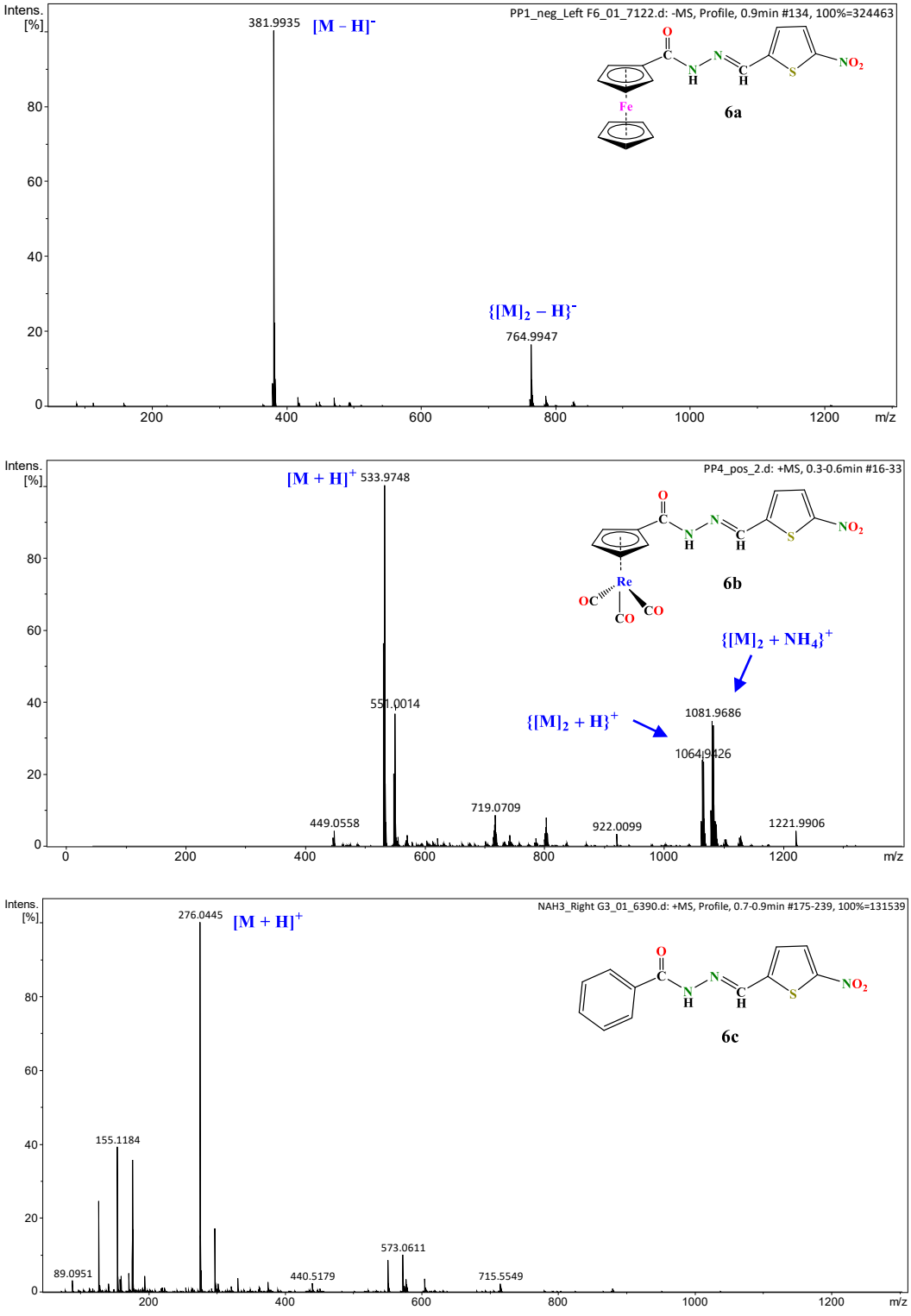

Figure S4. High-resolution mass spectra of compounds **7a**, **7b**, and **7c** (see also *section 2.2.1* of the manuscript).

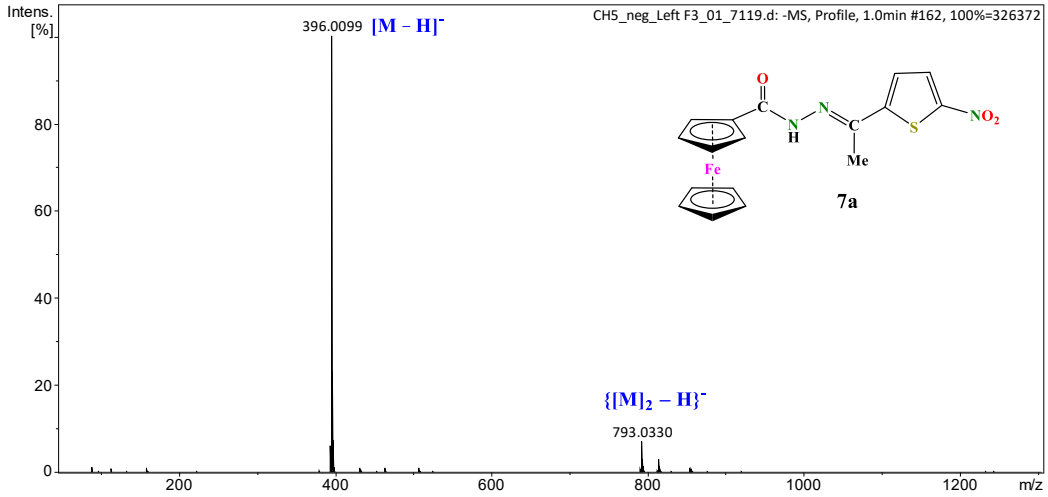

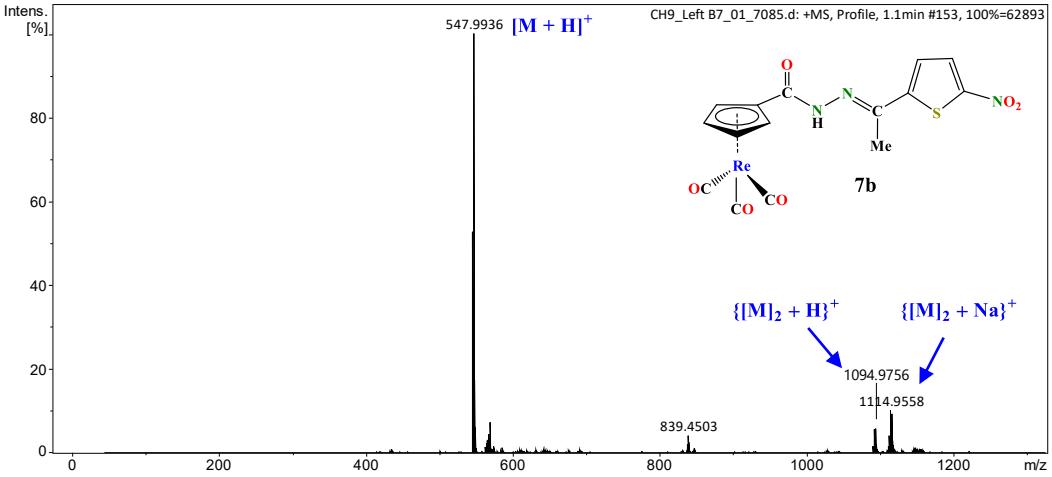

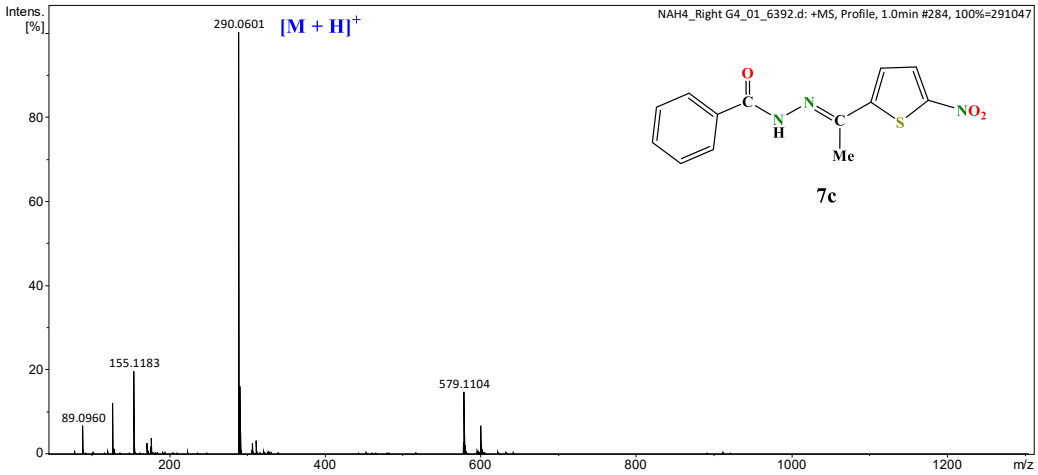

Figure S5. Mass spectra of compounds **4a** and **4b**.

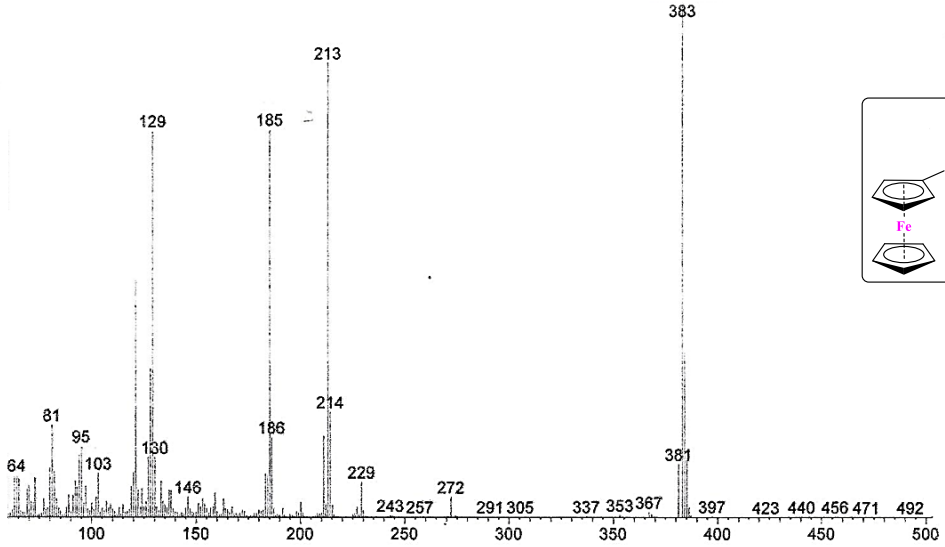

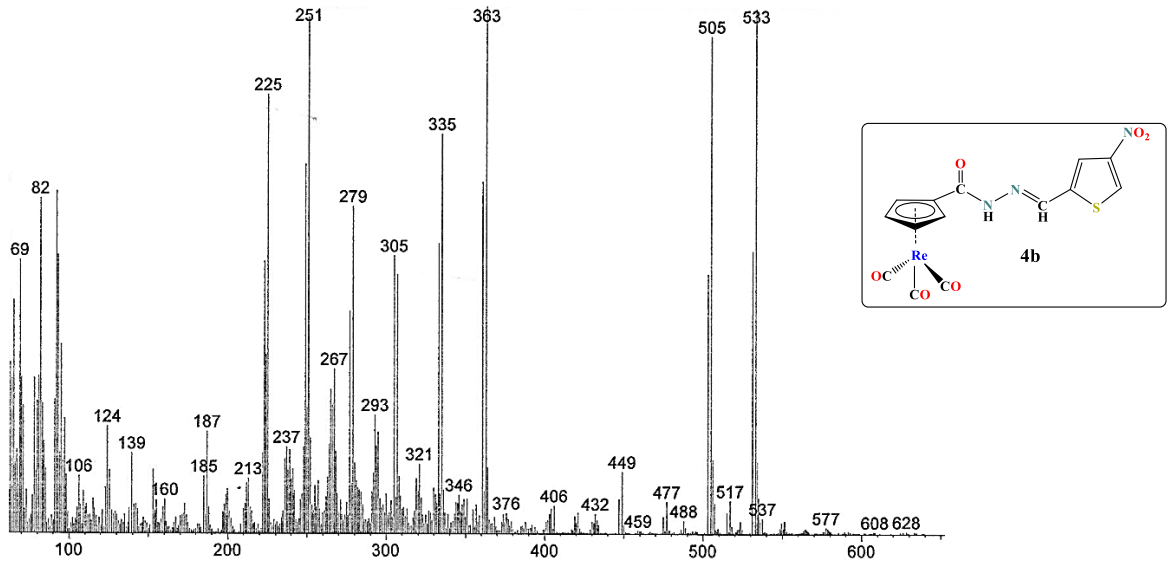

Figure S6. Mass spectra of compounds **5a** and **5b**.

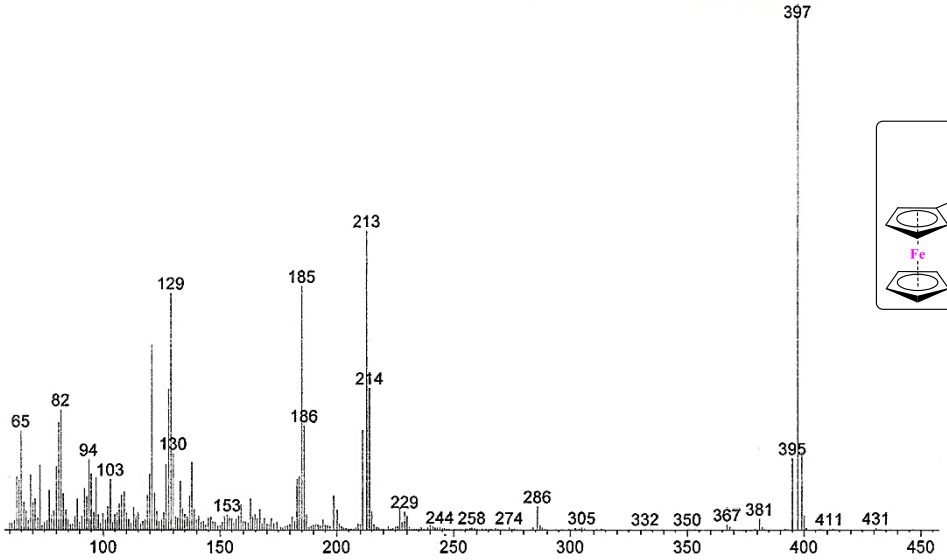

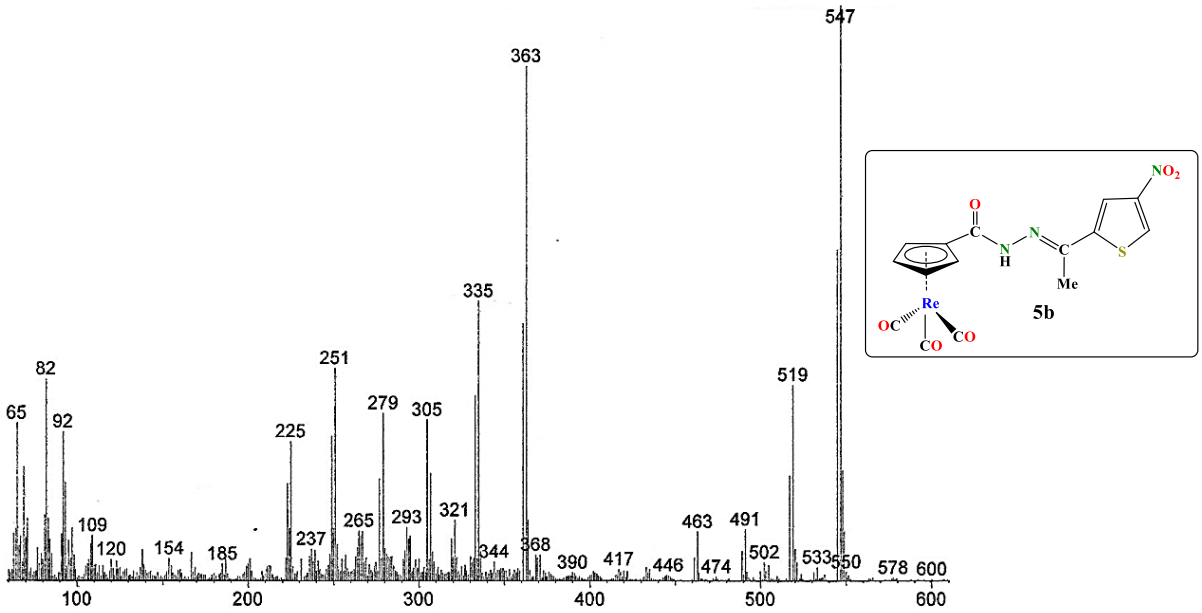

Figure S7. Mass spectra of compounds **6a** and **6b**.

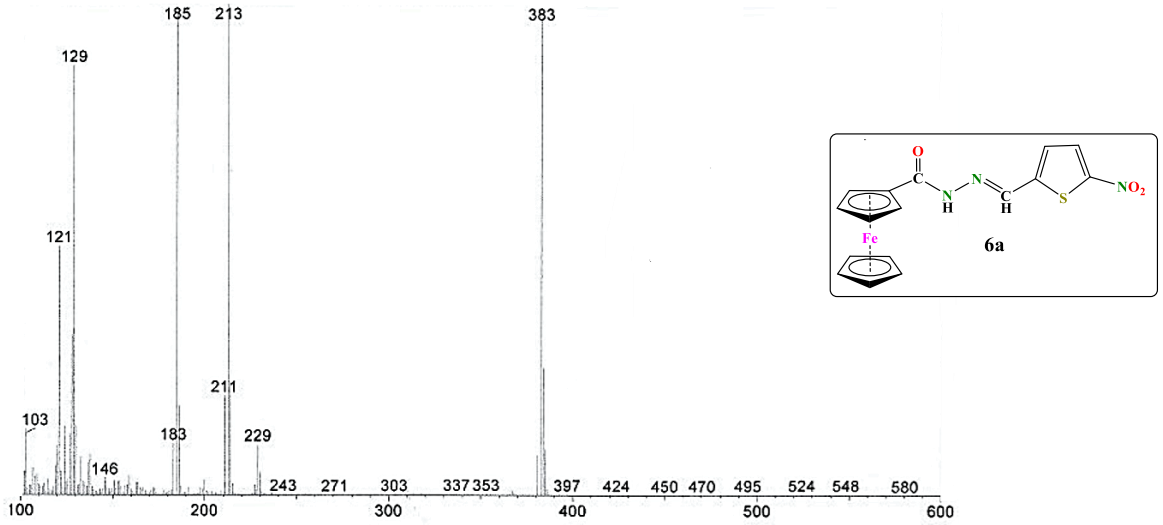

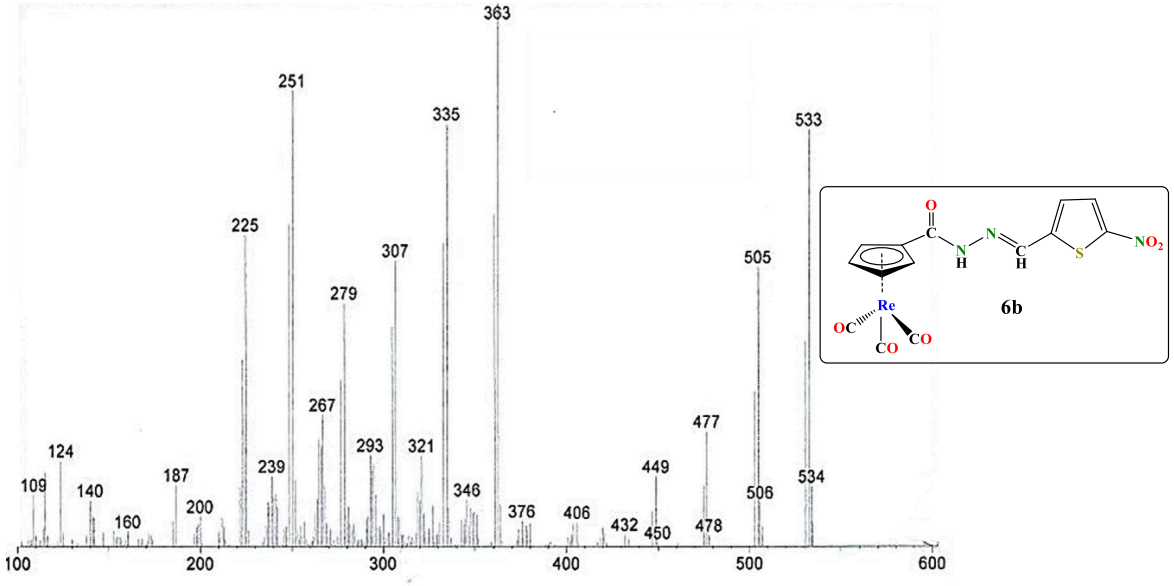

Figure S8. Mass spectra of compounds **7a** and **7b**.

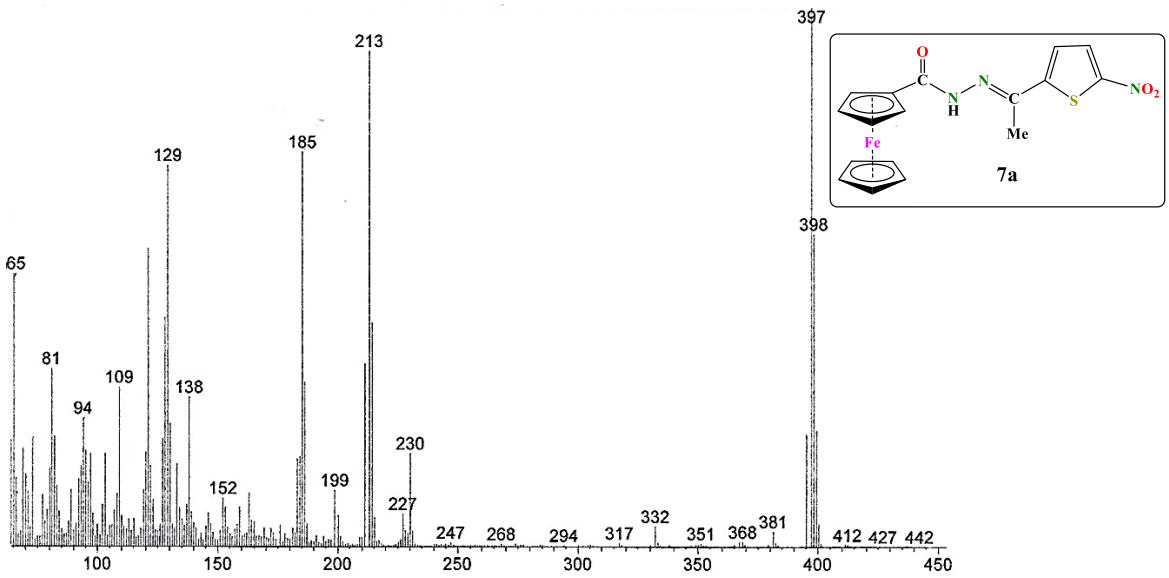

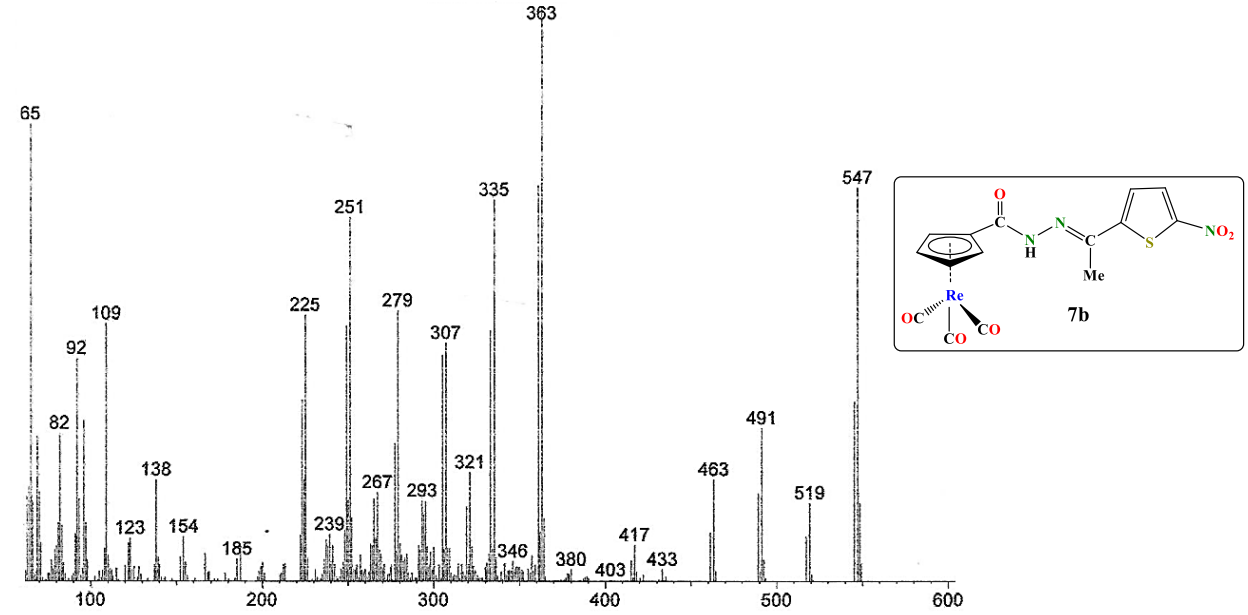

Figure S9. FT-IR spectra of compounds **4a**, **4b** and **4c**.

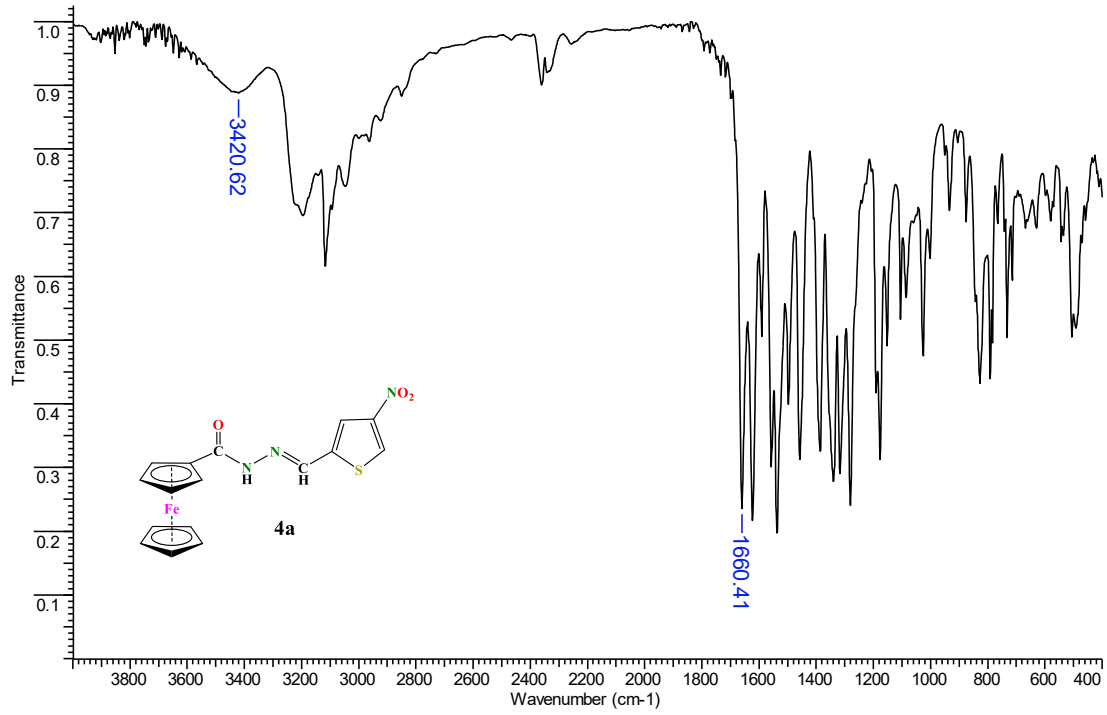

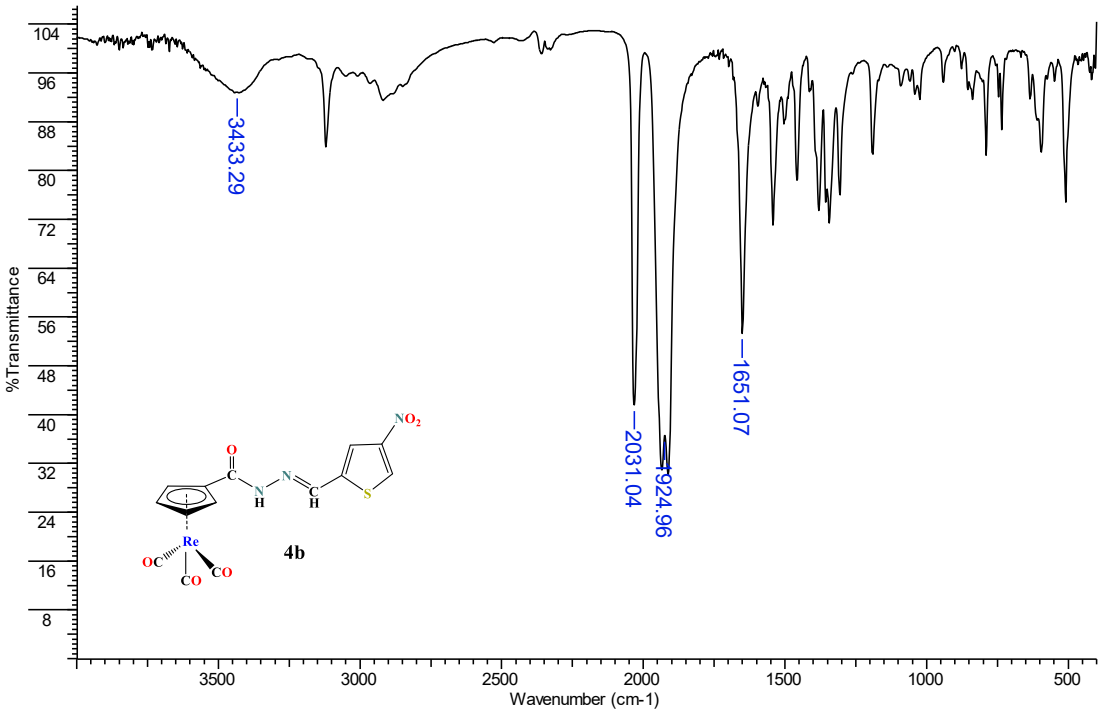

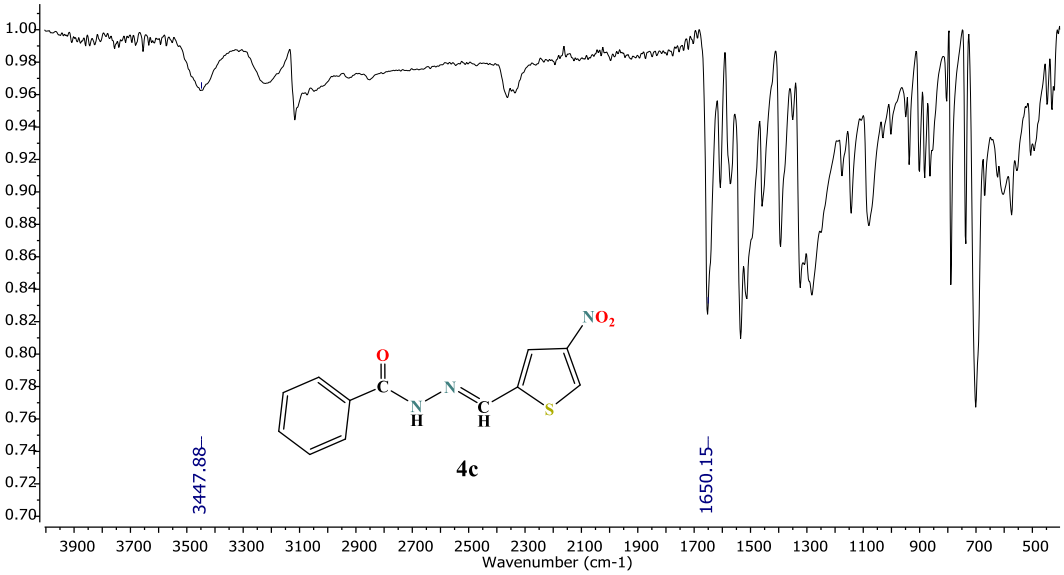
1.00
0.98
0.96
0.94
0.92
0.90
0.88
0.86
0.84
0.82
0.80
0.78
0.76
0.74
0.72
0.70
3447.88
1650.15
3900 3700 3500 3300 3100 2900 2700 2500 2300 2100 1900 1700 1500 1300 1100 900 700 500
Wavenumber (cm-1)
O
C
N
H
N
C
H
S
NO2

4c

Figure S10. FT-IR spectra of compounds **5a**, **5b** and **5c**.

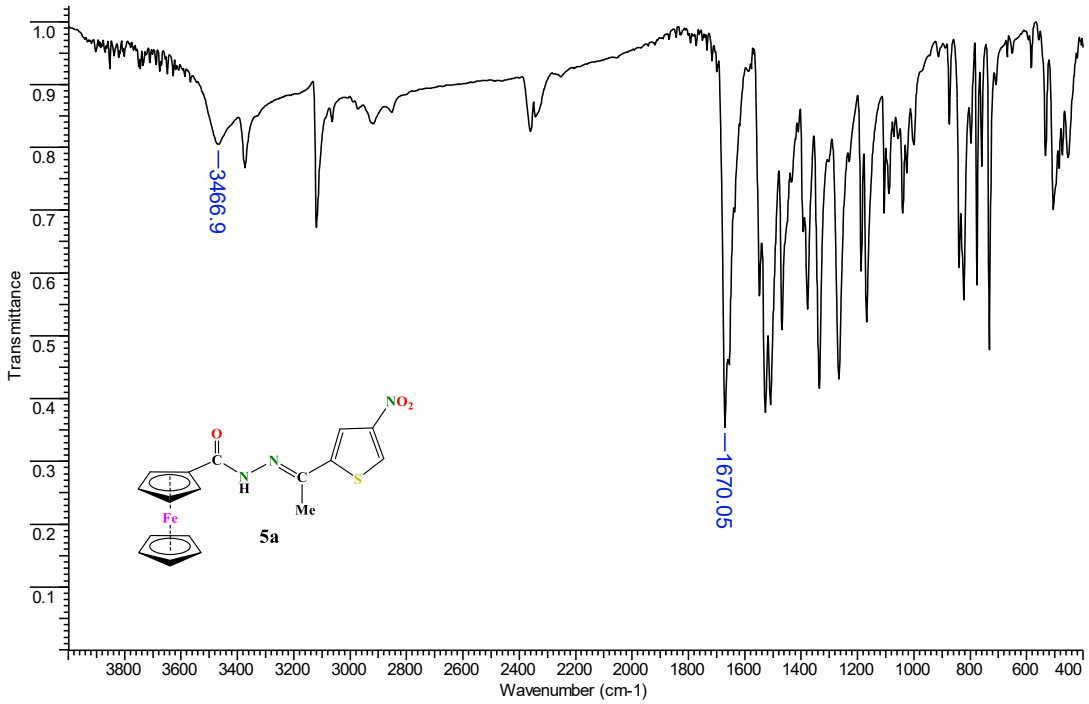

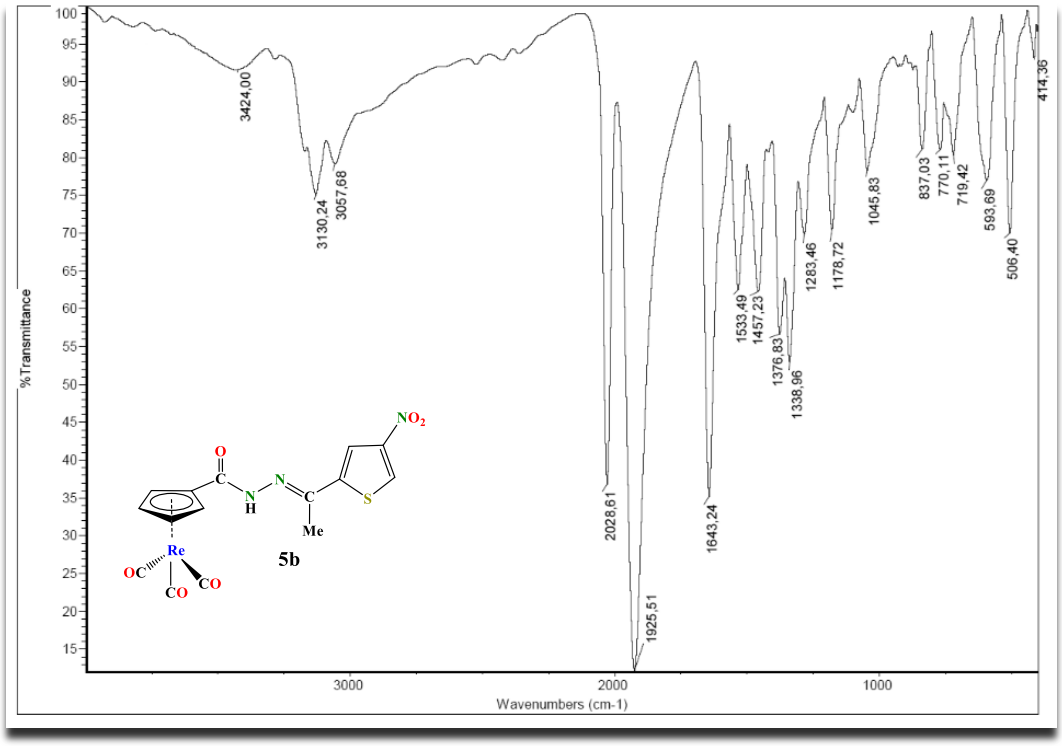

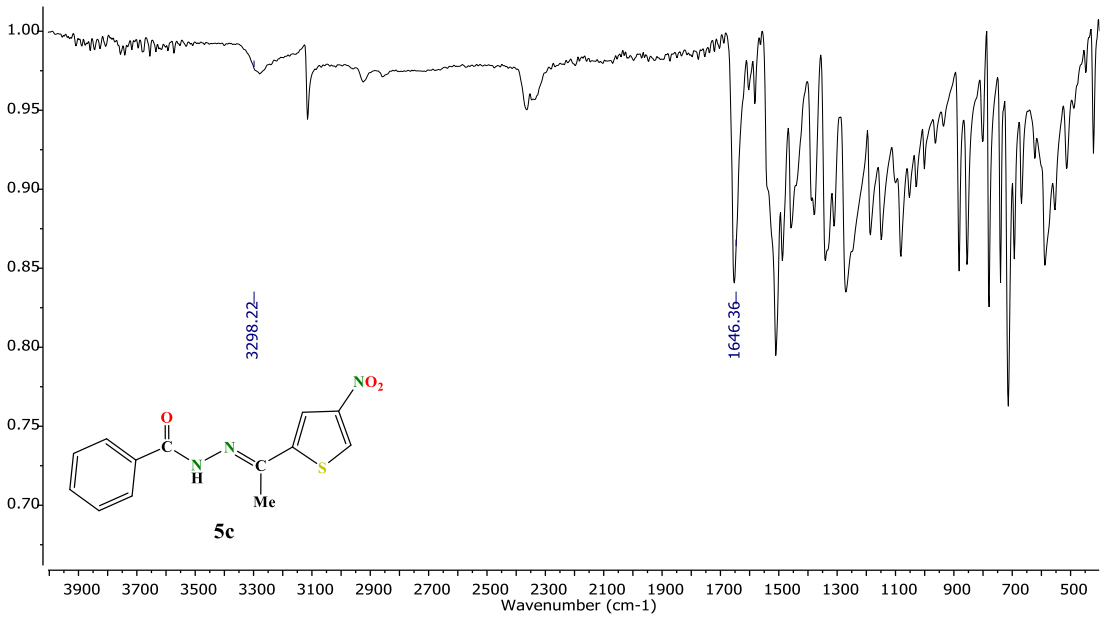
1.00
0.95
0.90
0.85
0.80
0.75
0.70
3298.22
1646.36
O
C
N
H
N
C
Me
S
NO2
5c
3900 3700 3500 3300 3100 2900 2700 2500 2300 2100 1900 1700 1500 1300 1100 900 700 500
Wavenumber (cm-1)

Figure S11. FT-IR spectra of compounds **6a**, **6b** and **6c**.

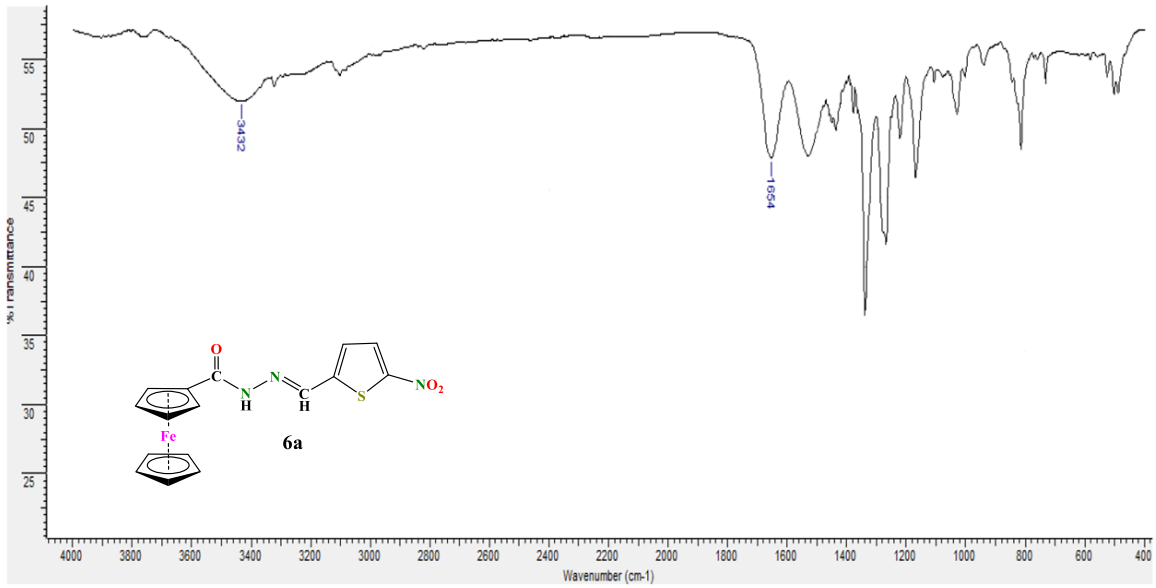

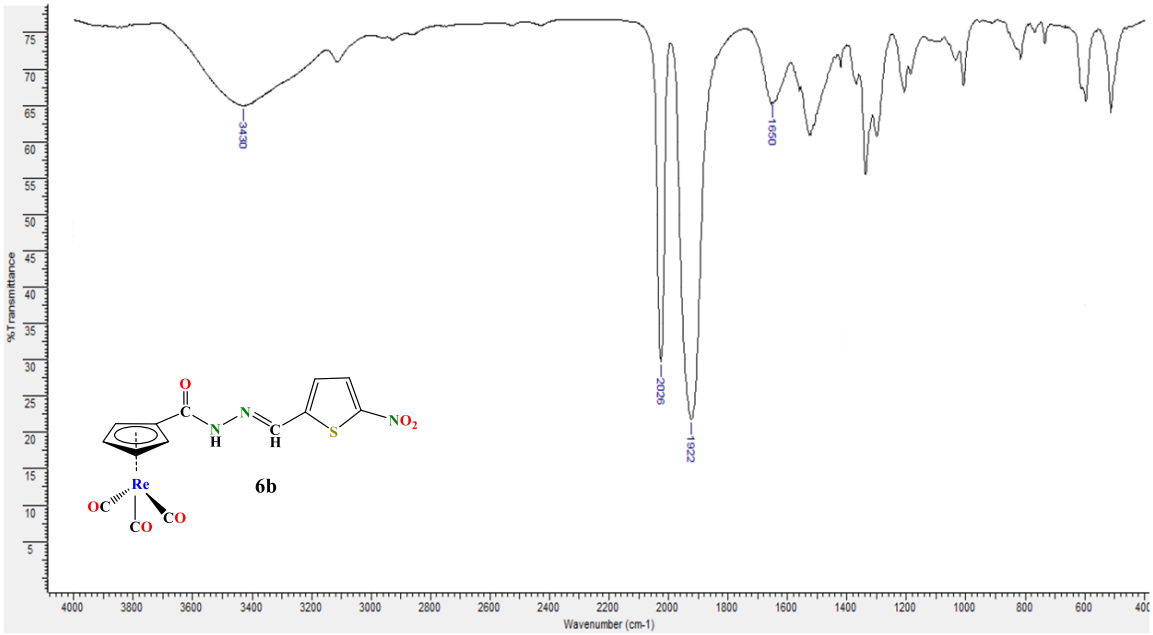

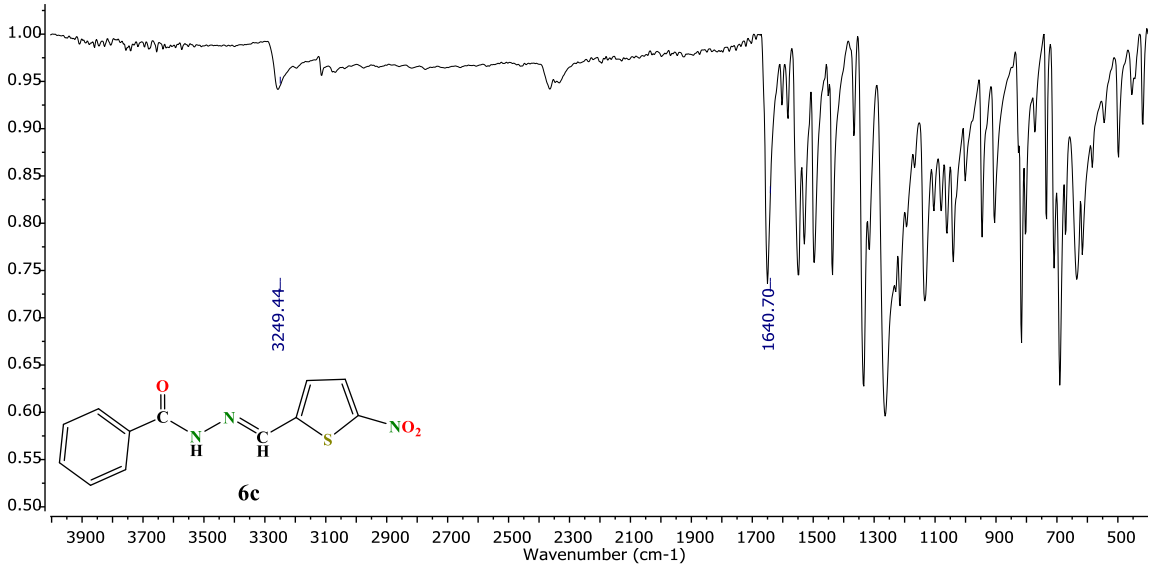
1.00
0.95
0.90
0.85
0.80
0.75
0.70
0.65
0.60
0.55
0.50
3249.44
1640.70
O
C
N
H
N
C
H
S
NO2
6c
3900 3700 3500 3300 3100 2900 2700 2500 2300 2100 1900 1700 1500 1300 1100 900 700 500
Wavenumber (cm-1)

Figure S12. FT-IR spectra of compounds **7a**, **7b** and **7c**.

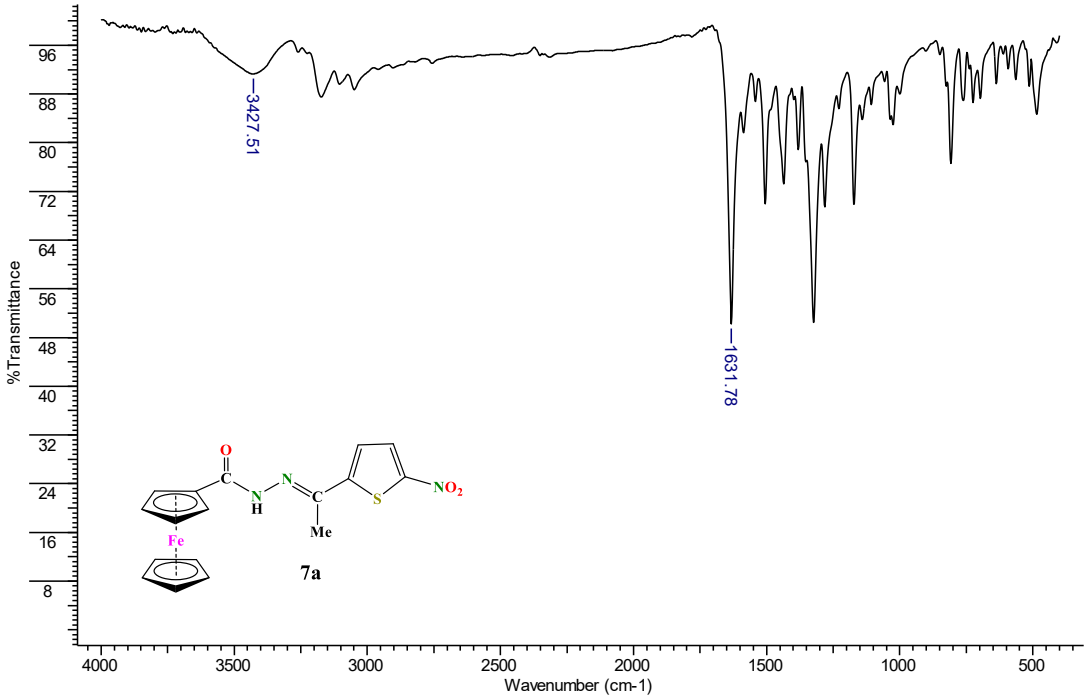

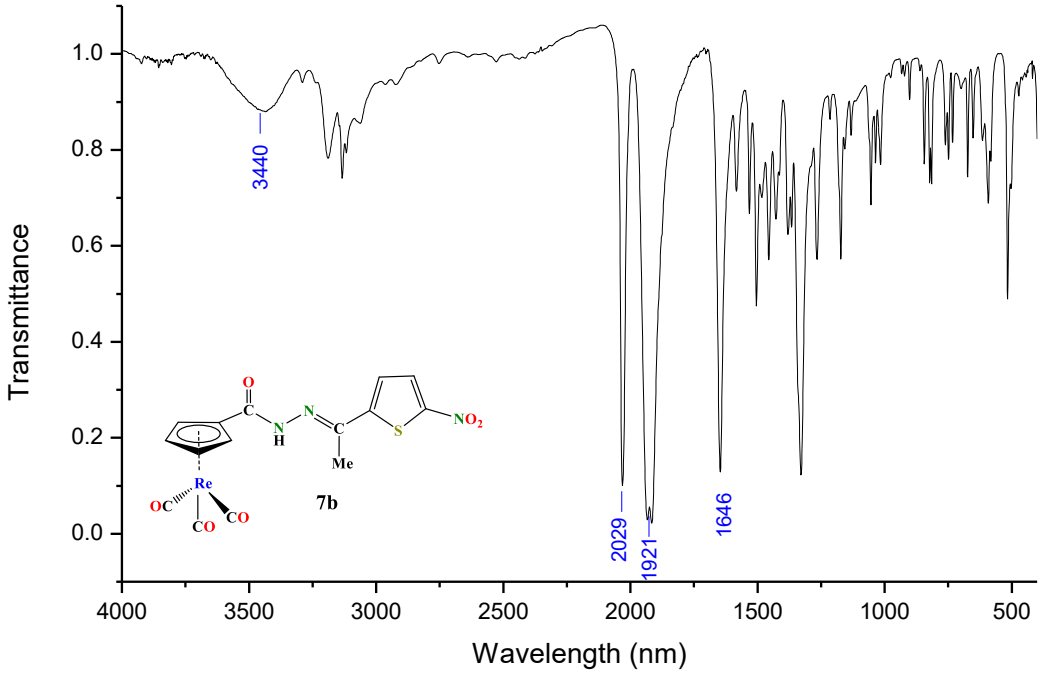

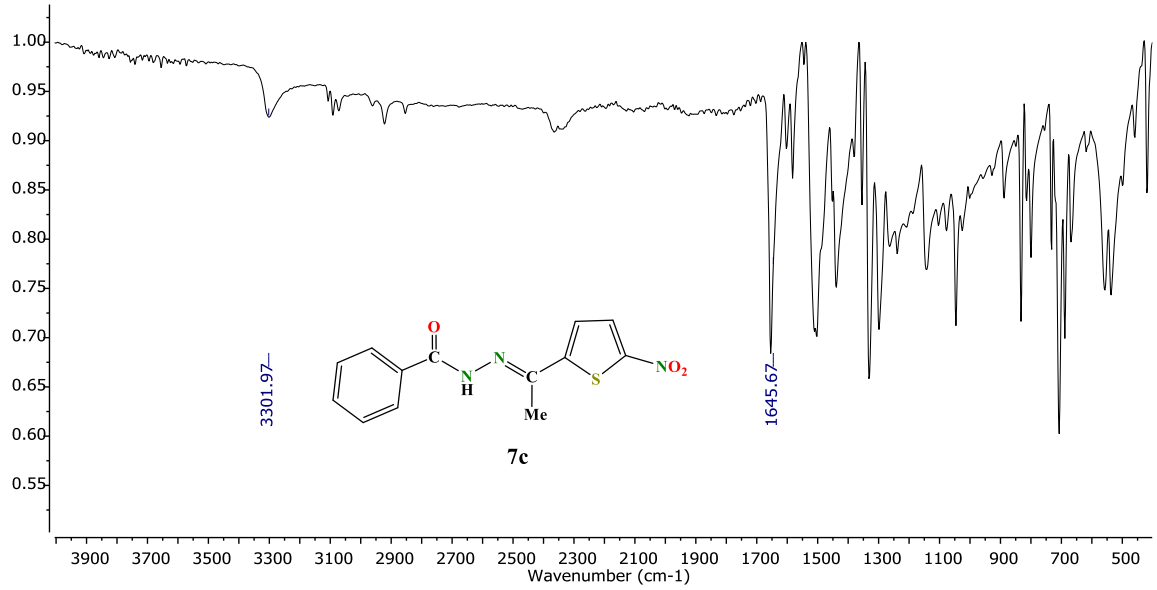
1.00
0.95
0.90
0.85
0.80
0.75
0.70
0.65
0.60
0.55
3301.97
1645.67
O
C
N
H
N
C
Me
S
NO2
3900 3700 3500 3300 3100 2900 2700 2500 2300 2100 1900 1700 1500 1300 1100 900 700 500
Wavenumber (cm-1)

7c

Figure S13. Intermolecular hydrogen bonds of **5a** along to [110] by N1–H1···O1 (1/2-x, 1/2-y, 1-z) and C9–H9···O2 (1-x, 2-y, 1-z). Donor-Acceptor distances (Å): N1–H1···O1, 2.918(5); C9–H9···O2, 3.353(7).

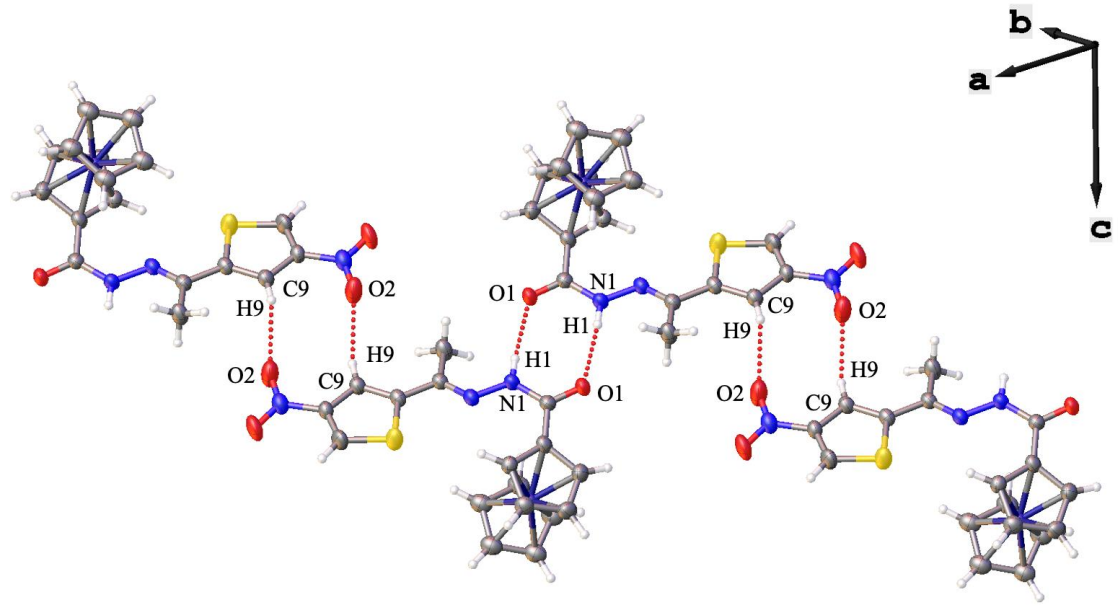

Figure S14. Crystal packing and the hydrogen bond N1–H1···O1 (2-x, 1-y, -z) in **6b**. Donor-Acceptor distance (Å): N1–H1···O1, 2.854(10); C10–H10···O6, 3.416(17).

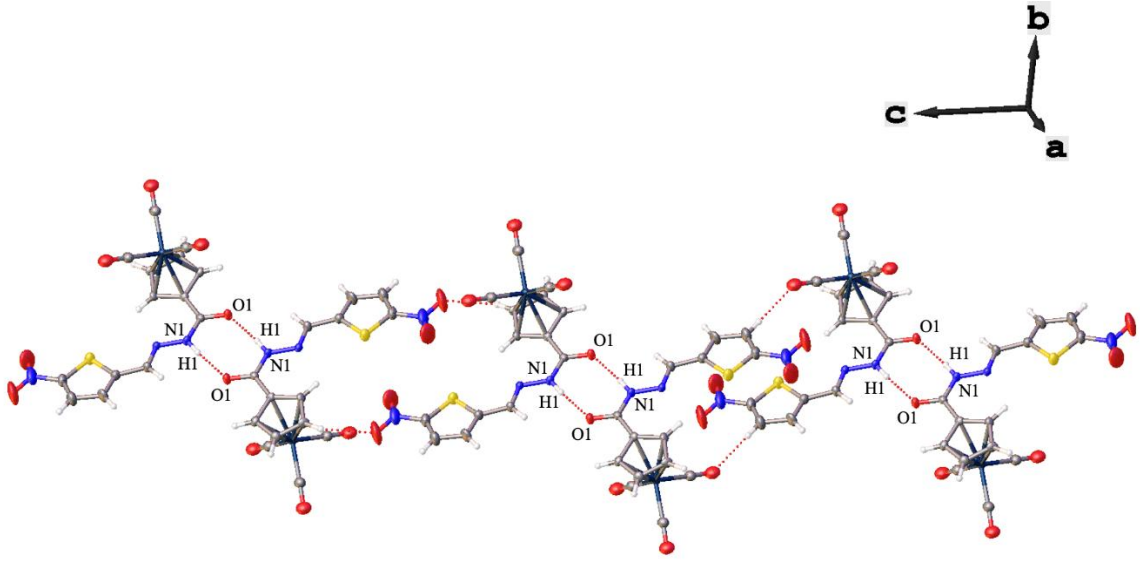

Figure S15. Crystal packing and the hydrogen bond N1–H1···O1 (-x, -y, 1-z) in **4b**. Donor-Acceptor distance (Å): N1–H1···O1, 2.884(5); C11–H11···O5, 3.360(8).

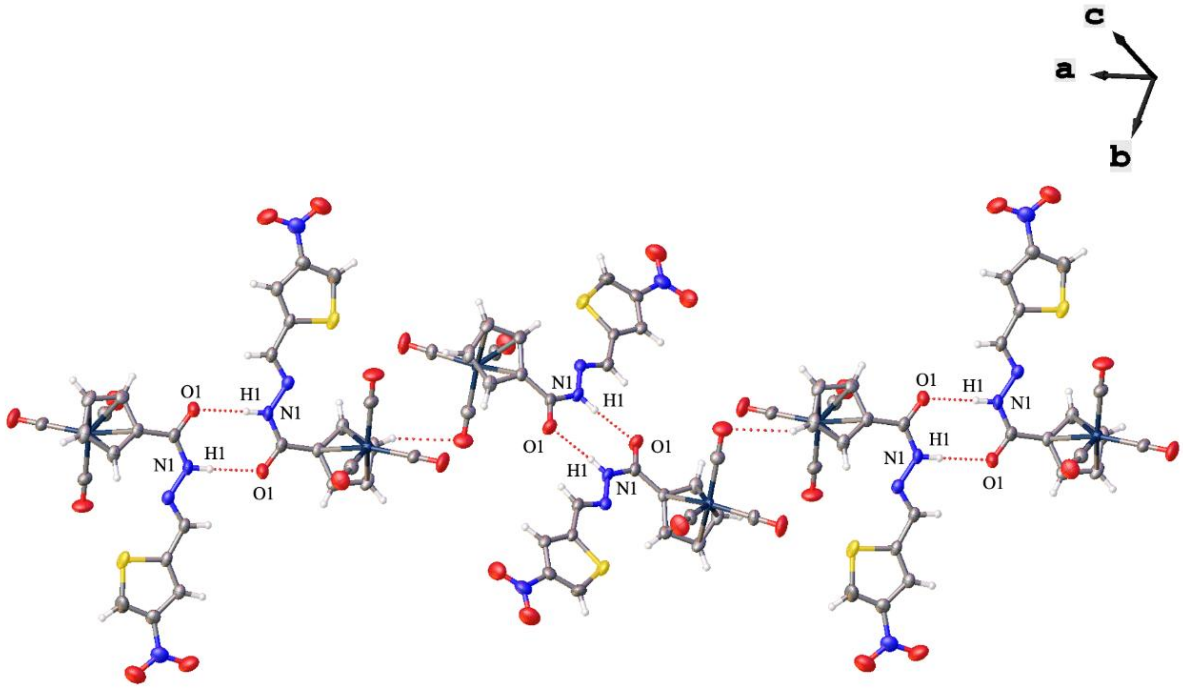

Figure S16. Crystal packing and the hydrogen bond N1–H1···O1 (1-x, 2-y, 2-z) in **5b**. Donor-Acceptor distance (Å): N1–H1···O1, 2.912(9); C11–H11···O5, 3.330(12).

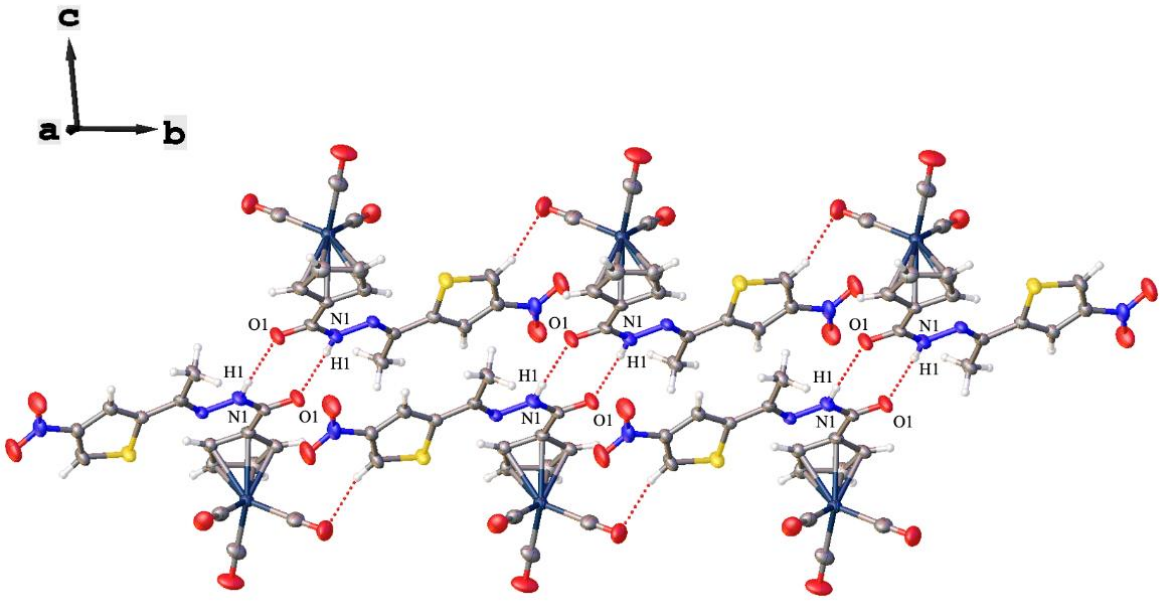

Figure S17. UV-Vis spectra of a freshly prepared solution of **4a** in a DMSO:Buffer solution (20:80) were recorded every 3 h up to 24 h and are shown in **A**. To facilitate visualization, a selection of those obtained at t = 0, 12, and 24 h is presented in **B**.

A)

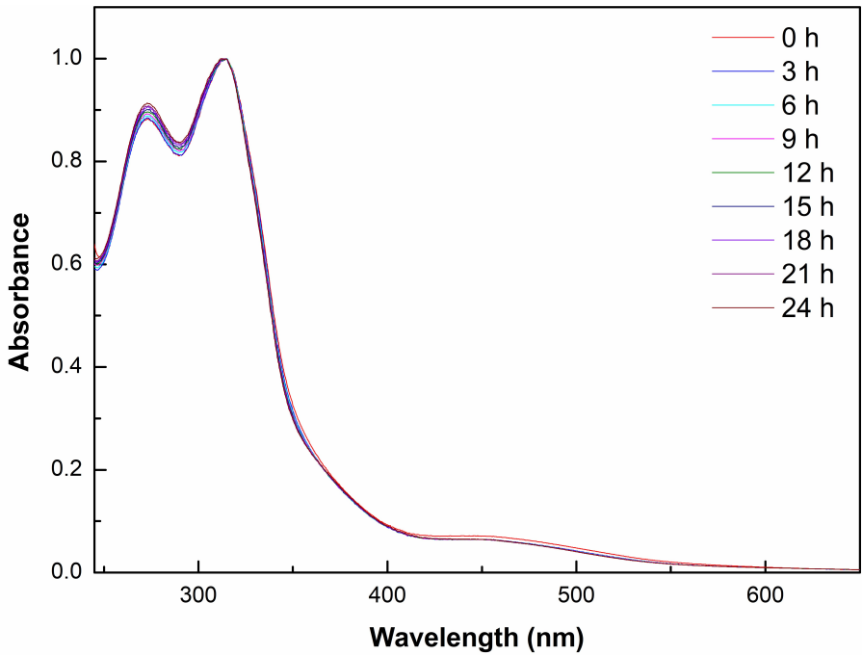

B)

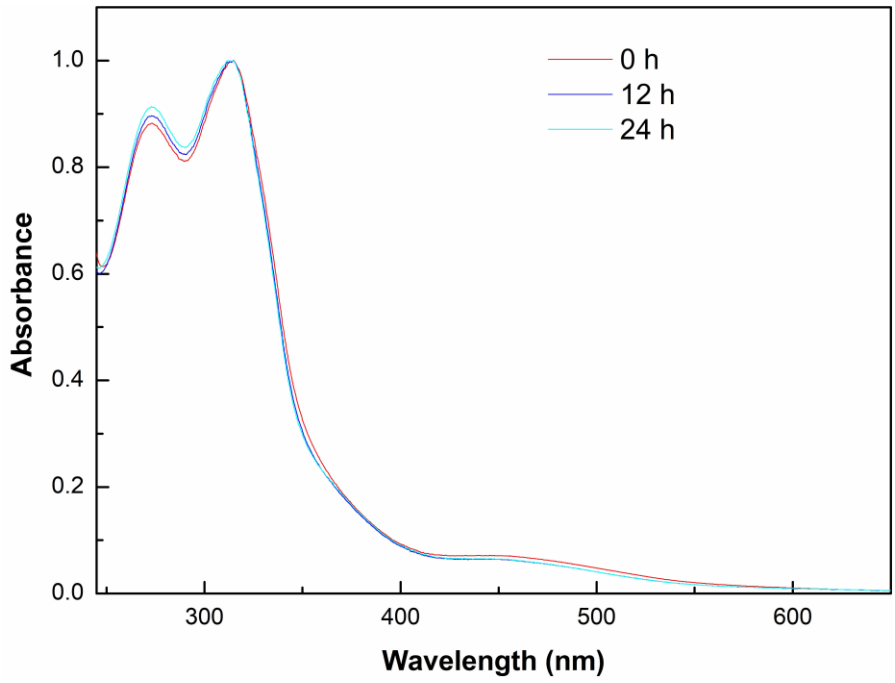

Figure S18. UV-Vis spectra of a freshly prepared solution of **5a** in a DMSO:Buffer solution (20:80) were recorded every 3 h up to 24 h and are shown in **A**. To facilitate visualization, a selection of those obtained at t = 0, 12, and 24 h is presented in **B**.

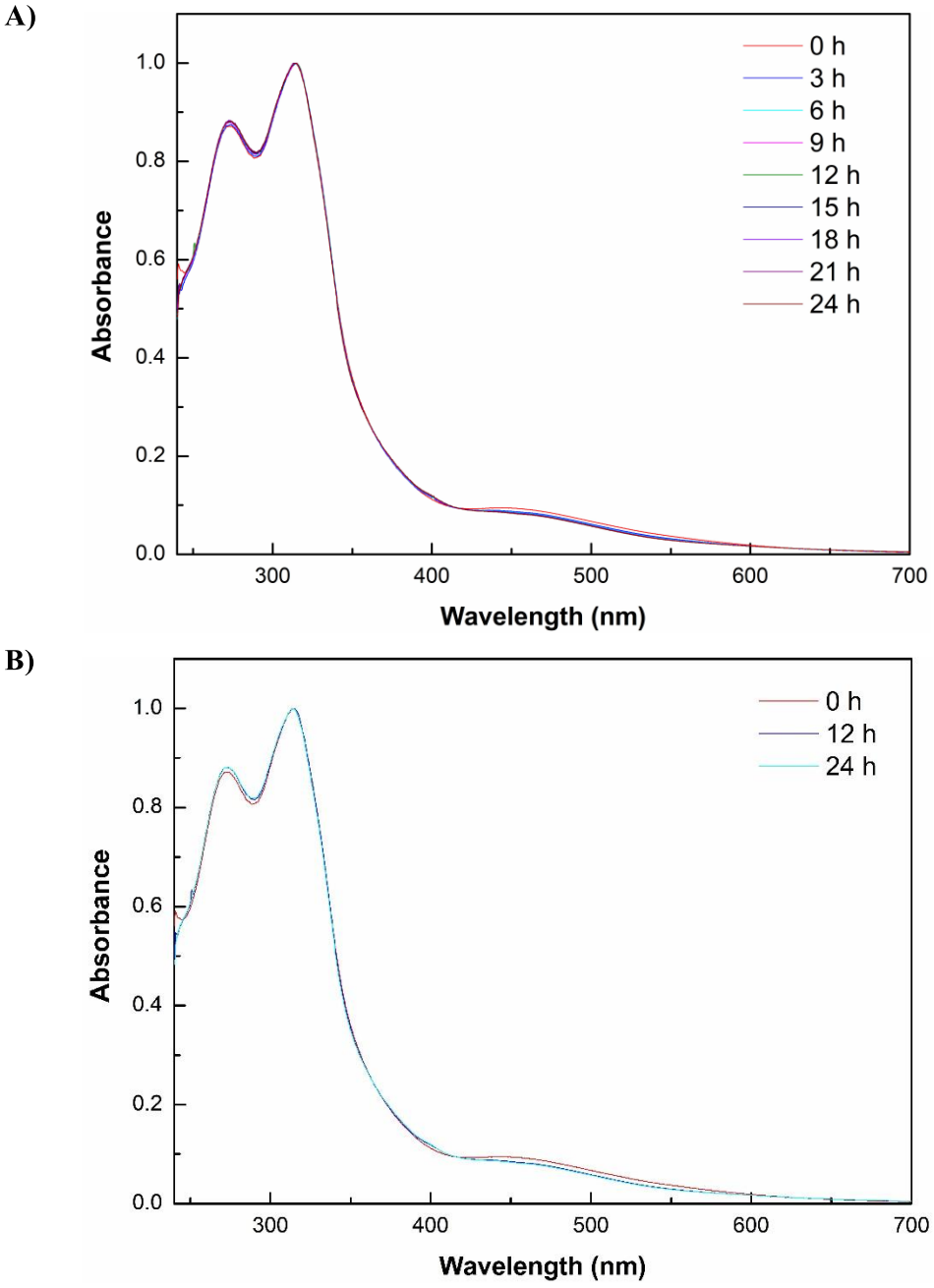

Figure S19. UV-Vis spectra of a freshly prepared solution of **6a** in a DMSO:Buffer solution (20:80) were recorded every 3 h up to 24 h and are shown in **A**. To facilitate visualization, a selection of those obtained at t = 0, 12, and 24 h is presented in **B**.

A)

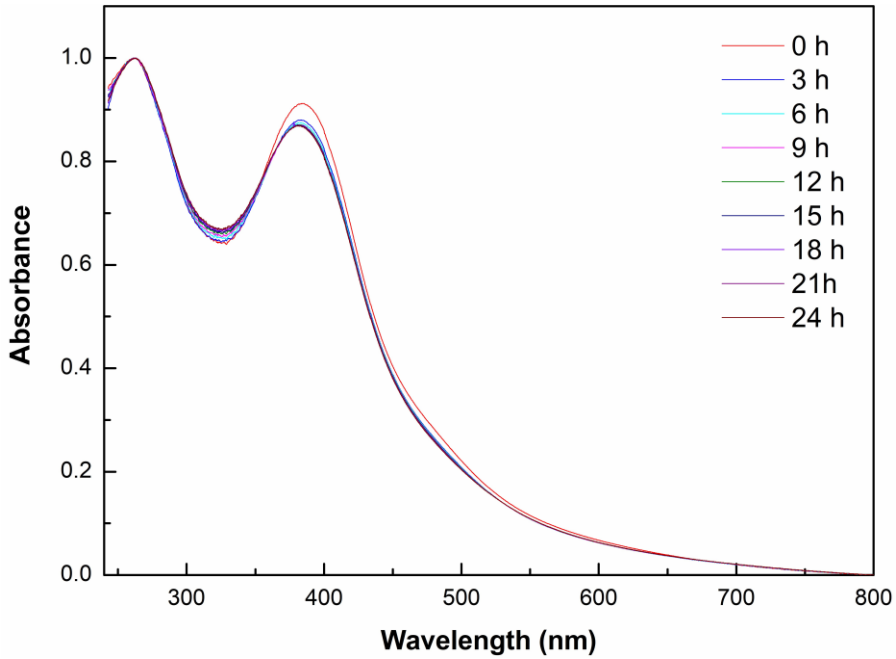

B)

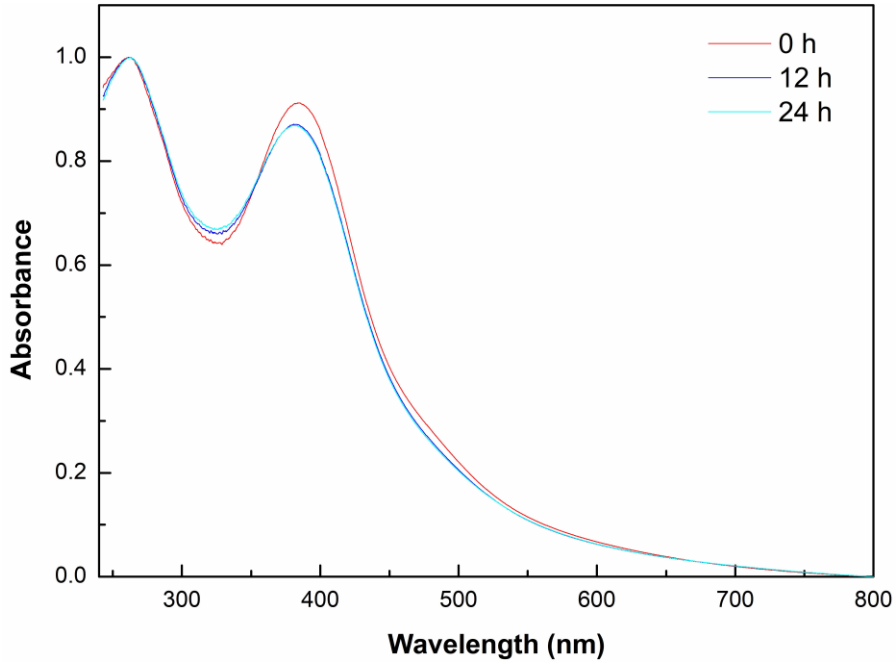

Figure S20. UV-Vis spectra of a freshly prepared solution of **7a** in a DMSO:Buffer solution (20:80) were recorded every 3 h up to 24 h and are shown in **A**. To facilitate visualization, a selection of those obtained at t = 0, 12, and 24 h is presented in **B**.

A)

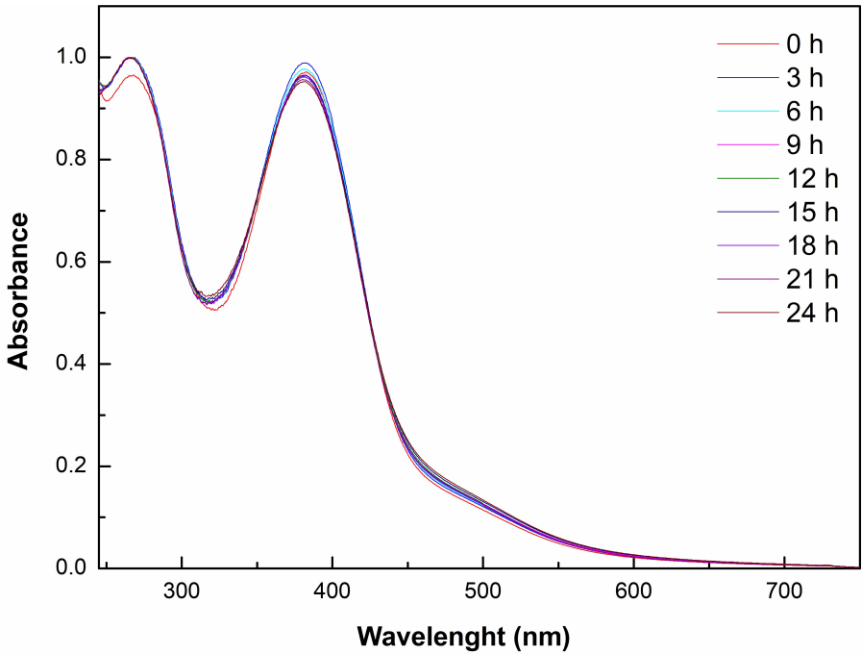

B)

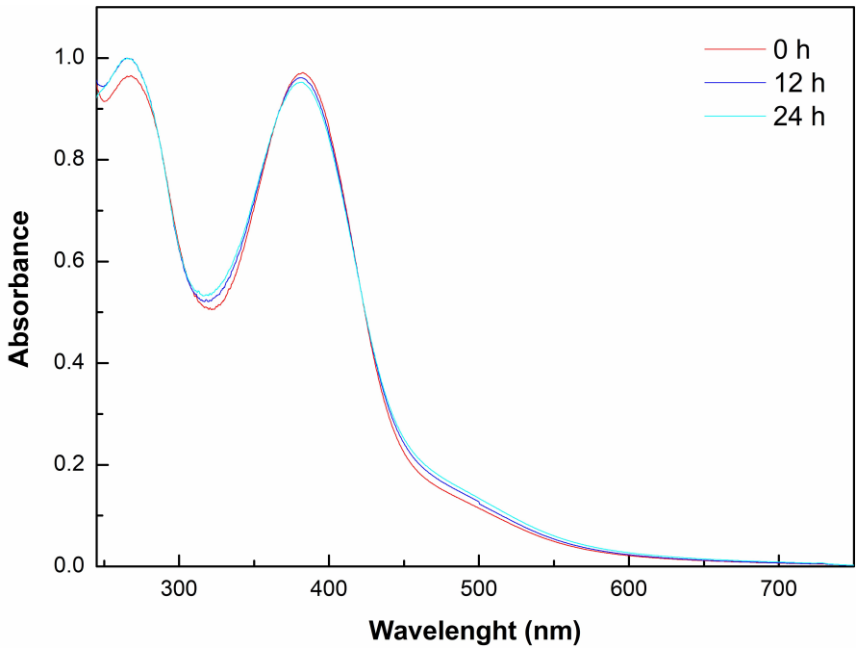

Figure S21. UV-Vis spectra of a freshly prepared solution of **4b** in a DMSO:Buffer solution (20:80) were recorded every 3 h up to 24 h and are shown in **A**. To facilitate visualization, a selection of those obtained at t = 0, 12, and 24 h is presented in **B**.

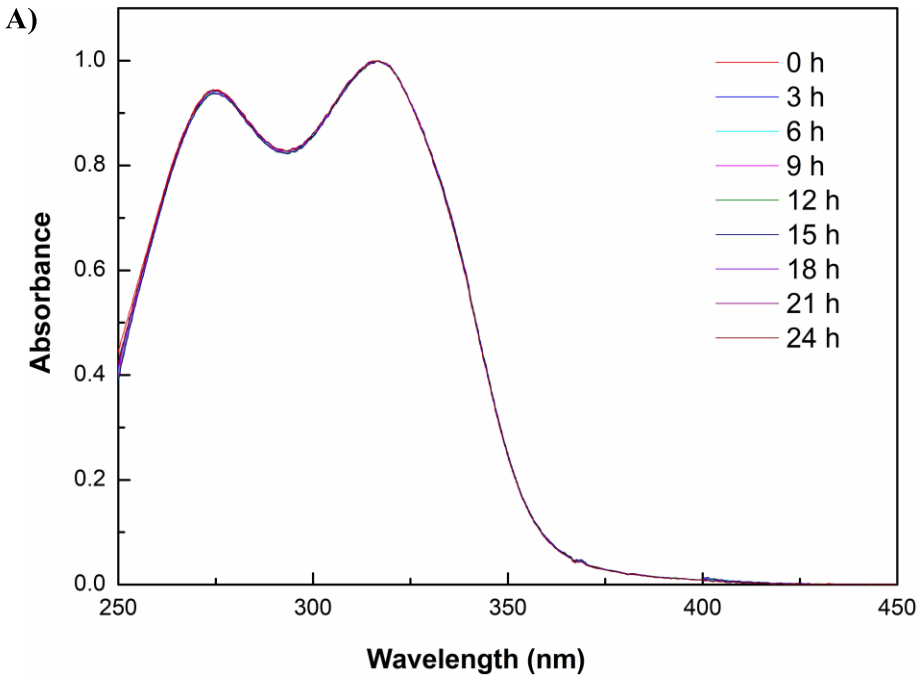

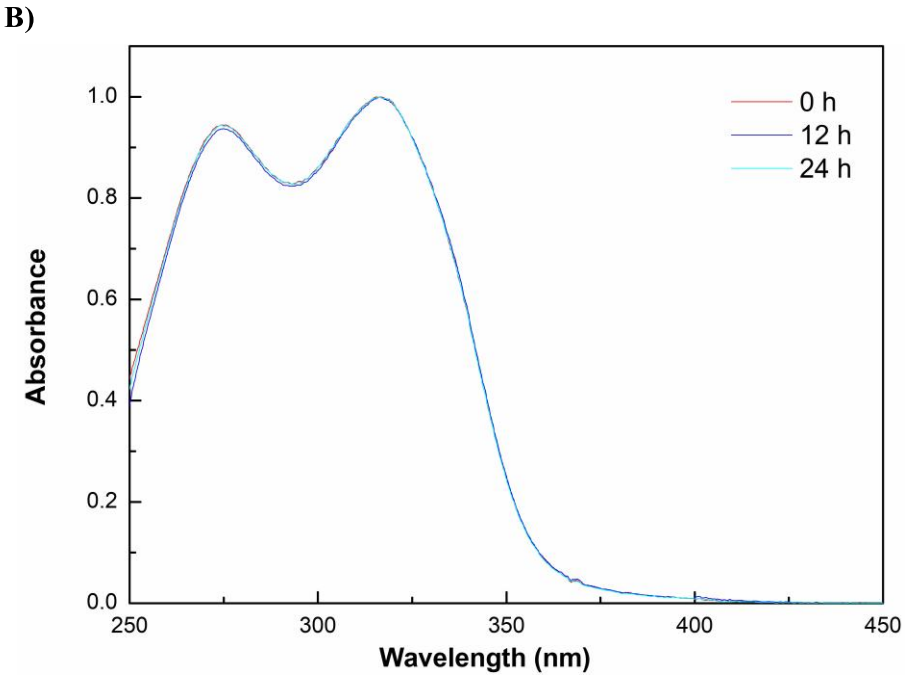

Figure S22. UV-Vis spectra of a freshly prepared solution of **5b** in a DMSO:Buffer solution (20:80) were recorded every 3 h up to 24 h and are shown in **A**. To facilitate visualization, a selection of those obtained at t = 0, 12, and 24 h is presented in **B**.

A)

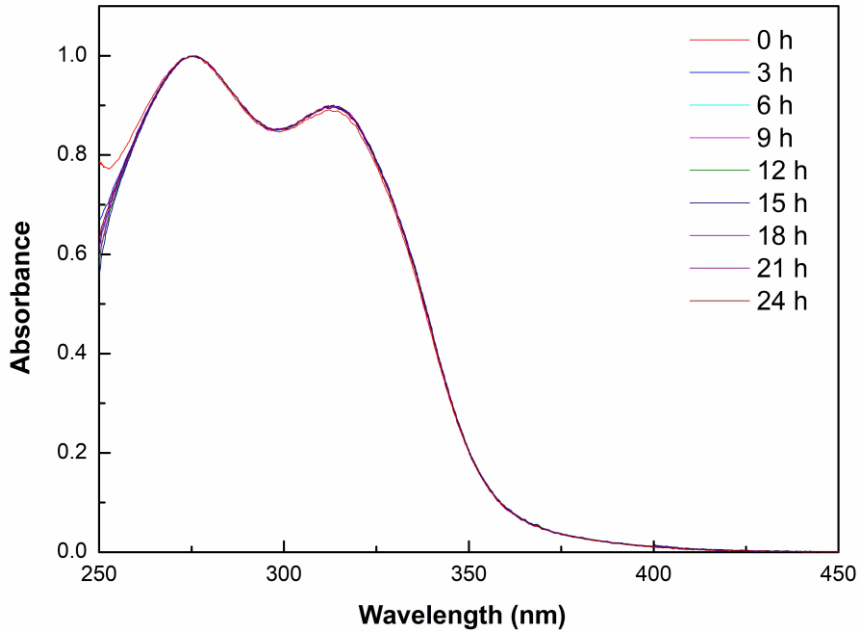

B)

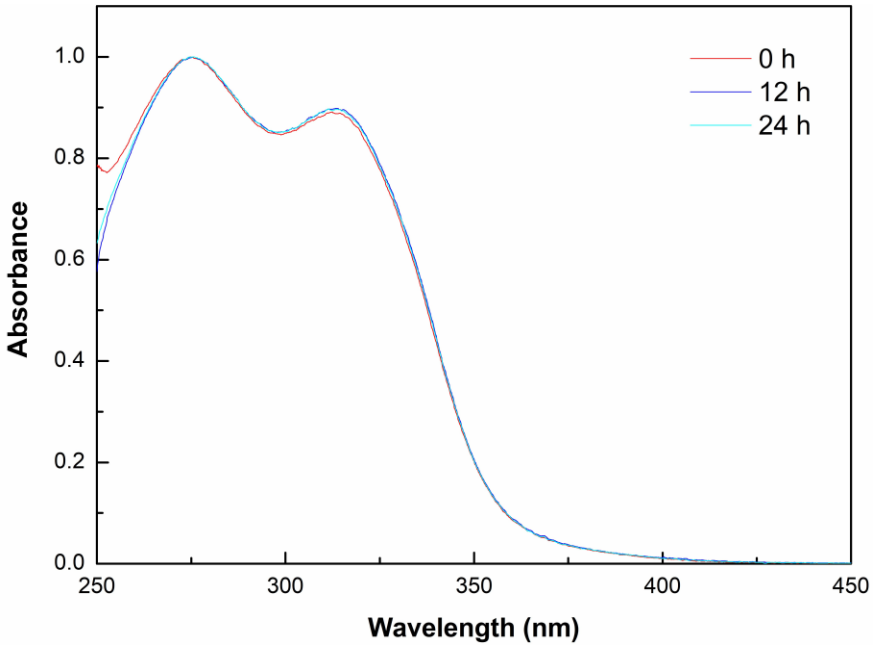

Figure S23. UV-Vis spectra of a freshly prepared solution of **6b** in a DMSO:Buffer solution (20:80) were recorded every 3 h up to 24 h and are shown in **A**. To facilitate visualization, a selection of those obtained at t = 0, 12, and 24 h is presented in **B**.

A)

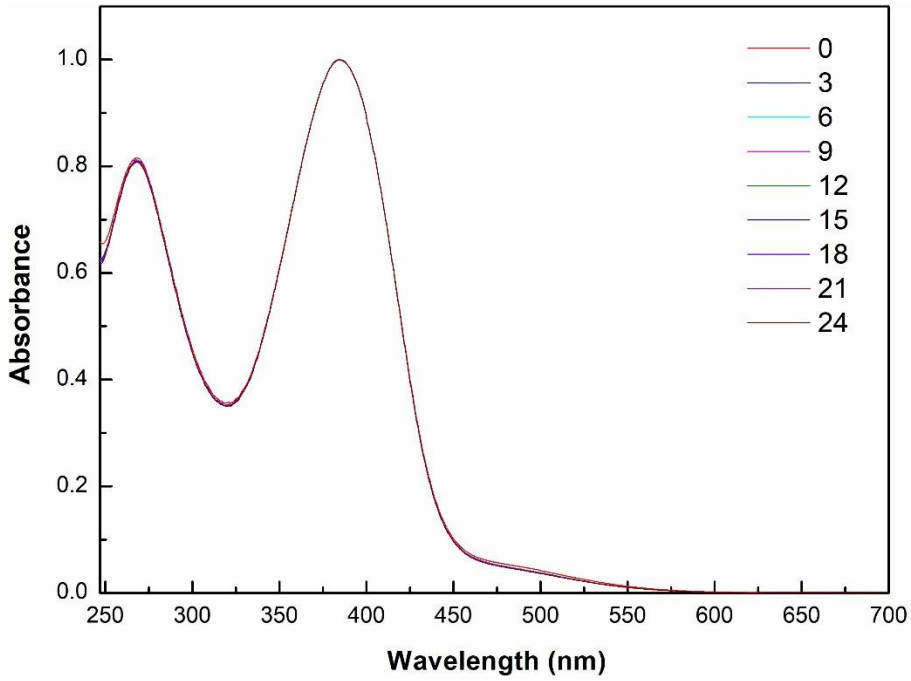

B)

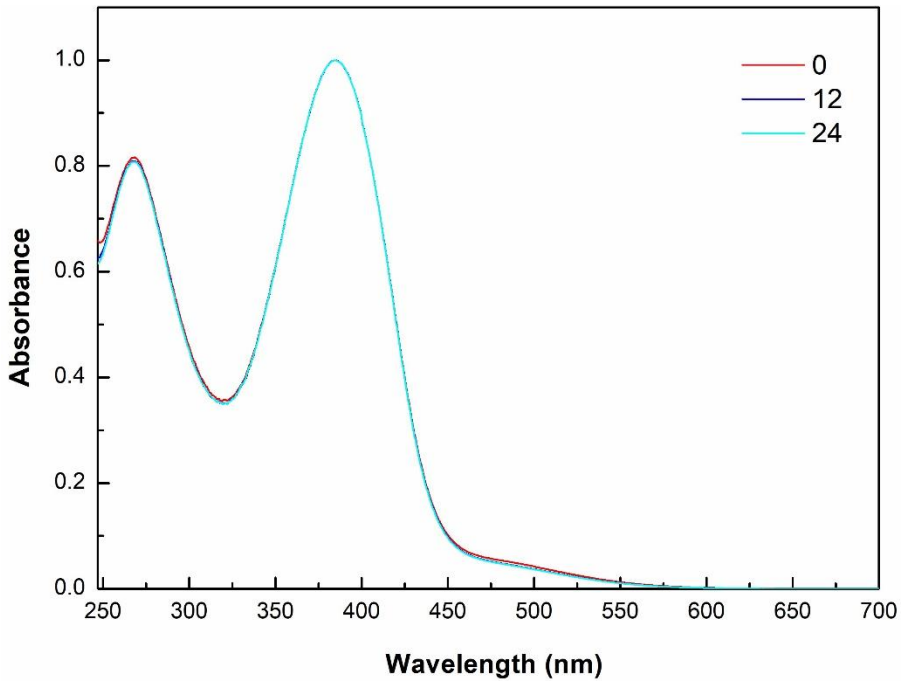

Figure S24. UV-Vis spectra of a freshly prepared solution of **7b** in a DMSO:Buffer solution (20:80) were recorded every 3 h up to 24 h and are shown in **A**. To facilitate visualization, a selection of those obtained at t = 0, 12, and 24 h is presented in **B**.

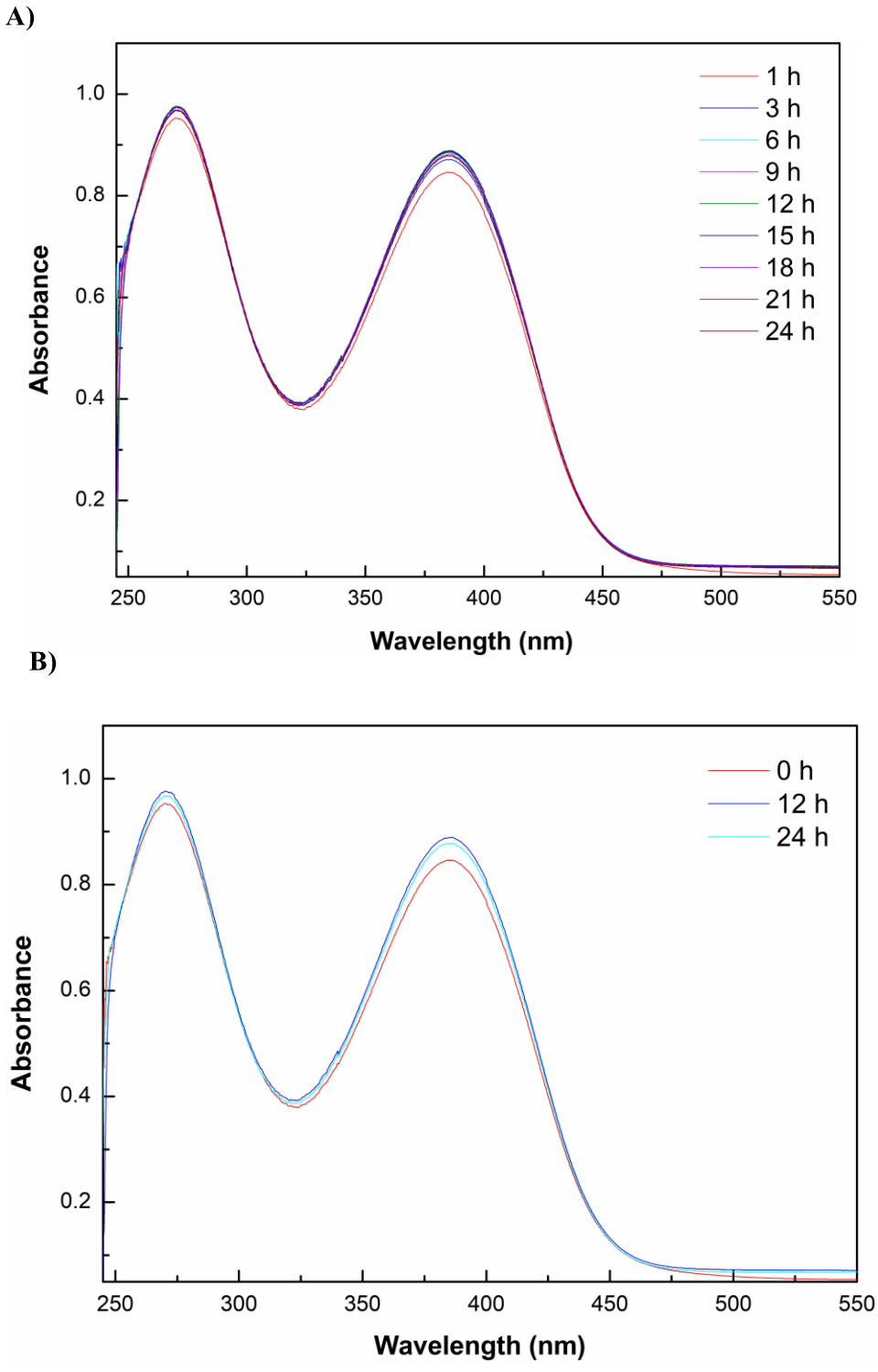

Figure S25. [1]H-NMR spectrum (300 MHz) of compound **4a** in DMSO-*d*$_6$.

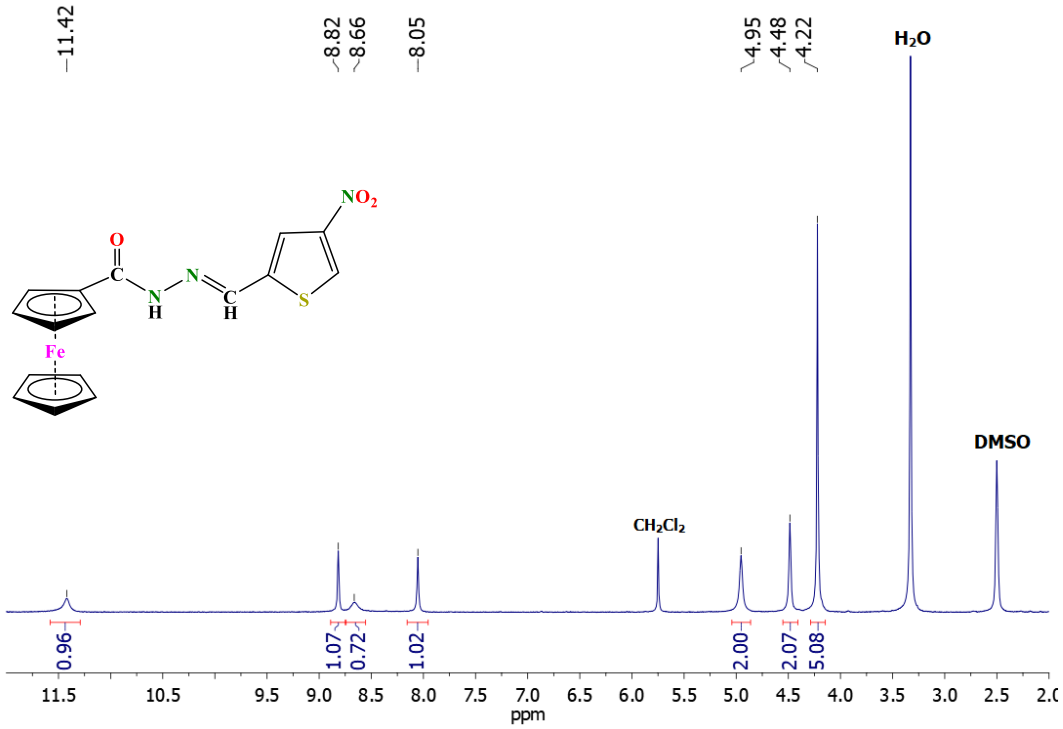

Figure S26. [1]H-NMR spectrum (300 MHz) of compound **5a** in DMSO-*d*$_6$.

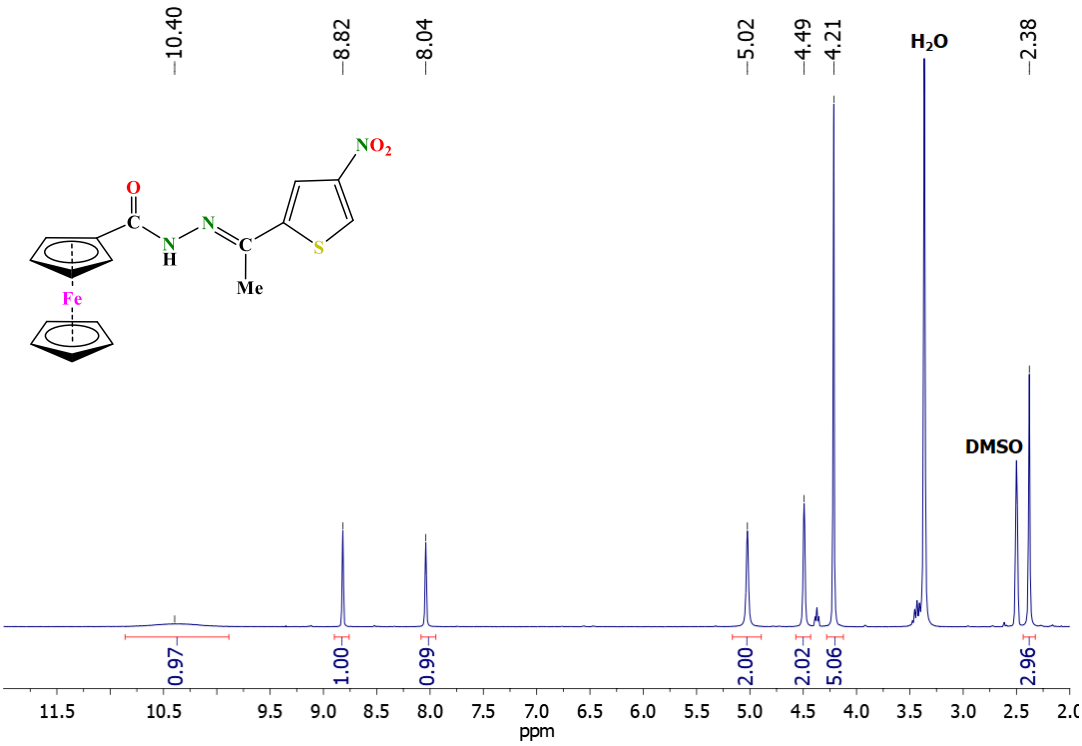

Figure S27. [1]H-NMR spectrum (300 MHz) of compound **6a** in DMSO-d_6.

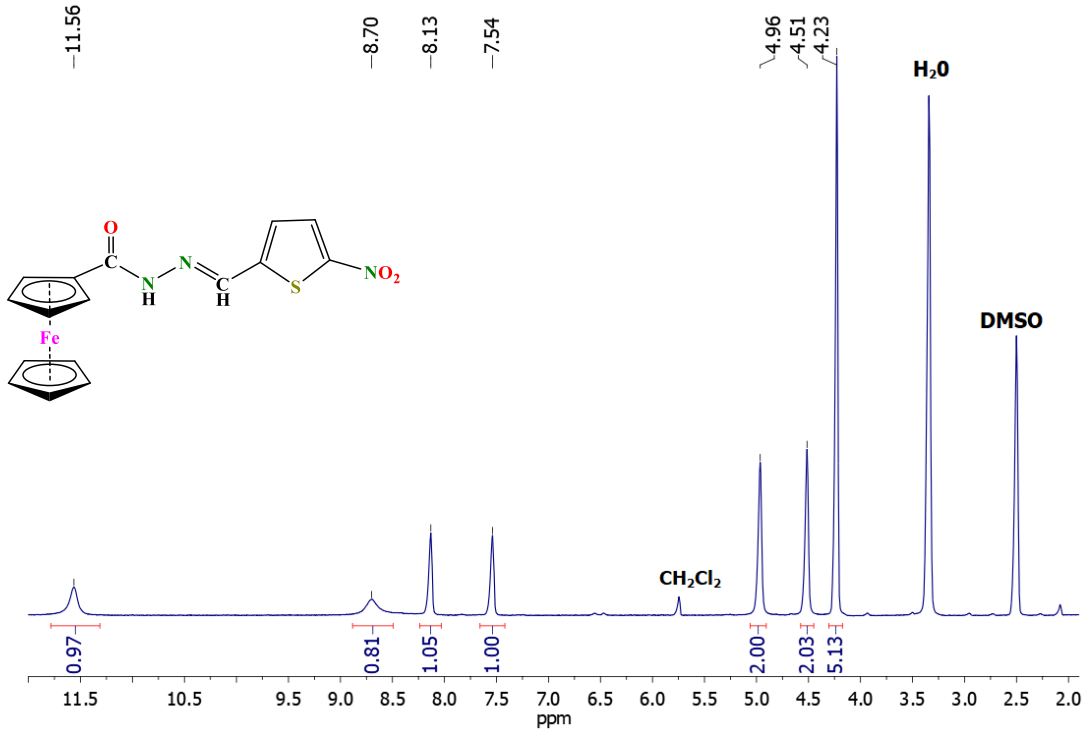

Figure S28. [1]H-NMR spectrum (300 MHz) of compound **7a** in DMSO-d_6.

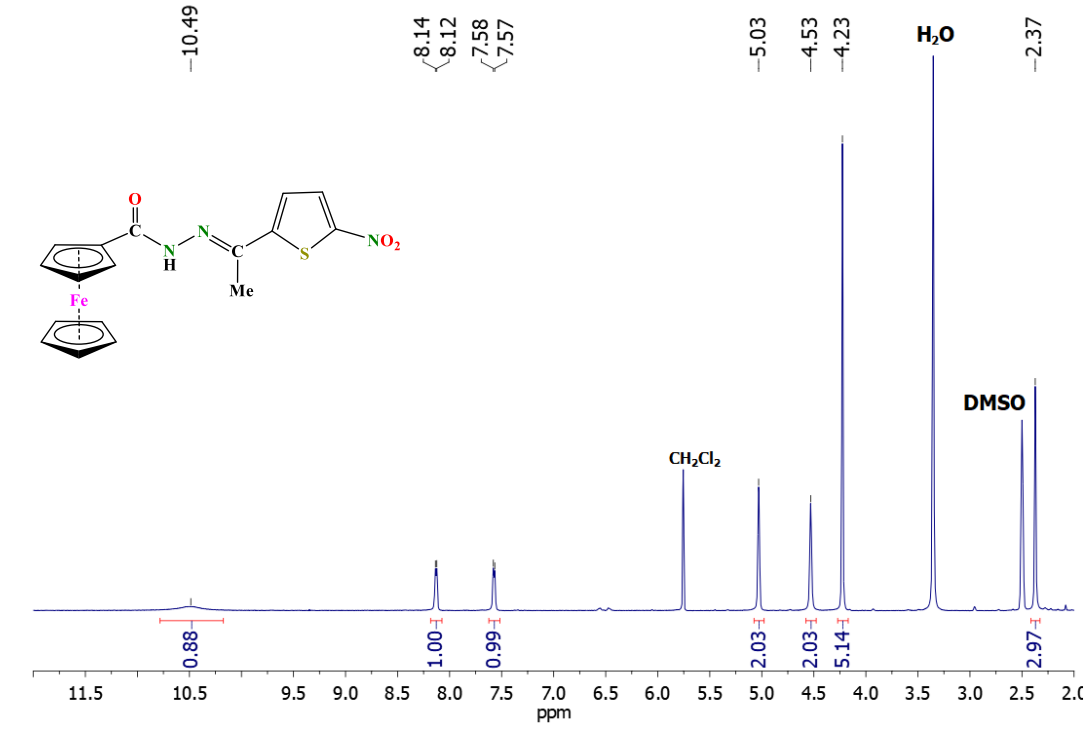

Figure S29. [1]H-NMR spectrum (300 MHz) of compound **4b** in DMSO-d_6.

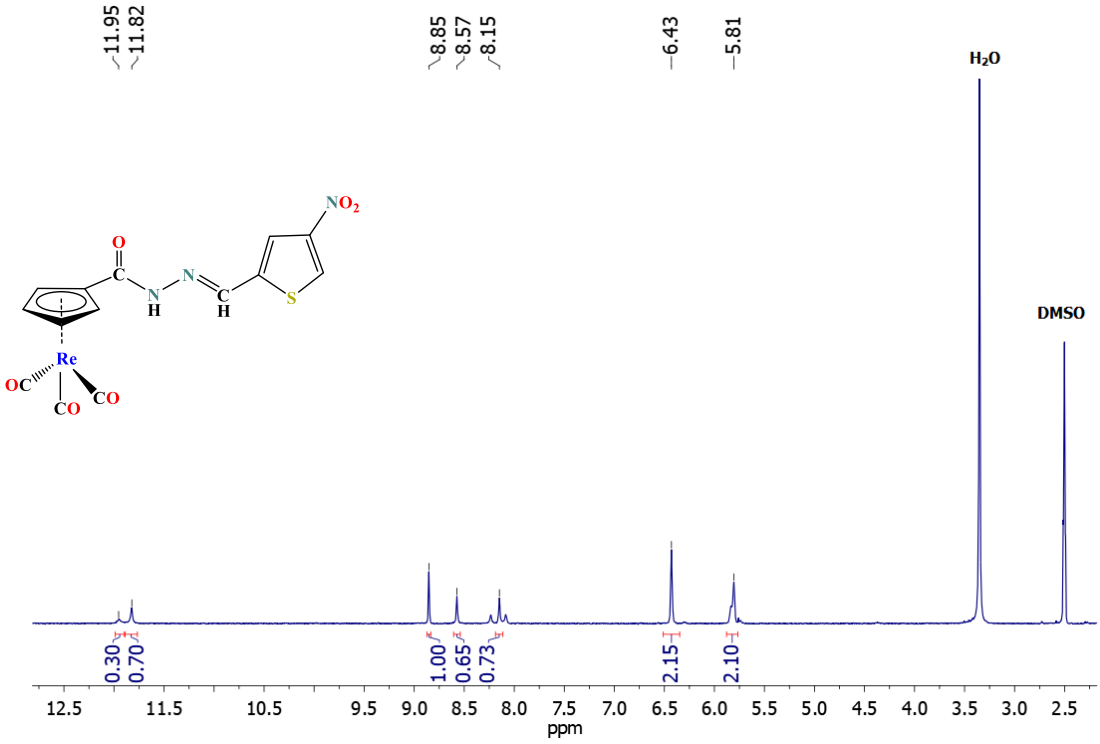

Figure S30. [1]H-NMR spectrum (300 MHz) of compound **5b** in DMSO-d_6.

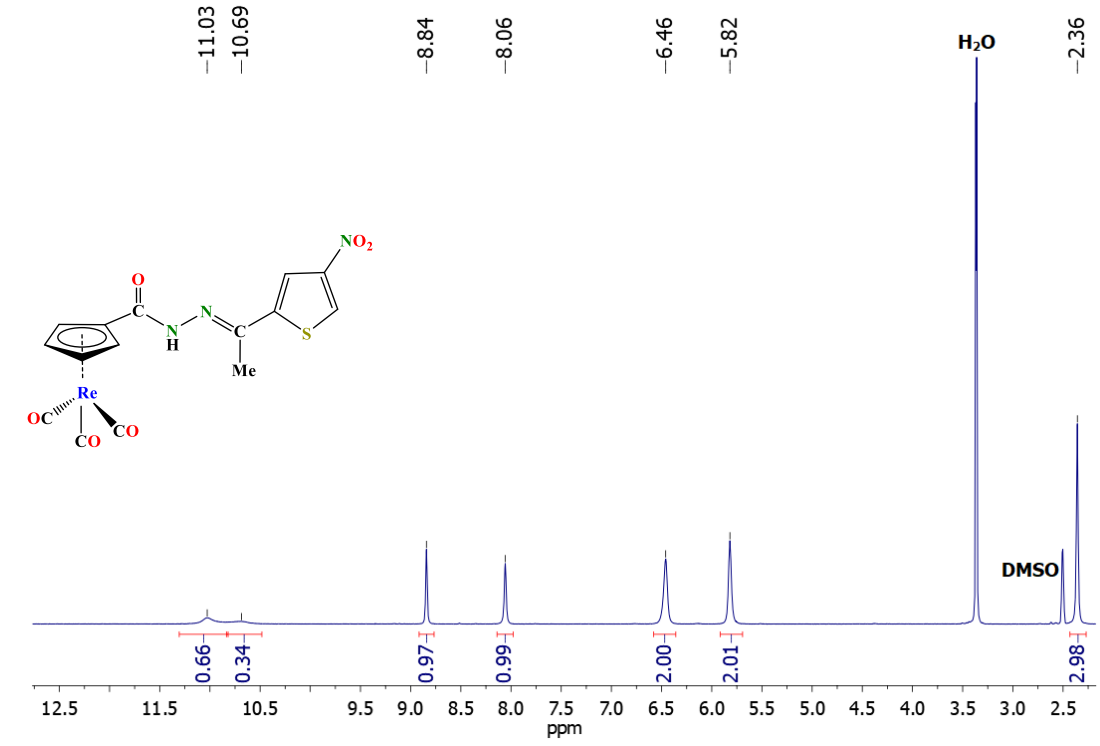

Figure S31. ^{1}H-NMR spectrum (300 MHz) of compound **6b** in DMSO-d_6.

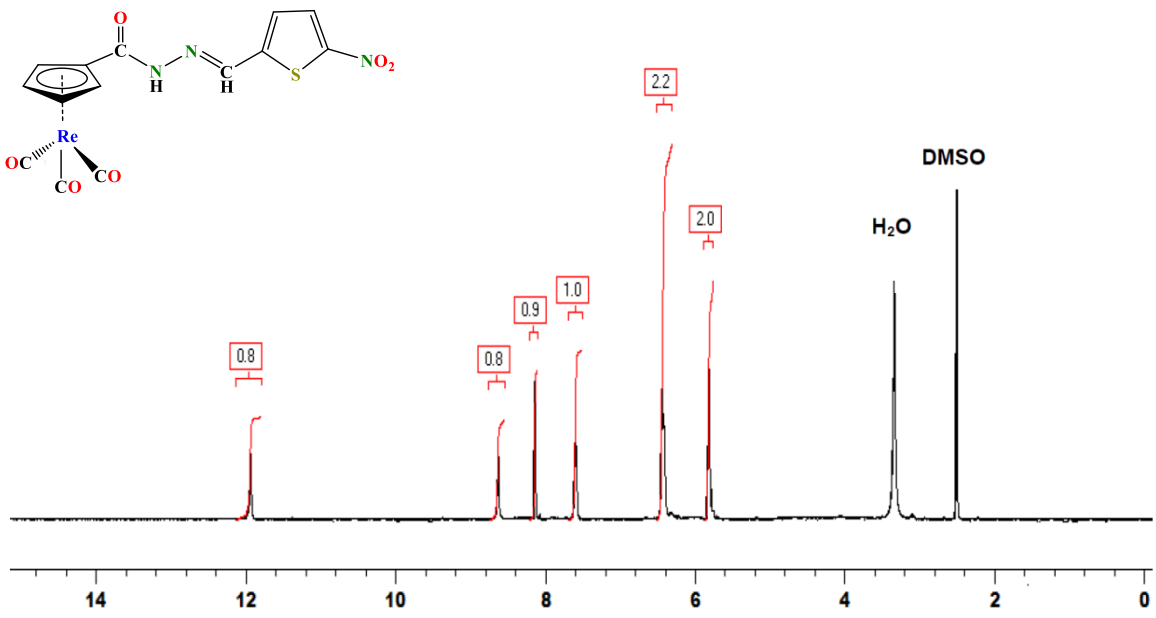

Figure S32. ^{1}H-NMR spectrum (300 MHz) of compound **7b** in DMSO-d_6.

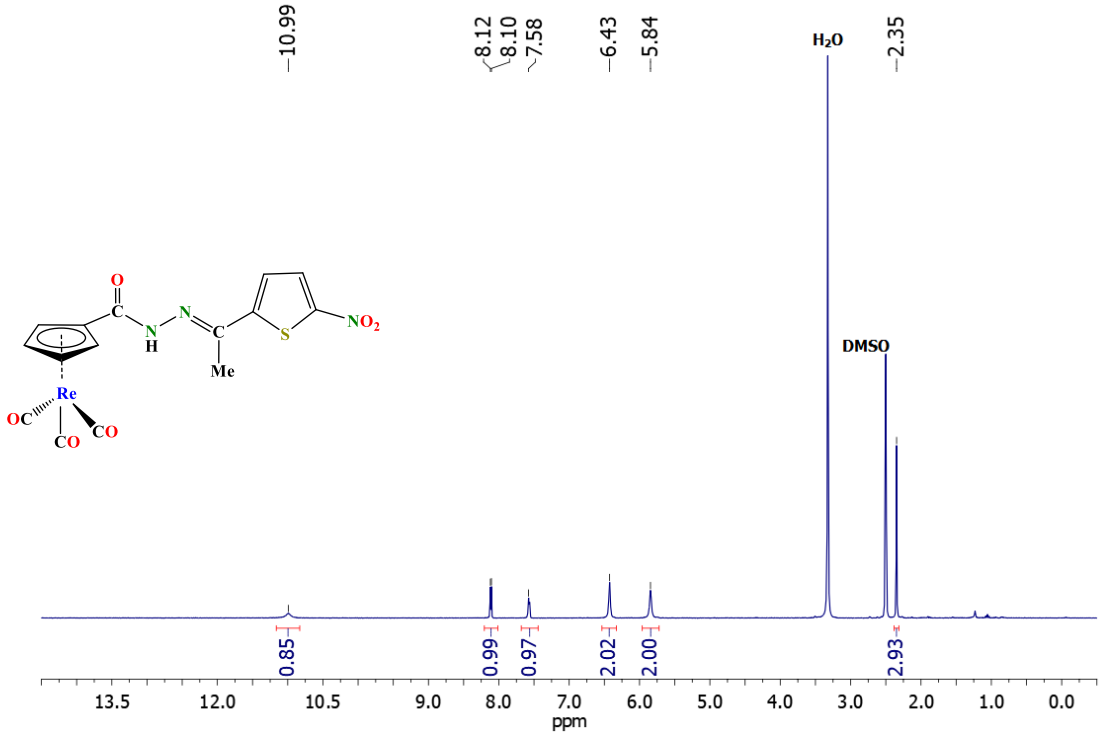

Figure S33. [1]H NMR spectrum (400 MHz) of compound **4c** in DMSO-d_6.

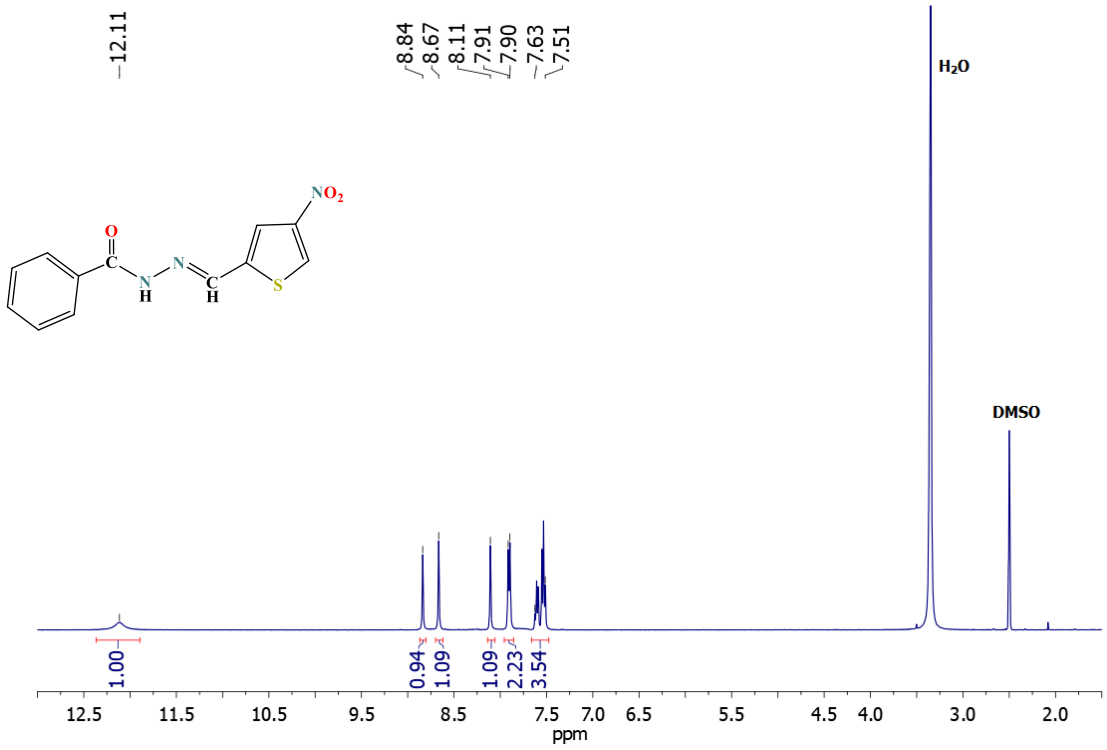

Figure S34. [1]H NMR spectrum (400 MHz) of compound **5c** in DMSO-d_6.

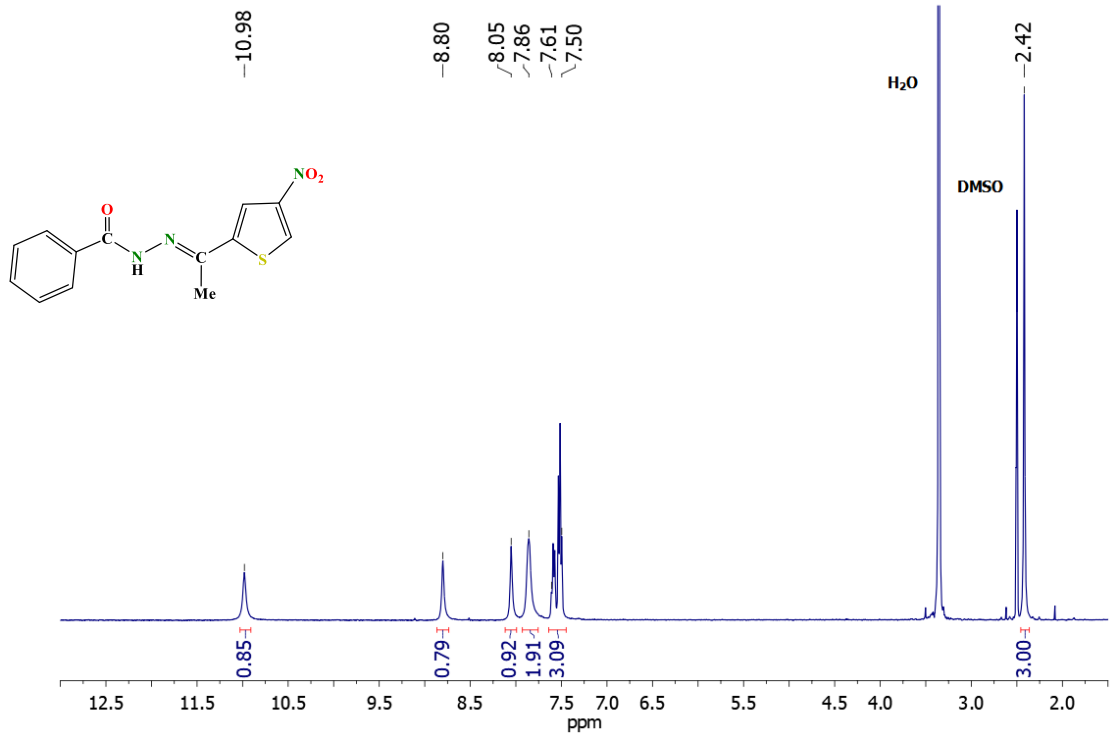

Figure S35. ^{1}H NMR spectrum (400 MHz) of compound **6c** in DMSO-d_6. The inserted plot shows an expansion of the region 8.0 – 7.5 ppm.

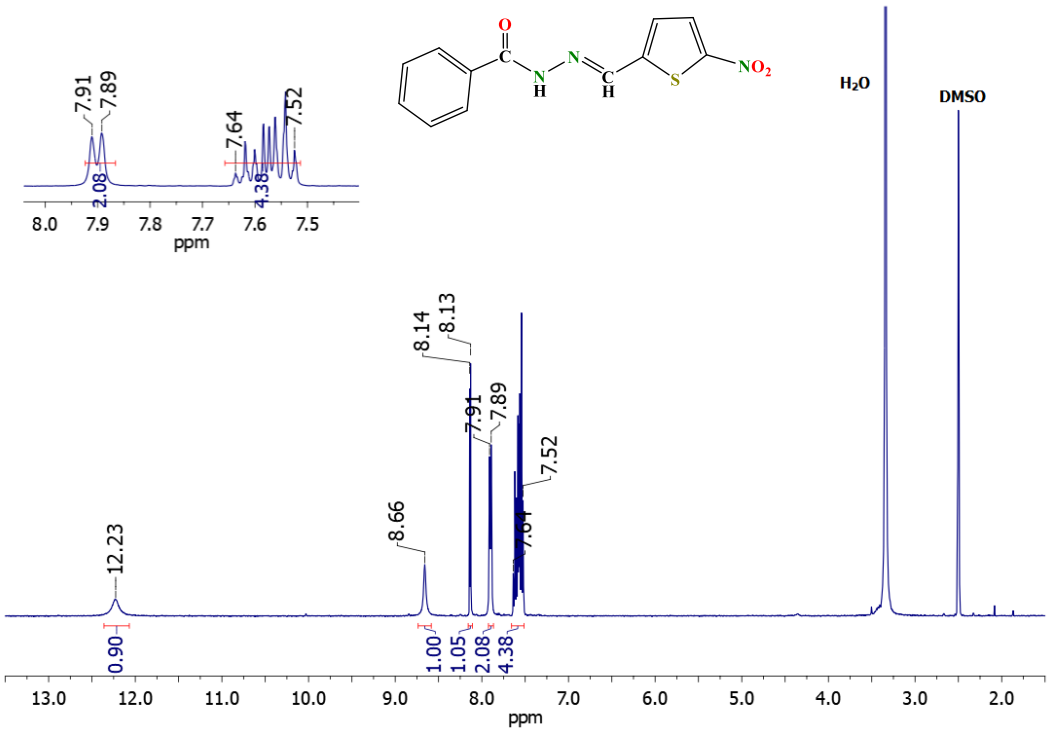

Figure S36. ^{1}H NMR spectrum (400 MHz) of compound **7c** in DMSO-d_6. The inserted plot shows an expansion of the region 8.0 – 7.4 ppm.

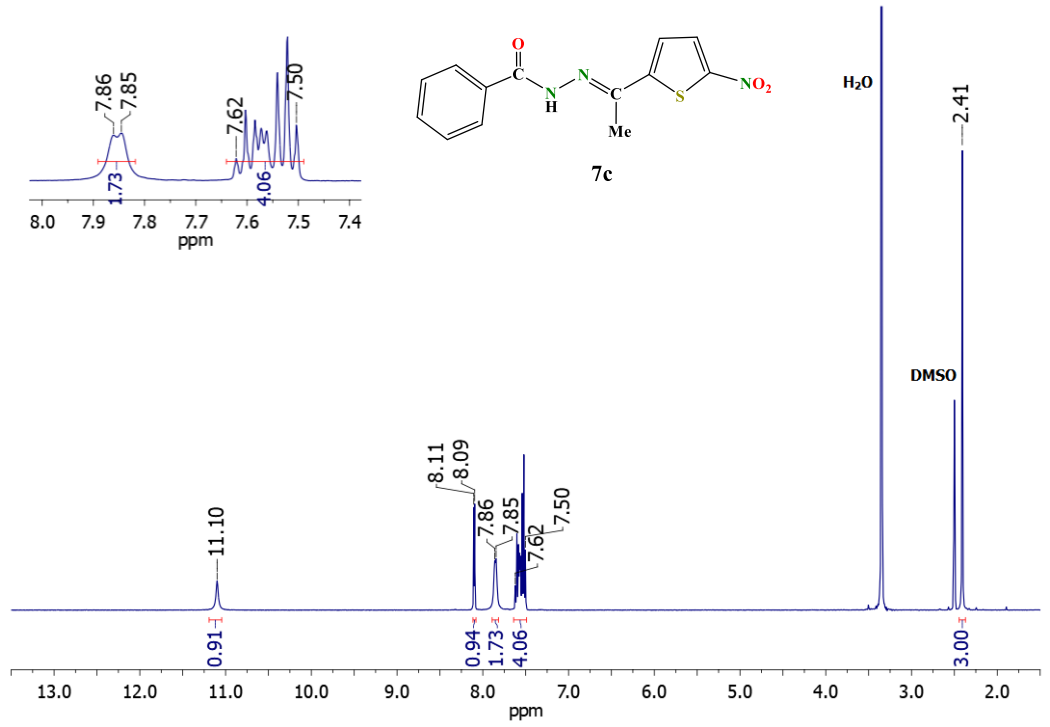

Figure S37. [^{1}H–^{1}H] NOESY spectrum (400 MHz) of compound **4a** in DMSO-d_6.

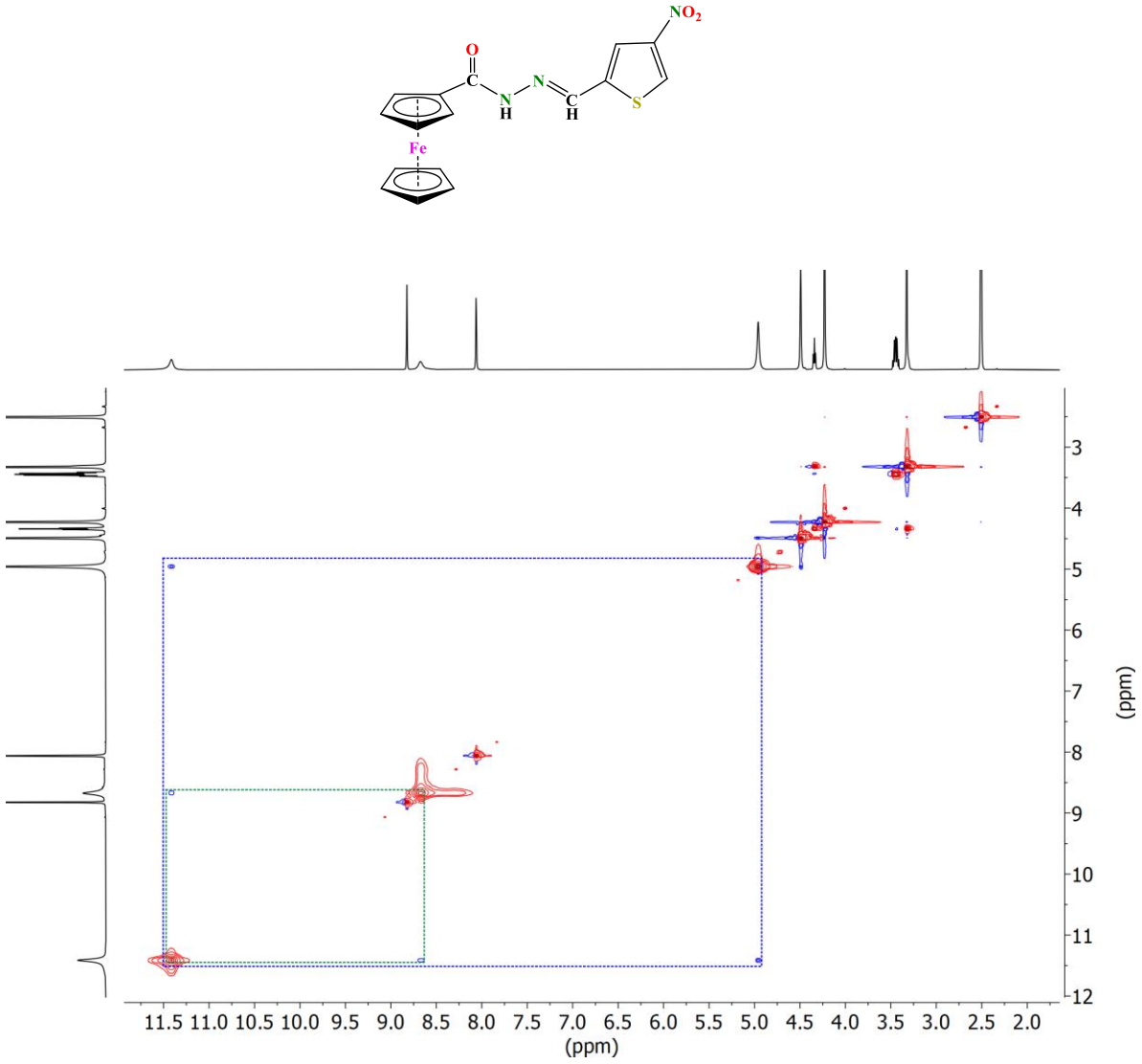

Figure S38. ^{1}H-NMR spectra (400 MHz) of complex **4b** in DMSO-d_6 registered at variable temperatures (300 to 340 K).

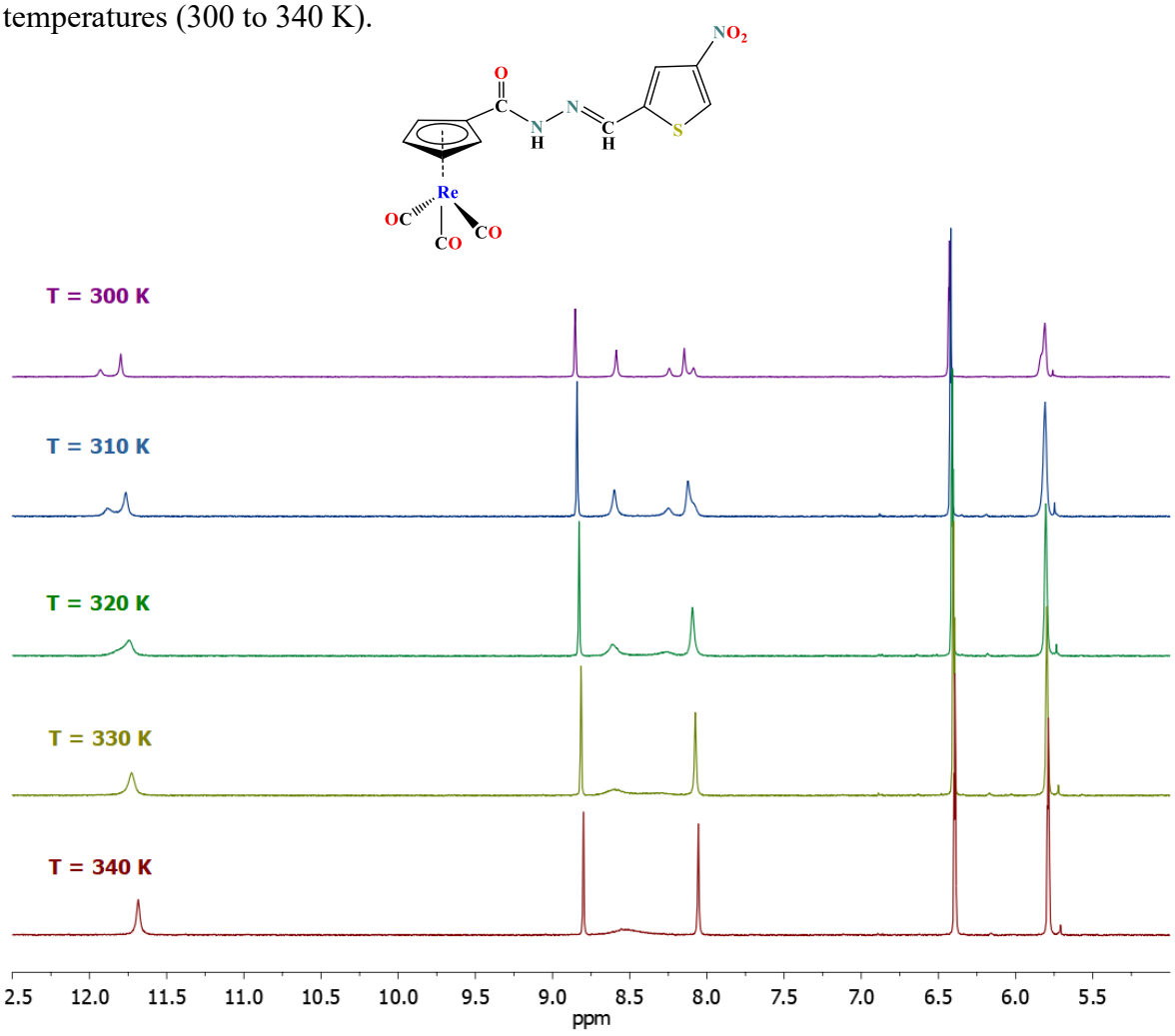

Figure S39. Zoom-in of the NH and aromatic region of the ^{1}H-NMR spectra (400 MHz) of **4b** recorded at different temperatures (300 to 340 K).

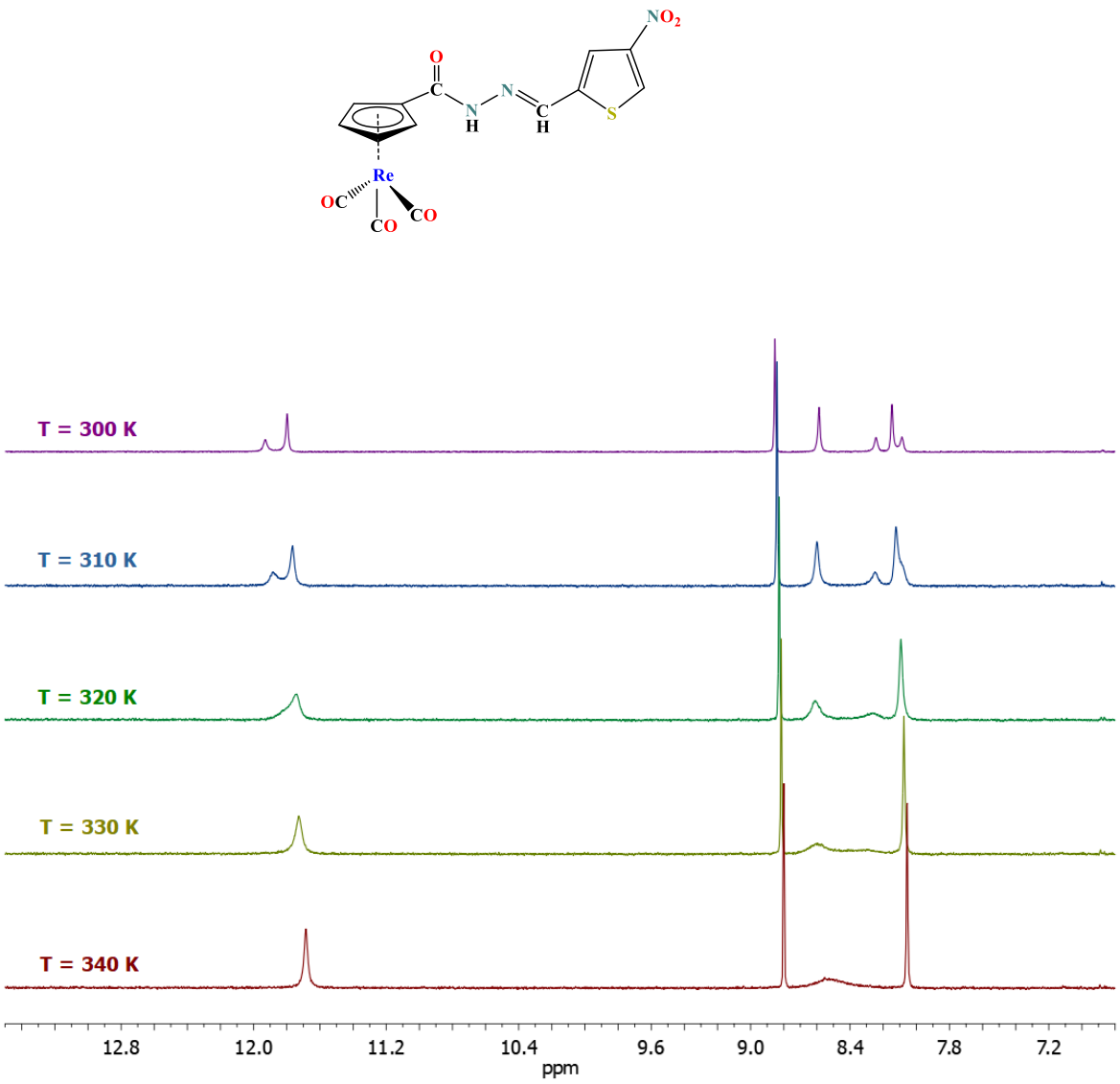

Figure S40. Cyclic voltammograms of **4a** at different scan rates of 0.1 – 2.00 V s^{-1} in DMSO (TBAP 0.1 M, HMDE, Pt, non-aqueous Ag/AgCl).

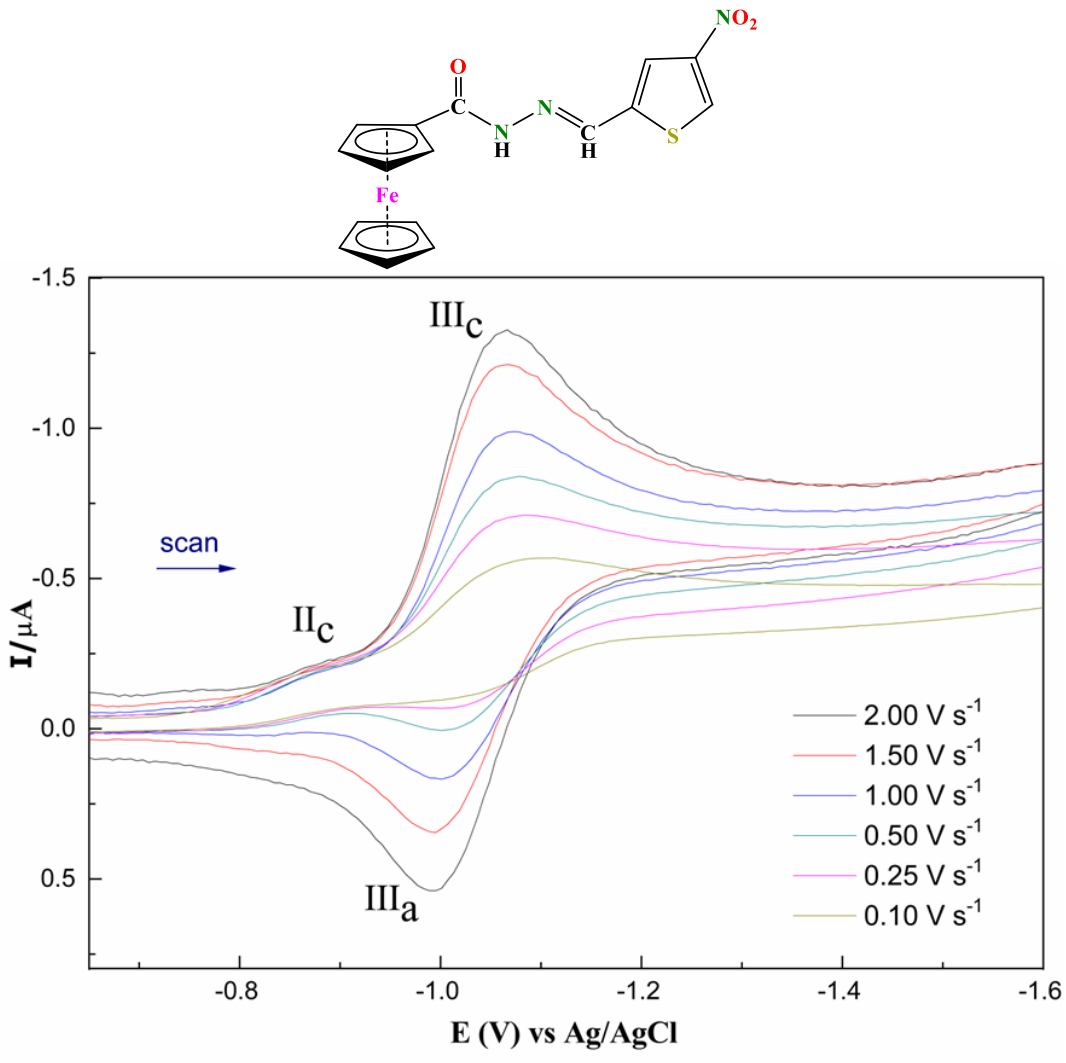

Figure S41. Cyclic voltammograms of **4b** at different scan rates of 0.1 – 2.00 V s^{-1} in DMSO (TBAP 0.1 M, HMDE, Pt, non-aqueous Ag/AgCl).

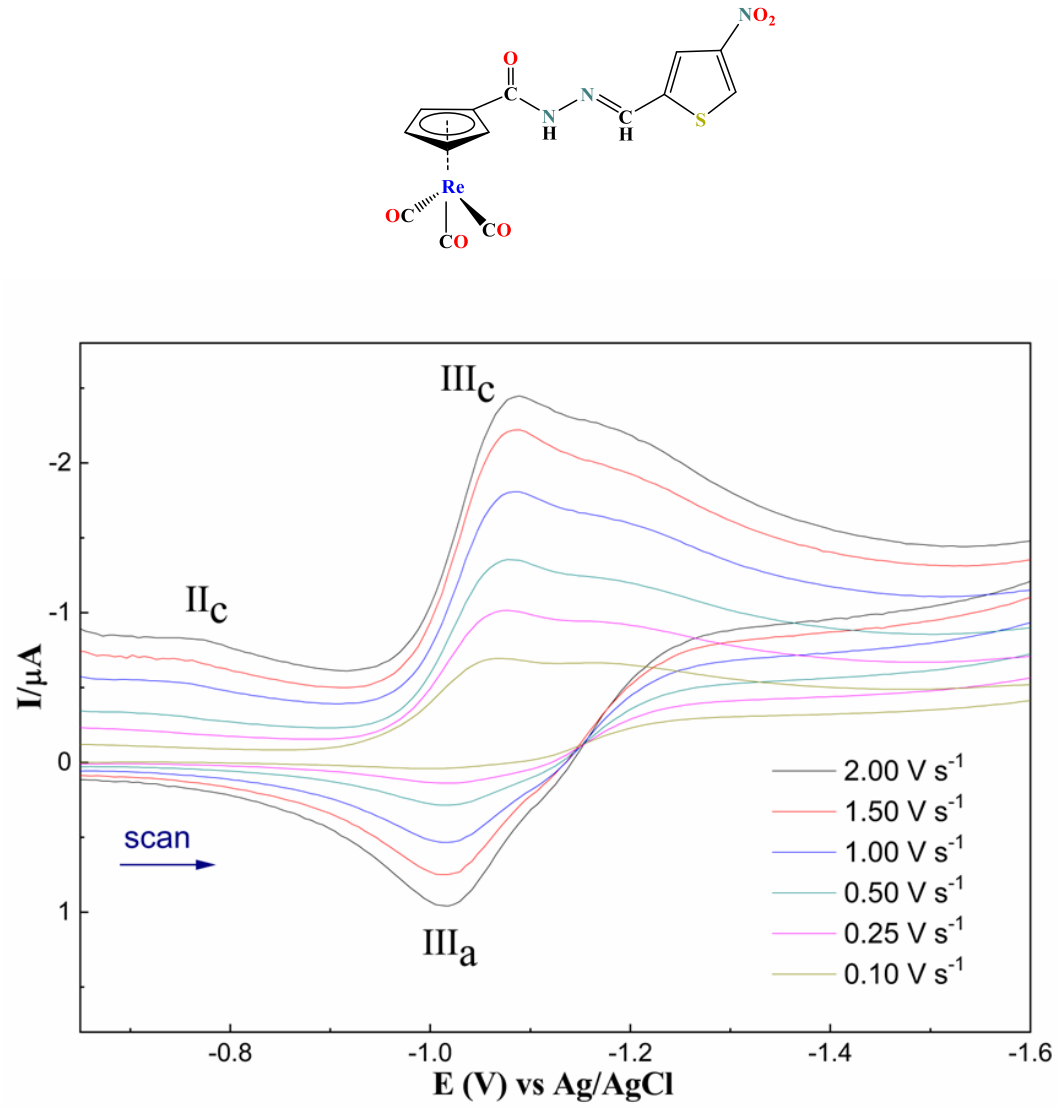

Figure S42. Cyclic voltammograms of **5a** at different scan rates of 0.1 – 2.00 V s^{-1} in DMSO (TBAP 0.1 M, HMDE, Pt, non-aqueous Ag/AgCl).

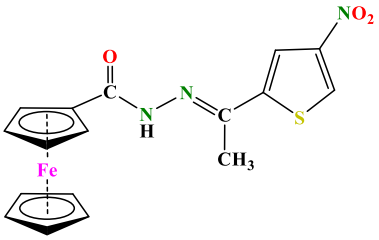

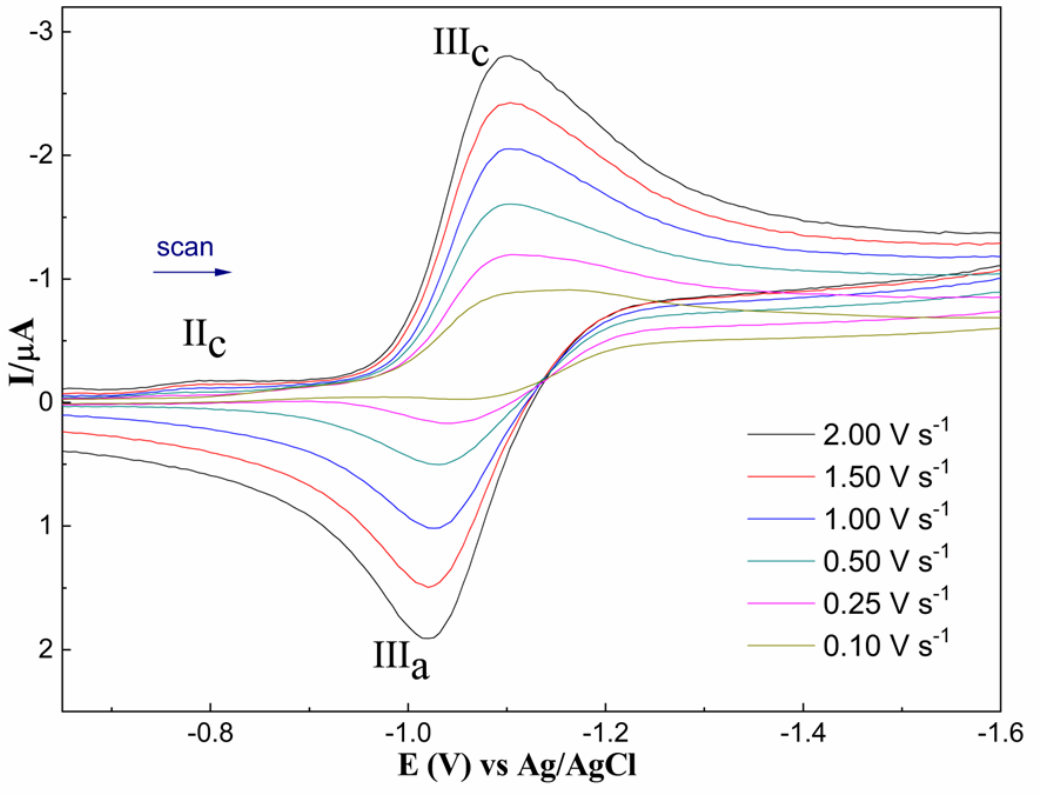

Figure S43. Cyclic voltammograms of **6a** at different scan rates of 0.1 – 2.00 V s^{-1} in DMSO (TBAP 0.1 M, HMDE, Pt, non-aqueous Ag/AgCl).

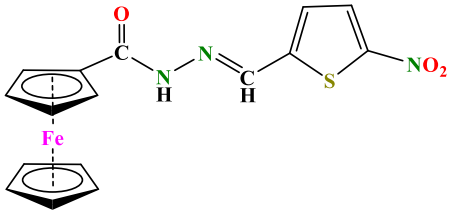

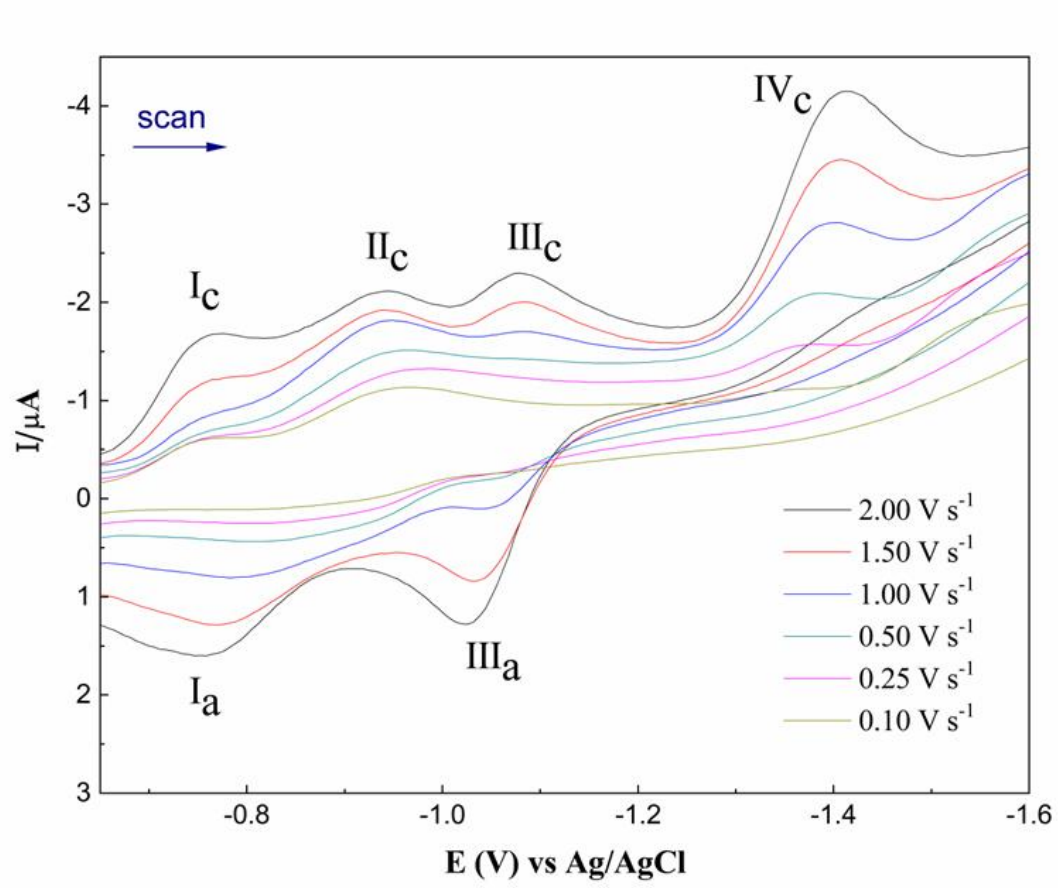

Figure S44. Cyclic voltammograms of **7a** at different scan rates of 0.1 – 2.00 V s^{-1} in DMSO (TBAP 0.1 M, HMDE, Pt, non-aqueous Ag/AgCl).

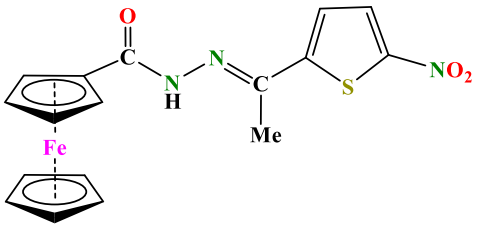

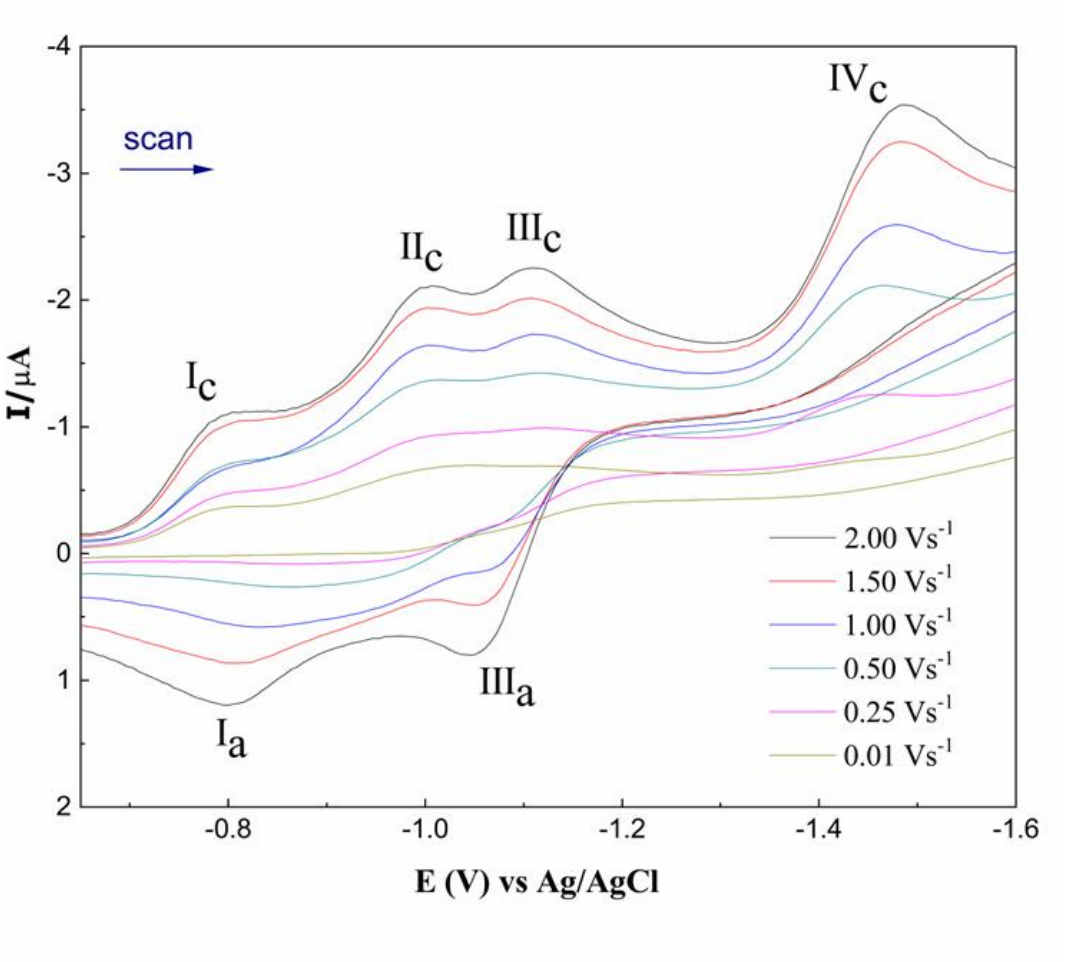

Figure S45. Cyclic voltammograms of **7b** at different scan rates of 0.1 – 2.00 V s^{-1} in DMSO (TBAP 0.1 M, HMDE, Pt, non-aqueous Ag/AgCl).

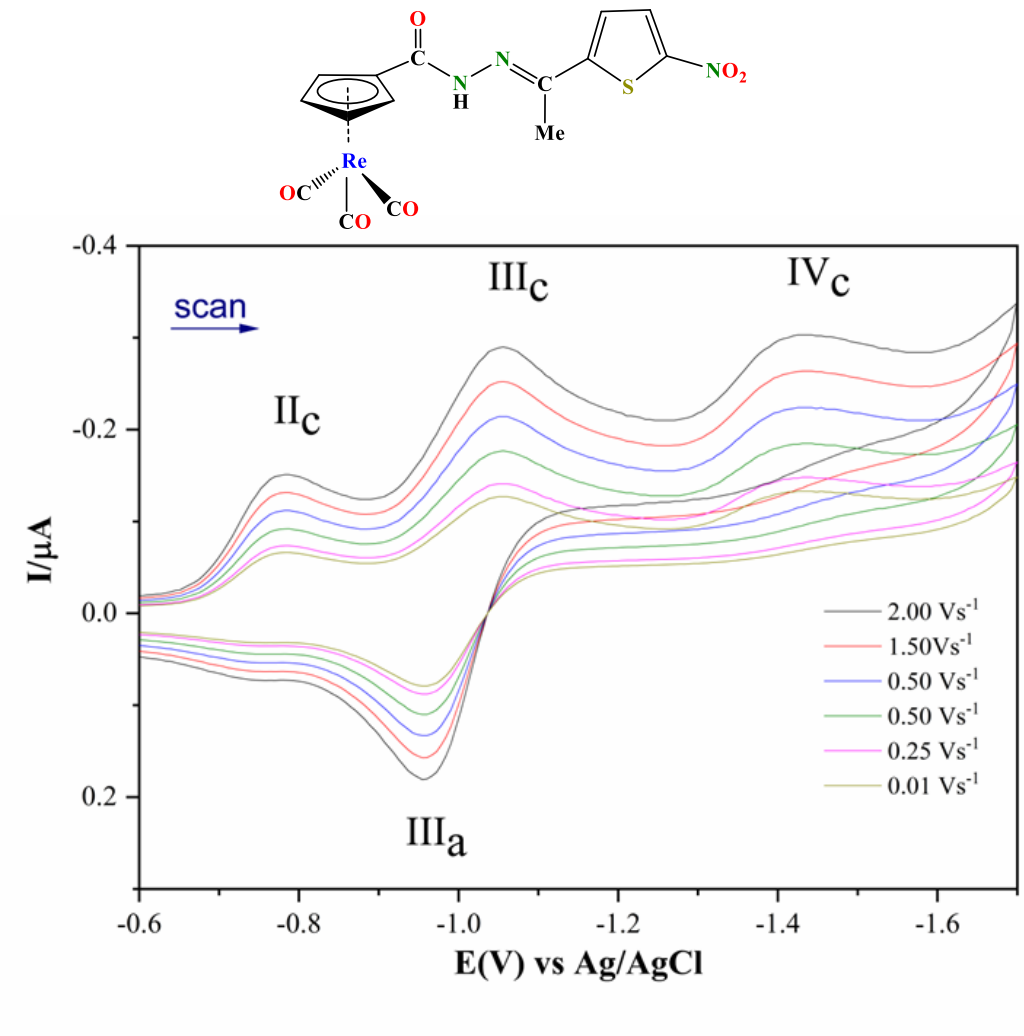

Figure S46. Differential pulse voltammograms of **5b** (**A**) and **6b** (**B**) derivatives. All experiments were performed in DMSO (TBAP 0.1 M, HMDE, Pt, non-aqueous Ag/AgCl).

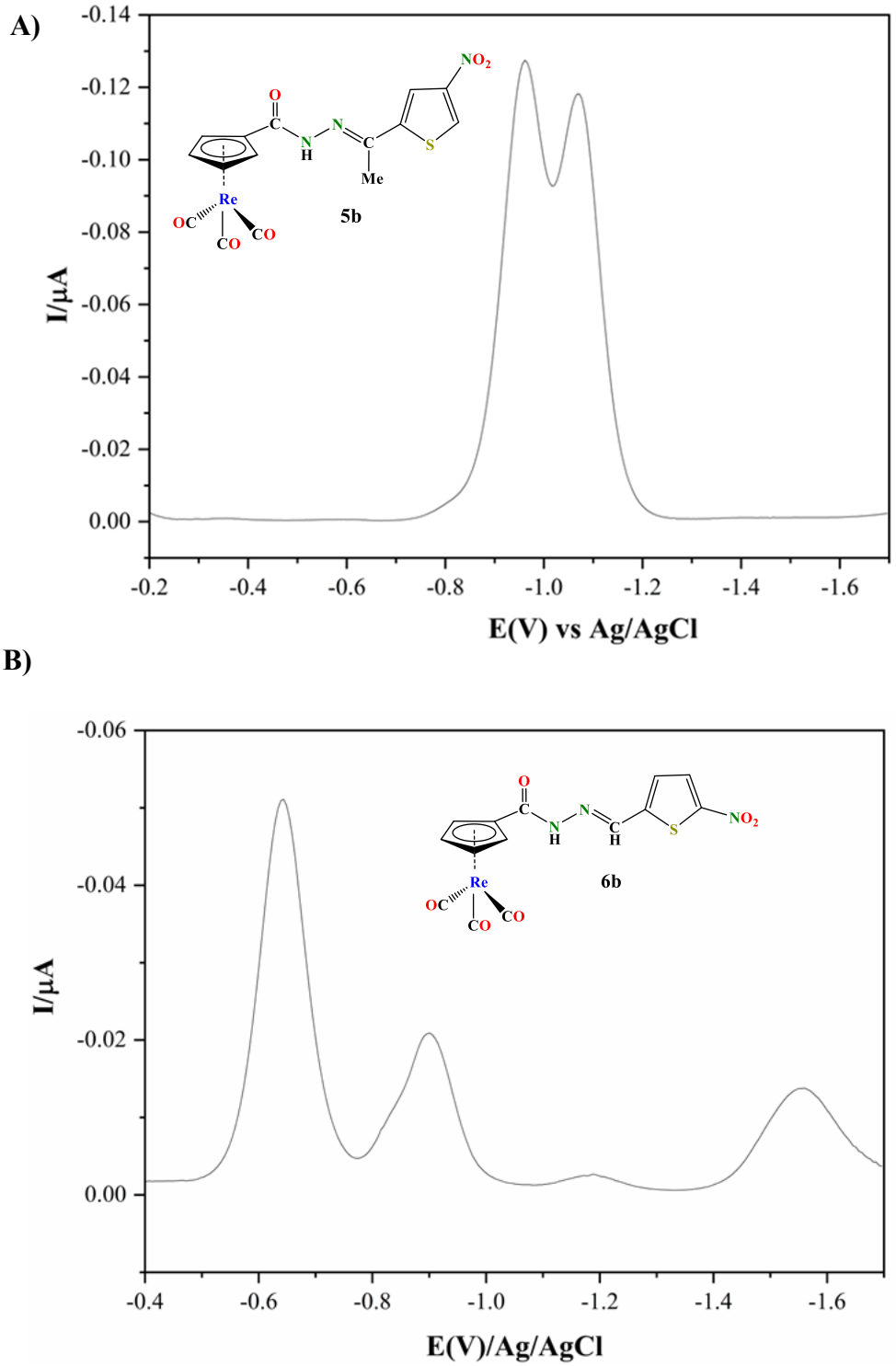

Figure S47. Comparative plot of the SI values obtained for NAH compounds (**4a**, **5a**, **6a**, **6b**, **7a**, and Nfx) in *T. cruzi* (**A**) and *T. brucei* (**B**).

A)

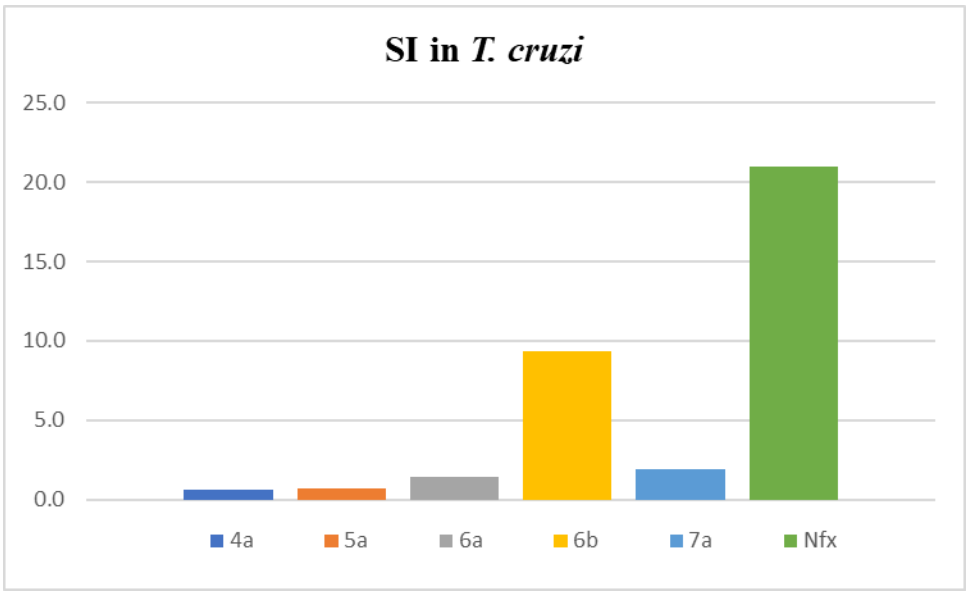

B)

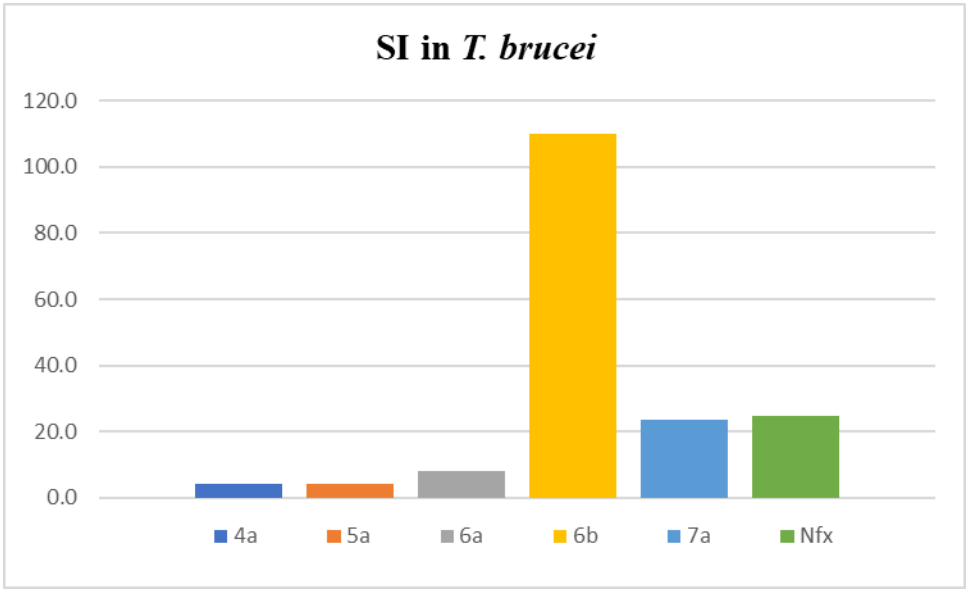

Figure S48. Comparative plot of all the NAH compounds (types **E**, **F**, and **G**, and **I** with R^2 = H) of their anti-*T. cruzi* activity (EC_{50}) and selectivity (SI).

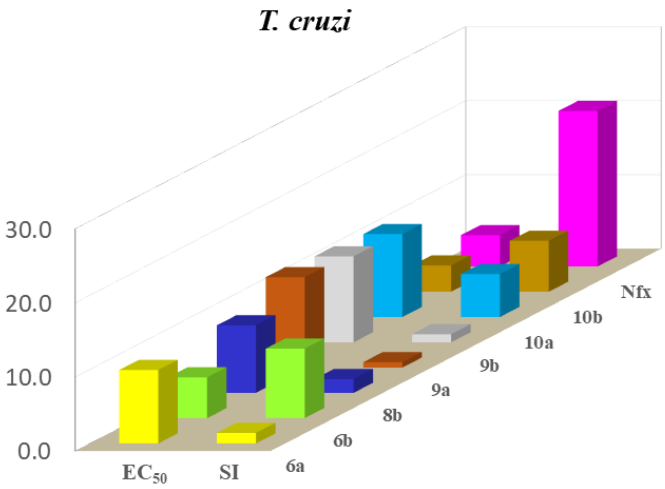

Type **I**

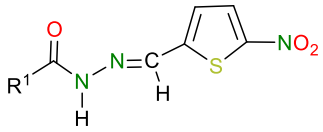

6a, **6b**

Type **G**

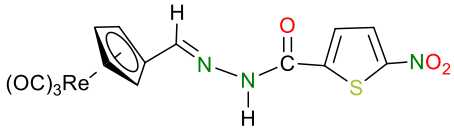

8b

Type **E**

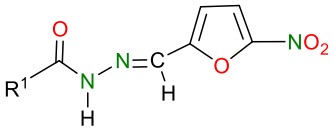

10a, **10b**

Type **F**

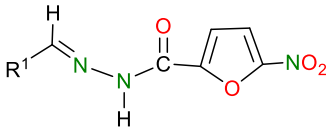

9a, **9b**

3. Supplementary Table

Table S1. Crystal data, experimental details, and refinement parameters for complexes [Re{(η^5-C_5H_4)-C(O)-NH-N=CH-(2-C_4H_2S-4-NO_2)}$(CO)_3$] (**4b**), [Fe(η^5-C_5H_5){(η^5-C_5H_4)-C(O)-NH-N=C(Me)-(2-C_4H_2S-4-NO_2)}] (**5a**), [Re{(η^5-C_5H_4)-C(O)-NH-N=C(Me)-(2-C_4H_2S-4-NO_2)}$(CO)_3$] (**5b**) and [Re{(η^5-C_5H_4)-C(O)-NH-N=CH-(2-C_4H_2S-5-NO_2)}$(CO)_3$] (**6b**).

Compound	**4b**	**5a**	**5b**	**6b**
Empirical formula	$C_{14}H_8N_3O_6ReS$	$C_{17}H_{15}FeN_3O_3S$	$C_{15}H_{10}N_3O_6ReS$	$C_{14}H_8N_3O_6ReS$
Formula weight	532.49	397.23	546.52	532.49
T (K)	295.9	295.5	295.7	296.9
λ (Å)	0.71073	1.54178	1.54178	1.54178
Crystal system	Monoclinic	Monoclinic	Triclinic	Triclinic
Space group	$P2_1/c$	C2/c	P-1	P-1
a (Å), α (°)	12.0195(9), 90	18.234(3), 90	7.5398(4), 95.862(3)	6.8710(12), 95.562(5)
b (Å), β (°)	9.3382(6), 98.538(2)	8.2285(13), 90.509(11)	10.0131(5), 92.381(4)	8.3059(13), 93.119(5)
c (Å), γ (°)	14.7444(9), 90	22.781(4), 90	11.6632(6), 99.689(3)	14.755(3), 94.287(5)
V (Å^3)	1636.58(19)	3417.9(10)	861.88(8)	834.1(2)
Z	4	8	2	2
D_{calc} (g/cm^3)	2.161	1.544	2.106	2.120
μ (mm^{-1})	7.589	8.412	15.285	7.445
F(000)	1008.0	1632.0	520.0	504.0
Crystal size (mm^3)	0.262 × 0.256 × 0.196	0.185 × 0.121 × 0.111	0.281 × 0.164 × 0.114	0.131 × 0.121 × 0.097
2θ range (°)	From 5.548 to 61.08	From 7.762 to 130.03	From 7.634 to 130.5	From 5.558 to 51.992
Index ranges	$-16 \le h \le 17$	$-21 \le h \le 21$	$-8 \le h \le 8$	$-8 \le h \le 8$
	$-13 \le k \le 13$	$-9 \le k \le 9$	$-11 \le k \le 11$	$-10 \le k \le 10$
	$-20 \le l \le 21$	$-26 \le l \le 26$	$-13 \le l \le 13$	$-18 \le l \le 18$
Reflections collected	38808	16251	10717	29299
Independent reflections	4928 [R_{int} = 0.0842]	2866 [R_{int} = 0.1260]	2883 [R_{int} = 0.0797]	3174 [R_{int} = 0.0968]
Data/parameters	4928/227	2866/202	2883/236	3174/202
Goodness-of-fit on F^2	1.094	1.018	1.091	1.105
Final *R* indices [$I > 2\sigma(I)$]	R_1 = 0.0402, wR_2 = 0.0464	R_1 = 0.0526, wR_2 = 0.1023	R_1 = 0.0468, wR_2 = 0.0985	R_1 = 0.0464, wR_2 = 0.1092
R indices (all data)	R_1 = 0.0972, wR_2 = 0.0571	R_1 = 0.1274, wR_2 = 0.1279	R_1 = 0.0681, wR_2 = 0.1060	R_1 = 0.0619, wR_2 = 0.1200

Table S2. Bond lengths [Å] and angles [°] for **4b**.

Atoms	Length/Å	Atoms	Length/Å
Re1-C1	2.292(4)	O6-C14	1.155(6)
Re1-C2	2.291(5)	N1-N2	1.375(5)
Re1-C3	2.296(5)	N1-C6	1.342(6)
Re1-C4	2.306(5)	N2-C7	1.270(6)
Re1-C5	2.310(5)	N3-C10	1.460(7)
Re1-C12	1.918(5)	C1-C2	1.420(7)
Re1-C13	1.895(6)	C1-C5	1.432(7)
Re1-C14	1.896(5)	C1-C6	1.481(6)
S1-C8	1.718(5)	C2-C3	1.401(7)
S1-C11	1.687(7)	C3-C4	1.409(8)
O1-C6	1.237(6)	C4-C5	1.418(7)
O2-N3	1.204(6)	C7-C8	1.448(7)
O3-N3	1.224(6)	C8-C9	1.350(6)
O4-C12	1.138(6)	C9-C10	1.399(7)
O5-C13	1.153(6)	C10-C11	1.337(7)
Atoms	**Angles/°**	**Atoms**	**Angles/°**
C1-Re1-C3	60.14(17)	C2-C2-Re1	71.9(3)
C1-Re1-C4	59.83(18)	C2-C1-C5	107.1(4)
C1-Re1-C5	36.25(17)	C2-C1-C6	120.5(5)
C2-Re1-C1	36.11(16)	C5-C1-Re1	72.6(3)
C2-Re1-C3	35.57(18)	C5-C1-C6	131.9(5)
C2-Re1-C4	59.1(2)	C6-C1-Re1	126.3(3)
C2-Re1-C5	59.8(2)	C1-C2-Re1	72.0(3)
C3-Re1-C4	35.6(2)	C3-C2-Re1	72.4(3)
C3-Re1-C5	59.9(2)	C3-C2-C1	109.1(5)
C4-Re1-C5	35.77(17)	C2-C3-Re1	72.0(3)
C12-Re1-C1	110.7(2)	C2-C3-C4	107.7(5)
C12-Re1-C2	146.6(2)	C4-C3-Re1	72.6(3)
C12-Re1-C3	150.3(2)	C3-C4-Re1	71.8(3)
C12-Re1-C4	114.7(2)	C3-C4-C5	109.0(5)
C12-Re1-C5	95.4(2)	C5-C4-Re1	72.3(3)
C13-Re1-C1	102.5(2)	C1-C5-Re1	71.2(3)
C13-Re1-C2	94.0(2)	C4-C5-Re1	72.0(3)
C13-Re1-C3	118.6(2)	C4-C5-C1	107.2(5)

C13-Re1-C4	152.6(2)	O1-C6-N1	119.1(5)
C13-Re1-C5	137.1(2)	O1-C6-C1	119.0(5)
C13-Re1-C12	90.5(2)	N1-C6-C1	121.9(5)
C13-Re1-C14	89.5(2)	N2-C7-C8	119.6(5)
C14-Re1-C1	156.74(18)	C7-C8-S1	119.6(4)
C14-Re1-C2	124.31(19)	C9-C8-S1	111.6(4)
C14-Re1-C3	96.6(2)	C9-C8-C7	128.8(5)
C14-Re1-C4	101.1(2)	C8-C9-C10	111.0(5)
C14-Re1-C5	133.0(2)	C9-C10-N3	122.9(5)
C14-Re1-C12	88.8(2)	C11-C10-N3	122.3(6)
C11-S1-C8	91.6(3)	C11-C10-C9	114.7(5)
C6-N1-N2	122.7(4)	C10-C11-S1	111.0(5)
C7-N2-N1	115.3(4)	O4-C12-Re1	178.7(5)
O2-N3-O3	124.7(6)	O5-C13-Re1	175.9(5)
O2-N3-C10	117.7(6)	O6-C14-Re1	179.4(5)
O3-N3-C10	117.6(6)		

Table S3. Bond lengths [Å] and angles [°] for **5a**.

Atoms	Length/Å	Atoms	Length/Å
Fe1-C1	2.017(4)	C1-C6	1.471(6)
Fe1-C2	2.033(5)	C2-C3	1.405(6)
Fe1-C3	2.048(5)	C3-C4	1.403(6)
Fe1-C4	2.054(5)	C4-C5	1.418(6)
Fe1-C5	2.031(5)	C7-C8	1.451(6)
Fe1-C17	2.020(7)	C7-C12	1.492(6)
Fe1-C13	2.006(6)	C8-C9	1.372(6)
Fe1-C14	2.009(6)	C8-S1	1.727(4)
Fe1-C15	2.025(6)	C9-C10	1.392(6)
Fe1-C16	2.031(6)	C10-C11	1.331(6)
Fe1-C17A	2.104(17)	C11-S1	1.701(5)
Fe1-C16A	2.090(16)	C17-C13	1.4200
O1-C6	1.222(5)	C17-C16	1.4200
O2-N3	1.218(5)	C13-C14	1.4200
O3-N3	1.219(5)	C14-C15	1.4200
N1-N2	1.371(5)	C15-C16	1.4200
N1-C6	1.360(6)	C17A-C13A	1.4200
N2-C7	1.300(5)	C17A-C16A	1.4200
N3-C10	1.451(6)	C13A-C14A	1.4200
C1-C2	1.428(6)	C14A-C15A	1.4200
C1-C5	1.432(6)	C15A-C16A	1.4200
Atoms	**Angles/°**	**Atoms**	**Angles/°**
C1-Fe1-C2	41.30(18)	C2-C1-C5	106.9(4)
C1-Fe1-C3	68.95(19)	C2-C1-C6	121.0(4)
C1-Fe1-C4	68.81(18)	C5-C1-Fe1	69.8(2)
C1-Fe1-C5	41.44(17)	C5-C1-C6	132.1(4)
C1-Fe1-C17	120.1(3)	C6-C1-Fe1	124.0(3)
C1-Fe1-C15	160.2(3)	C1-C2-Fe1	68.7(3)
C1-Fe1-C16	156.7(3)	C3-C2-Fe1	70.4(3)
C1-Fe1-C17A	129.7(6)	C3-C2-C1	108.6(5)
C1-Fe1-C15A	169.2(7)	C2-C3-Fe1	69.3(3)
C2-Fe1-C3	40.28(18)	C4-C3-Fe1	70.2(3)
C2-Fe1-C4	67.7(2)	C4-C3-C2	108.3(5)
C2-Fe1-C17A	168.7(7)	C3-C4-Fe1	69.8(3)

C2-Fe1-C16A	149.5(7)	C3-C4-C5	108.7(4)
C3-Fe1-C4	40.00(18)	C5-C4-Fe1	68.8(3)
C3-Fe1-C17A	150.2(6)	C1-C5-Fe1	68.8(3)
C3-Fe1-C16A	119.7(5)	C4-C5-Fe1	70.6(3)
C4-Fe1-C17A	118.2(5)	C4-C5-C1	107.6(4)
C4-Fe1-C16A	113.1(4)	O1-C6-N1	118.5(4)
C5-Fe1-C2	68.86(19)	O1-C6-C1	120.6(5)
C5-Fe1-C3	68.4(2)	N1-C6-C1	120.9(4)
C5-Fe1-C4	40.63(17)	N2-C7-C8	113.4(4)
C5-Fe1-C16	121.7(3)	N2-C7-C12	126.7(4)
C5-Fe1-C17A	108.8(4)	C8-C7-C12	119.9(4)
C5-Fe1-C16A	133.1(7)	C7-C8-S1	119.5(4)
C17-Fe1-C2	155.8(3)	C9-C8-C7	130.2(4)
C17-Fe1-C3	162.6(3)	C9-C8-S1	110.3(3)
C17-Fe1-C4	126.1(3)	C8-C9-C10	111.4(4)
C17-Fe1-C5	107.6(2)	C9-C10-N3	122.9(5)
C17-Fe1-C15	69.24(17)	C11-C10-N3	121.5(4)
C17-Fe1-C16	41.04(13)	C11-C10-C9	115.7(5)
C13-Fe1-C1	105.17(19)	C10-C11-S1	110.5(4)
C13-Fe1-C2	119.5(3)	C13-C17-Fe1	68.8(2)
C13-Fe1-C3	155.1(4)	C16-C17-Fe1	69.9(2)
C13-Fe1-C4	162.3(4)	C16-C17-C13	108
C13-Fe1-C5	124.0(3)	C17-C13-Fe1	69.9(2)
C13-Fe1-C17	41.31(13)	C14-C13-Fe1	69.4(2)
C13-Fe1-C14	41.43(11)	C14-C13-C17	108
C13-Fe1-C15	69.51(16)	C13-C14-Fe1	69.2(2)
C13-Fe1-C16	69.38(17)	C13-C14-C15	108
C14-Fe1-C1	122.4(3)	C15-C14-Fe1	70.0(2)
C14-Fe1-C2	105.6(2)	C14-C15-Fe1	68.8(2)
C14-Fe1-C3	120.0(3)	C14-C15-C16	108
C14-Fe1-C4	155.9(4)	C16-C15-Fe1	69.8(2)
C14-Fe1-C5	160.8(3)	C17-C16-Fe1	69.0(2)
C14-Fe1-C17	69.55(17)	C15-C16-Fe1	69.3(2)
C14-Fe1-C15	41.23(11)	C15-C16-C17	108
C14-Fe1-C16	69.32(16)	C13A-C17A-Fe1	71.9(6)
C15-Fe1-C2	123.5(3)	C16A-C17A-Fe1	69.7(6)
C15-Fe1-C3	107.4(2)	C16A-C17A-C13A	108
C15-Fe1-C4	121.7(3)	C17A-C13A-Fe1	69.0(6)

C15-Fe1-C5	157.0(3)	C14A-C13A-Fe1	71.0(6)
C15-Fe1-C16	40.99(12)	C14A-C13A-C17A	108
C16-Fe1-C2	161.2(3)	C13A-C14A-Fe1	70.3(6)
C16-Fe1-C3	125.4(3)	C15A-C14A-Fe1	69.4(6)
C16-Fe1-C4	109.2(2)	C15A-C14A-C13A	108
C16A-Fe1-C17A	39.6(3)	C14A-C15A-Fe1	71.8(6)
C6-N1-N2	122.4(4)	C14A-C15A-C16A	108
C7-N2-N1	117.7(4)	C16A-C15A-Fe1	69.2(6)
O2-N3-O3	123.3(5)	C17A-C16A-Fe1	70.7(6)
O2-N3-C10	117.8(4)	C17A-C16A-C15A	108
O3-N3-C10	118.9(5)	C15A-C16A-Fe1	71.4(6)
C2-C1-Fe1	70.0(3)	C11-S1-C8	92.2(3)

Table S4. Bond lengths [Å] and angles [°] for **5b**.

Atoms	Length/Å	Atoms	Length/Å
Re1-C1	2.308(8)	N1-N2	1.376(10)
Re1-C2	2.293(9)	N1-C6	1.358(11)
Re1-C3	2.303(10)	N2-C7	1.283(11)
Re1-C4	2.294(9)	N3-C10	1.463(12)
Re1-C5	2.283(9)	C1-C2	1.434(12)
Re1-C13	1.899(11)	C1-C5	1.431(12)
Re1-C14	1.927(12)	C1-C6	1.463(12)
Re1-C15	1.897(10)	C2-C3	1.394(13)
S1-C8	1.727(8)	C3-C4	1.400(14)
S1-C11	1.696(10)	C4-C5	1.396(12)
O1-C6	1.219(10)	C7-C8	1.466(12)
O2-N3	1.208(10)	C7-C12	1.484(11)
O3-N3	1.236(10)	C8-C9	1.356(12)
O4-C13	1.158(12)	C9-C10	1.392(12)
O5-C14	1.134(12)	C10-C11	1.342(13)
O6-C15	1.153(12)		
Atoms	**Angles/°**	**Atoms**	**Angles/°**
C2-Re1-C1	36.3(3)	C2-C1-C6	119.6(8)
C2-Re1-C3	35.3(3)	C5-C1-Re1	70.9(5)
C2-Re1-C4	58.8(4)	C5-C1-C2	105.2(8)
C3-Re1-C1	60.2(3)	C5-C1-C6	135.1(8)
C4-Re1-C1	59.8(3)	C6-C1-Re1	124.4(6)
C4-Re1-C3	35.5(4)	C1-C2-Re1	72.4(5)
C5-Re1-C1	36.3(3)	C3-C2-Re1	72.7(6)
C5-Re1-C2	59.7(3)	C3-C2-C1	109.7(9)
C5-Re1-C3	59.6(4)	C2-C3-Re1	72.0(5)
C5-Re1-C4	35.5(3)	C2-C4-C4	107.3(8)
C13-Re1-C1	103.6(4)	C4-C3-Re1	71.9(6)
C13-Re1-C2	138.5(4)	C3-C4-Re1	72.6(6)
C13-Re1-C3	153.7(4)	C5-C4-Re1	71.8(5)
C13-Re1-C4	119.4(4)	C5-C4-C3	109.3(8)
C13-Re1-C5	94.8(4)	C1-C5-Re1	72.8(5)
C13-Re1-C14	90.1(4)	C4-C5-Re1	72.7(5)
C14-Re1-C1	108.2(4)	C4-C5-C1	108.5(8)

C14-Re1-C2	94.3(4)	O1-C6-N1	118.8(8)
C14-Re1-C3	114.0(5)	O1-C6-C1	120.3(8)
C14-Re1-C4	149.4(4)	N1-C6-C1	120.8(8)
C14-Re1-C5	144.2(4)	N2-C7-C8	114.2(7)
C15-Re1-C1	157.1(4)	N2-C7-C12	126.5(8)
C15-Re1-C2	130.7(4)	C8-C7-C12	119.3(8)
C15-Re1-C3	99.7(4)	C7-C8-S1	119.0(6)
C15-Re1-C4	97.6(4)	C9-C8-S1	110.9(6)
C15-Re1-C5	125.9(4)	C9-C8-C7	130.1(7)
C15-Re1-C13	90.5(4)	C8-C9-C10	111.6(8)
C15-Re1-C14	89.4(4)	C9-C10-N3	123.3(8)
C11-S1-C8	91.9(4)	C11-C10-N3	121.6(8)
C6-N1-N2	122.4(7)	C11-C10-C9	115.0(8)
C7-N2-N1	118.4(7)	C10-C11-S1	110.6(7)
O2-N3-O3	124.6(9)	O4-C13-Re1	177.5(9)
O2-N3-C10	118.1(8)	O5-C14-Re1	176.8(10)
O3-N3-C10	117.2(9)	O6-C15-Re1	178.6(11)
C2-C1-Re1	71.3(5)		

Table S5. Bond lengths [Å] and angles [°] for **6b**.

Re1-C1	2.288(9)	O5-C13	1.144(14)
Re1-C2	2.301(9)	N1-N2	1.380(10)
Re1-C3	2.302(10)	N1-C6	1.338(11)
Re1-C4	2.296(9)	N2-C7	1.285(12)
Re1-C5	2.300(9)	C1-C2	1.421(13)
Re1-C12	1.882(13)	C1-C5	1.425(12)
Re1-C13	1.903(11)	C1-C6	1.490(12)
Re1-C14	1.887(11)	C2-C3	1.399(13)
S1-C8	1.717(10)	C3-C4	1.406(14)
S1-C11	1.714(12)	C4-C5	1.417(13)
O1-C6	1.234(10)	C7-C8	1.458(13)
N3-O2	1.28(2)	C8-C9	1.348(15)
N3-O3	1.15(2)	C9-C10	1.412(16)
N3-C11	1.472(17)	C10-C11	1.318(18)
O4-C12	1.169(15)	C14-O6	1.163(14)
Atoms	**Angles/°**	**Atoms**	**Angles/°**
C1-Re1-C2	36.1(3)	C2-C1-Re1	72.5(5)
C1-Re1-C3	59.8(3)	C2-C1-C5	107.4(8)
C1-Re1-C4	59.9(3)	C2-C1-C6	119.6(8)
C1-Re1-C5	36.2(3)	C5-C1-Re1	72.4(5)
C2-Re1-C3	35.4(3)	C5-C1-C6	132.9(8)
C4-Re1-C2	59.3(3)	C6-C1-Re1	122.7(6)
C4-Re1-C3	35.6(4)	C1-C2-Re1	71.5(5)
C4-Re1-C5	35.9(3)	C3-C2-Re1	72.3(5)
C5-Re1-C2	59.8(3)	C3-C2-C1	108.4(8)
C5-Re1-C3	59.7(4)	C2-C3-Re1	72.3(5)
C12-Re1-C1	98.9(4)	C2-C3-C4	108.4(8)
C12-Re1-C2	98.1(4)	C4-C3-Re1	72.0(5)
C12-Re1-C3	127.2(4)	C3-C4-Re1	72.4(6)
C12-Re1-C4	156.7(4)	C3-C4-C5	108.4(8)
C12-Re1-C5	130.2(4)	C5-C4-Re1	72.2(5)
C12-Re1-C13	90.3(5)	C1-C5-Re1	71.4(5)
C12-Re1-C14	90.1(5)	C4-C5-Re1	71.9(5)
C13-Re1-C1	153.0(4)	C4-C5-C1	107.4(8)

C13-Re1-C2	117.7(4)	O1-C6-N1	118.9(8)
C13-Re1-C3	94.6(4)	O1-C6-C1	118.7(8)
C13-Re1-C4	104.8(4)	N1-C6-C1	122.4(8)
C13-Re1-C5	139.3(4)	N2-C7-C8	119.6(8)
C14-Re1-C1	116.0(4)	C7-C8-S1	121.7(7)
C14-Re1-C2	151.7(4)	C9-C8-S1	113.0(8)
C14-Re1-C3	142.4(5)	C9-C8-C7	125.3(10)
C14-Re1-C4	107.5(4)	C8-C9-C10	112.0(12)
C14-Re1-C5	94.4(4)	C11-C10-C9	111.5(11)
C14-Re1-C13	89.1(5)	N3-C11-S1	116.4(12)
C11-S1-C8	88.8(5)	C10-C11-S1	114.8(9)
O2-N3-C11	111.5(17)	C10-C11-N3	128.9(13)
O3-N3-O2	127.7(16)	O4-C12-Re1	177.8(10)
O3-N3-C11	120.8(16)	O5-C13-Re1	177.2(11)
C6-N1-N2	123.9(7)	O6-C14-Re1	176.2(11)
C7-N2-N1	113.9(7)		

Table S6. Hydrogen bonds for **4b**.

D	H	A	d(D-H)/Å	d(H-A)/Å	d(D-A)/Å	D-H-A/°
N1	H1	O1[1]	0.86	2.03	2.884(5)	170.9
C3	H3	O4[2]	0.93	2.73	3.450(7)	135.0
C4	H4	O5[3]	0.93	2.71	3.481(7)	140.5
C7	H7	O2[4]	0.93	2.51	3.298(7)	142.6
C9	H9	O2[4]	0.93	2.67	3.389(7)	135.1
C11	H11	O5[5]	0.93	2.61	3.360(8)	138.6
[1]-x,-y,1-z; [2]+x,1/2-y,1/2+z; [3]1-x,1/2+y,3/2-z; [4]-x,-1/2+y,1/2-z; [5]+x,1+y,+z						

Table S7. Hydrogen bonds for **5a**.

D	H	A	d(D-H)/Å	d(H-A)/Å	d(D-A)/Å	D-H-A/°
N1	H1	O1[1]	0.86	2.08	2.918(5)	164.7
C9	H9	O2[2]	0.93	2.48	3.353(7)	157.3
C13	H13	O3[3]	0.93	2.53	3.422(5)	159.5
C15	H15	O3[4]	0.93	2.50	3.420(5)	171.8
[1]1/2-x,1/2-y,1-z; [2]1-x,2-y,1-z; [3]-1/2+x,-1/2+y,+z; [4]1-x,-1+y,3/2-z						

Table S8. Hydrogen bonds for **5b**.

D	H	A	d(D-H)/Å	d(H-A)/Å	d(D-A)/Å	D-H-A/°
N1	H1	O1[1]	0.86	2.08	2.912(9)	162.6
C3	H3	O4[2]	0.93	2.68	3.408(13)	135.4
C11	H11	O5[3]	0.93	2.43	3.330(12)	161.8
[1]1-x,2-y,2-z; [2]-1+x,+y,+z; [3]+x,-1+y,+z						

Table S9. Hydrogen bonds for **6b**.

D	H	A	d(D-H)/Å	d(H-A)/Å	d(D-A)/Å	D-H-A/°
C3	H3	O4[1]	0.93	2.63	3.442(14)	146.1
C4	H4	O2[2]	0.93	2.49	3.265(15)	140.4
C5	H5	O5[3]	0.93	2.84	3.420(14)	121.3
C7	H7	O5[4]	0.93	2.60	3.421(14)	146.9
C9	H9	O5[4]	0.93	2.68	3.462(17)	142.3
C10	H10	O6[5]	0.93	2.49	3.416(17)	172.8
[1]-1+x,+y,+z; [2]1-x,1-y,1-z; [3]+x,-1+y,+z; [4]1+x,-1+y,+z; [5]2-x,1-y,1-z						

Table S10. Summary of experimental ultraviolet-visible spectroscopic data: position of the bands detected [wavelengths λ_i (nm)] and logarithms of their molar extinction coefficients [log ε_i (ε_i in M^{-1} cm^{-1})] for the new organometallic NAHs (**4a**,**b – 7a**,**b**) [Types **H** and **I** in Figure 3).

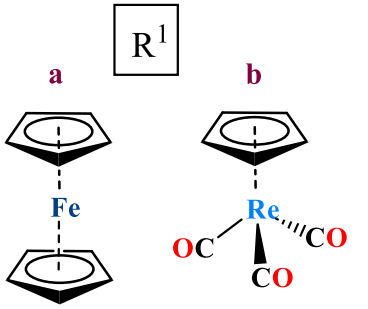

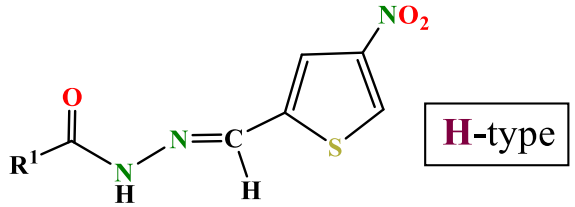

H-type

R^2 = H (**4a-4b**) R^2 = Me (**5a-5b**)

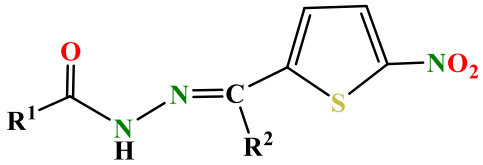

I-type

R^2 = H (**6a-6b**) R^2 = Me (**7a-7b**)

Compounds [a] →	**4a**	**4b**	**5a**	**5b**	**6a**	**6b**	**7a**	**7b**
λ_1 (log ε_1)	273 (4.0)	275 (4.0)	273 (3.9)	275 (4.0)	260 (4.0)	268 (3.9)	266 (4.0)	271 (4.0)
λ_2 (log ε_2)	313 (4.0)	316 (4.0)	314 (4.0)	313 (4.0)	383 (3.9)	385 (4.0)	380 (4.0)	385 (4.0)
λ_3 (log ε_3)	≈460 (2.8) [b]	——	≈468 (2.9) [b]	——	——	——	≈498[c]	——

[a] Data obtained from the spectra recorded from fresh solutions of the compounds (t = 0 h).

[b] Broad band {see also figures S17 (for **4a**) and S21 (for **4b**)}.

[c] This absorption appears as a shoulder (see figure S20).

4. Supplementary References

S1. P. Toro, C. Suazo, A. Acuña, M. Fuentealba, V. Artigas, R. Arancibia, C. Olea-Azar, M. Moncada, S. Wilkinson, A. H. Klahn, Cyrhetrenylaniline and new organometallic phenylimines derived from 4- and 5-nitrothiophene: Synthesis, characterization, X-Ray structures, electrochemistry and in vitro anti-T. brucei activity, J. Organomet. Chem., 2018, **862**, 13.

S2. B.P. Fabrichnyi, S.M. Kostrova, G.P. Gromova, Y. L. Gol'dfarb, Directive nature of the nitration of the oximes of 2-acetylthiophene and 2-propionylthiophene, Chem. Heterocycl. Compd. 1973, **9**, 1341.

S3. D. J. van Dijken, P. Kovaříček, S. P. Ihrig, S. Hecht, Acylhydrazones as Widely Tunable Photoswitches, J. Am. Chem. Soc., 2015, **137**, 14982–14991.

S4. M. Mallea, A. Acuña, A. H. Klahn, V. Artigas, F. Rogério Pavan, F. Manaia Demarqui, L. Lemus, D. H. Jara, P. M. Toro, Cyrhetrenyl and cymantrenyl N-acylhydrazone complexes based on isoniazid: Synthesis, characterization, X-ray crystal structures and antitubercular activity evaluation, J. Organomet. Chem., 2022, **964**, 122299.